Design, Syntheses and Applications of MOFs as Sensory Probes for Anion Recognition

A Thesis

Submitted in Partial Fulfillment of the Requirements

For the Degree of

Doctor of Philosophy

by

Avishek Karmakar

ID: 20113131

Indian Institute of Science Education and Research (IISER), Pune

2017

Dedicated

To Ma and Babi (my Parents)

IISER PUNE

Certificate

Certified that the work described in this thesis entitled "***Design, Syntheses and Applications of MOFs as Sensory Probes for Anion Recognition***"submitted by *Mr.* ***Avishek Karmakar*** was carried out by the candidate, under my supervision. The work presented here or any part of it has not been included in any other thesis submitted previously for the award of any degree or diploma from any other university or institution.

Date: 10th January 2017

Dr. Sujit K. Ghosh

Research Supervisor

IISER PUNE

Declaration

I declare that this written submission represents my ideas in my own words and wherever other's ideas have been included; I have adequately cited and referenced the original sources. I also declare that I have adhered to all principles of academic honesty and integrity and have not misrepresented or fabricated or falsified any idea/data/fact/source in this submission. I understand that violation of the above will result in disciplinary actions by the Institute and can also evoke penal action from the sources, which have thus not been properly cited or from whom appropriate permission has not been taken when needed.

Date: 10th January 2017

Avishek Karmakar

Reg. No: 20113131

Acknowledgement

*Prima facie, I am grateful to my supervisor **Dr. Sujit K. Ghosh**, whose constant motivation, support and encouragement has propelled my research forward for the last five years. It has been a privilege to work under his supervision and I feel his guidance has helped me to develop as an independent researcher for the future. His outstanding research ideas and his pro-active nature has always enthralled in me a keen source of energy, which has helped me achieve whatever I have achieved till date. I am also thankful to **Professor K.N.Ganesh**, Director IISER Pune, for the world-class research facilities and being a pioneer in setting up the IISER-Pune campus. I think his visionary owe due credit in making IISER-Pune one of the leading academic institutes of India. I am also thankful to my research advisory committee (RAC) members, **Dr. Nirmalya Ballav** (IISER-Pune) and **Dr. Avinash Kumbhar** (University of Pune) for their valuable suggestions and supportive nature throughout the tenure of five years. The annual meeting with my RAC members always ended in a fruitful manner, and there were always a lot of take-home messages after the scientific discussions. I would also use this opportunity to thanks all the other faculty members of IISER-Pune who have, in their own particular way, ensured that the outstanding standard of IISER-Pune is maintained. I think the present group of enthusiastic faculty members have played a crucial part in the progress of this premier institutes. I am sure that IISER-Pune will continue to prosper in all facets, in the wonderful years to come.*

I am also thankful to all the members of our lab "Microporous Materials Lab" which includes the present and past members as well. My sincere thanks go out for Dr. Sanjog Nagarkar, Dr. Biplab Joarder, Dr. Biplab Manna, Dr. Soumya Mukherjee and the current members: Dr. Tarak Nath Mandal, Aamod V. Desai, Partha Samanta, Arunabha Sen, Samraj Mollick, Yogeshwar More, Shivani Sharma, Prateek Agarwal and Subhajit Dutta. Of them, Aamod and Partha need special mention as they have been an integral part of my success so far. I would also like to mention about two MS students of IISER-Pune, Amrit Singh and Naveen Kumar who carried out their 5^{th} year project work under my guidance and successfully completed the two projects that they worked on. I would also like to thank all the other project students like Abhijeet Chaudhari and Arif Inamdar who also were key figures in our lab during my tenure. I would like to wish all the above mentioned members (past and present) of our lab all the very best for their future endeavors.

I would also like to thank American Chemical Society (ACS), Royal Society of Chemistry (RSC), John Wiley & Sons (Wiley-VCH), Elsevier for the various research and review articles that I managed to publish in my Ph.D tenure. I acknowledge Ministry of Human Resource Development (MHRD), India and IISER-Pune for providing the necessary funding required for my research.

I also take this opportunity to acknowledge all the instrument operators of IISER-Pune who made sure that the swift working of the instruments were possible and I could collect data without any hitch. I would also like to mention special thanks to our non-teaching administrative staffs for extending their generous support, whenever required.

Apart from the time I spend in lab, hostel life is one thing that added the fuel needed to carry out my research work. The fun filled time I spent in the hostel was entertaining to say the least. The heated arguments regarding politics, sports and entertainment was not only fun, but I learned a lot things from constructive discussions as well. Among my friends here at IISER-Pune, Abhik, Arindamda, Sudebda, Parthada, Supratik, Sunil, Koushikda, Barun, Maidul, Chandramouli, Rajkumar, Shyama, Reja, Tanmay, Amit, Sagar, Soumendu, Sapatashwa and Sushil formed the inner sphere of my circle and we have at various occasions, spent memorable times. Also, I would like to mention about our Bengali football and cricket team, of which I was a part for the last five years and I wish the members all the success in the forthcoming years.

Lastly, I would like to thank ***my parents*** *who stood beside me at every juncture of my life so far. Without their support and motivation, I would not have reached so far. My elder sister* ***Mausita*** *and brother-in-law,* ***Arnab*** *who are also pursuing research career themselves as well, in the U.S.A, have been the pillars of my life and my go-to persons in whatever tough situations I have faced in my life. Recently, they were blessed with a baby boy* ***Rohan*** *and I shower all my blessings and love to this little angel. Other than the above mentioned names,* ***Arijita*** *is one person who has formed a special bonding with me over the last 11 years. Currently pursuing her doctoral studies at IIT-Chennai, I am sure she will reach extraordinary heights in whatever she chooses to do in the future. My life is incomplete without these persons and I am blessed to have their support and love throughout my journey so far.*

Avishek Karmakar

Table of Contents

Synopsis

Metal-organic Frameworks (MOFs) have emerged as a promising class of materials in the regime of sensory materials mostly due to the rational designing based on the ligand and metal ions/clusters, tunable architectures and suitable host-guest interactions in such open frameworks. The wide choice of metal and ligands used in the synthesis of MOFs bestow ample opportunities to modulate the opto-electronic properties of such porous networked structures. Also, often, the inherent ionicity rendered by usage of neutral ligands in the MOF synthesis can be useful in sensing/recognition of anion(s) which are realized most by anion exchange processes. Whereas ligands play their specific part in recognition of anions, metal centers also have a pivotal role to play in such selective sensing processes in response to the changes in their sensitive electronic environment. Another strategy that can be employed in recognition of a particular anion is the post-synthetic modification, which imparts specific identification sites in the framework. Such functionalization in the organic part can also be employed to sense a particular anionic species inducing suitable signal transduction. In this regard sensing and capture of toxic anions can be fruitful in waste-water treatment and other environmental remediation purposes. If toxic anions can be rendered inactive by using MOFs as a molecular level reaction vessel in heterogeneous phase, then many pertinent problems involving such environmental hazardous entities can be addressed. I have systematically developed strategies for such sensing by anions by judicious choice of ligand or metal and also by post-functionalization of the MOF resulting in optical responses (fluorescence/visual) as signal output. Finally, I have successfully used a bio-compatible MOF for the capture of a toxic anion and rendered its activity less by a reaction based approach inside the MOF.

In a nut shell, my 1st chapter deals with the anion sensing properties of MOF which is achieved by ligand design resulting in tunable luminescence behaviors upon anion exchange. Following up, in the 2nd chapter the judicious choice of the metal center for the construction of MOF has been utilized to achieve colorimetric sensing of an anion. In the next (3rd) chapter I have show the Post-synthetic Modification (PSM) approach in a MOF to achieve selective sensing of a toxic anion, and finally in the 5th chapter I have shown how an anionic MOF can also be utilized to achieve selective sensing of a toxic anion and have also shown its reusability and sensing performance in human cell lines.

Chapter 1. *Introduction*

At the very outset, in this chapter I have discussed about the importance of anion sensing and the various aspects that are desired to fabricate a good chemical sensors for anions. Then, I have discussed briefly about MOFs and its utility as chemical sensors. Further, I have discussed about the role of MOFs in sensing of anions the various methodologies employed in sensing of anions. This is mostly achieved by anion exchange processes in cationic MOFs and therefore I have discussed about the various ways to construct cationic MOFs. I have also discussed about the two major modes of sensing of anions in MOFs i.e. by luminescence and by colorimetry. I have also discussed about post-synthetic modification (PSM) which can be employed in MOFs to achieve highly selective and sensitive detection of anions. Finally, I have given some insight towards the applicability of MOFs for practical purposes and/or for biological sensing which can be useful for designing devices for anion sensing in the future.

Chapter 2. *Dynamic Metal–Organic Framework with Anion-Triggered Luminescence Modulation Behavior*

In this chapter, a three-dimensional cationic framework based on a flexible neutral nitrogen-donor ligand was synthesized and undergoes guest-driven structural dynamics in a reversible way. Size-selective anion-exchange selective anion-exchange results prove the affinity of the host framework towards anions of similar nature (**Figure 1**) and can be an efficient system for ion separation. Also, anion-exchanged compounds show anion-dependent tunable luminescence and therefore have potential to develop as smart materials for chemical sensors, light-emitting devices, and other optoelectronic design strategies (*Inorg. Chem.* **2014**, *53*, 12225-12227).

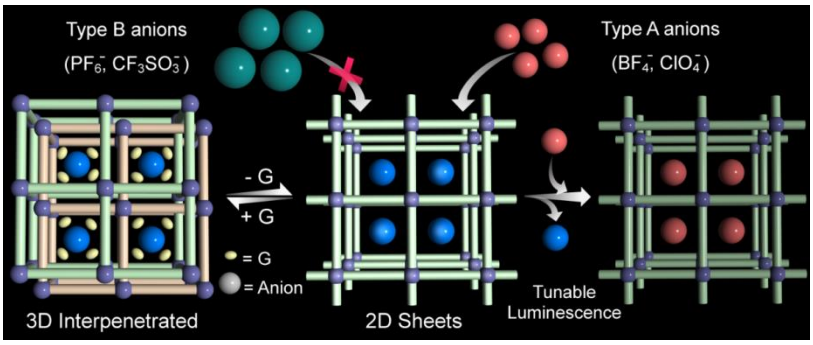

Figure 1: Schematic Representation of a Guest- and Anion-Responsive Dynamic Framework

Chapter 3. *An Amide-Functionalized Dynamic Metal–Organic Framework Exhibiting Visual Colorimetric Anion Exchange and Selective Uptake of Benzene over Cyclohexane*

In this chapter, I have synthesized a novel 1D metal–organic framework (MOF) based on a flexible neutral amide-based N-donor ligand. The framework underwent an interesting structural transformation upon desolvation, and this guest-free phase could be utilized for separation of CO_2 and other non-polar gases such as N_2, H_2, and CH_4 at low temperatures. Moreover, the combination of structural flexibility and guest-responsive enzymatic behavior has been used to address one of the important challenges of chemical industries, namely the separation of benzene and cyclohexane. In view of achieving further versatility, visual colorimetric detection of SCN^- anions has also been studied by an anion exchange process, which has been rarely reported previously. Such incorporation of multi-functionality in MOFs (**Figure 2**) is an important aspect, and if achieved in an economical fashion could be a most sought-after material in chemical industry in the future (*Chem. Eur. J.* **2015**, *21*, 7071 – 7076).

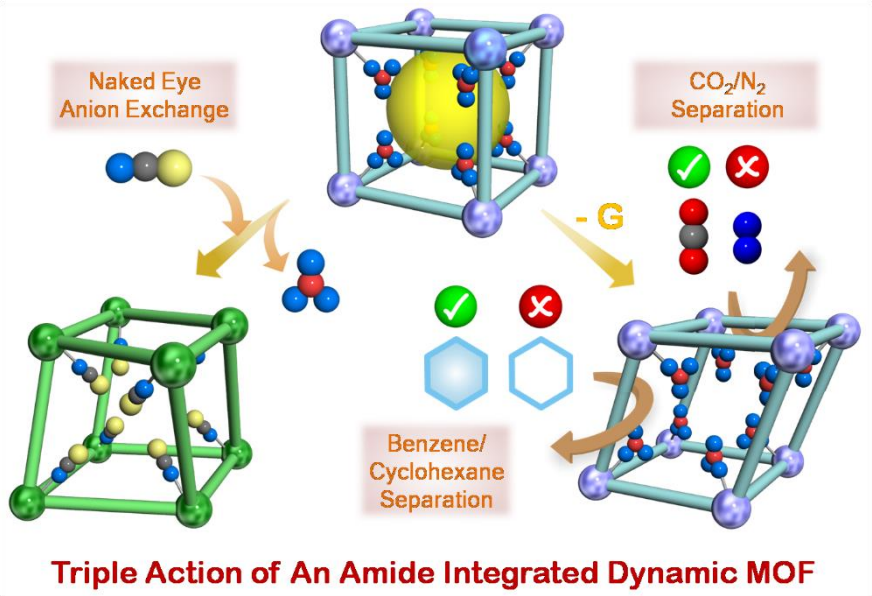

Figure 2: Representation of the multifunctional behavior of an amide functionalized Metal-organic Framework.

Chapter 4. *A Post-Synthetically Modified Metal-organic Framework for Selective and Sensitive Aqueous-Phase Detection of Highly Toxic Cyanide Ions*

In this chapter, selective and sensitive detection of toxic cyanide (CN^-) by a post-synthetically altered metal–organicframework (MOF) has been achieved. A post-syntheticmodification was employed in the MOF to incorporate thespecific recognition site with the CN^- ion over all otheranions, such as Cl^-, Br^-, and SCN^- etc. (**Figure 3**). The aqueous-phasesensing and very low detection limit, the essential pre-requisitesfor an effective sensory material, have been fulfilledby the MOF. Moreover, the detection level meetsthe standard set by the World Health Organization (WHO)for the permissible limit of cyanide concentration in drinkingwater. The utilization of MOF-based materials as thefluorometric probes for selective and sensitive detection of CN^-ions had not been explored till then (*Chem. Eur. J*. **2016**,*22*,864 – 868).

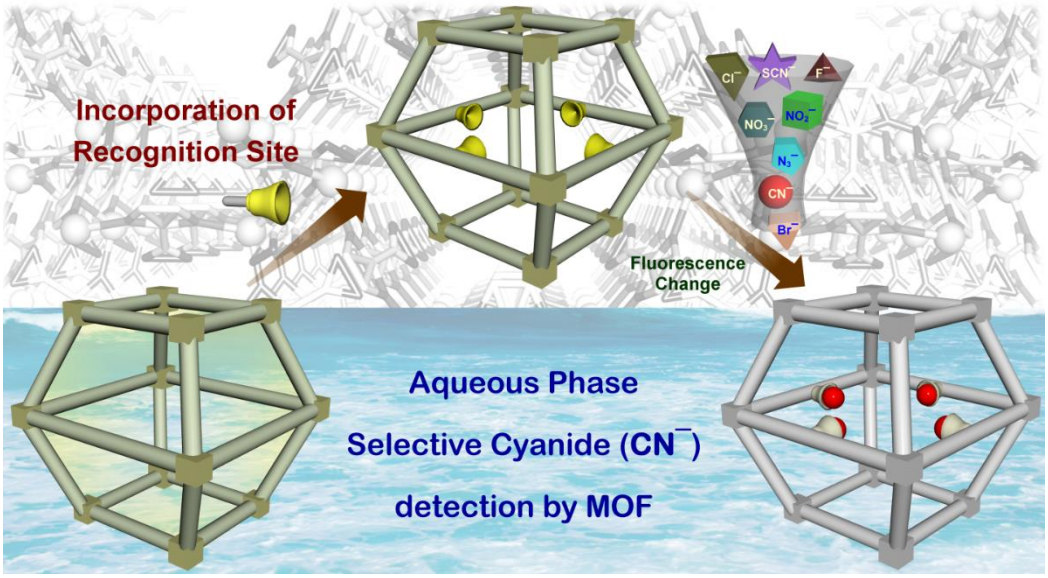

Figure 3: Figure showing the post-synthetic modification in MOF leading to selective sensing of cyanide ion.

Chapter 5. *Aqueous Phase Sensing of Cyanide Ion Using a Hydrolytically Stable Metal-organic Framework*

Moving on, in the last chapter, a fluorescent bio-compatible anionic metal-organic framework (MOF) for pure aqueous phase recognition and detoxification of cyanide ion (CN^-) has been shown. The MOF acts as a molecular reaction vessel exclusively for cyanide ions among all other competing anions inducing a signal turn on response in pure aqueous media (**Figure 4**). The chemodosimetric approach in heterogeneous phase results in ultrafast response and very low detection limit (5.2ppb) for CN^- ions by the MOF. Moreover, the MOF has been utilized to visualize the cytoplasmic cyanide concentration via in vitro studies and detect even trace amount of CN^- in living cells. Importantly the MOF could even be recycled via reversible cation exchange process to trigger almost the same response towards CN^- ion. The simultaneous recognition and detoxification of a highly chemically toxic agent like CN^- has not been demonstrated in the regime of porous materials till date. (*Chem. Commun*. **2016**, DOI: 10.1039/C6CC08557A).

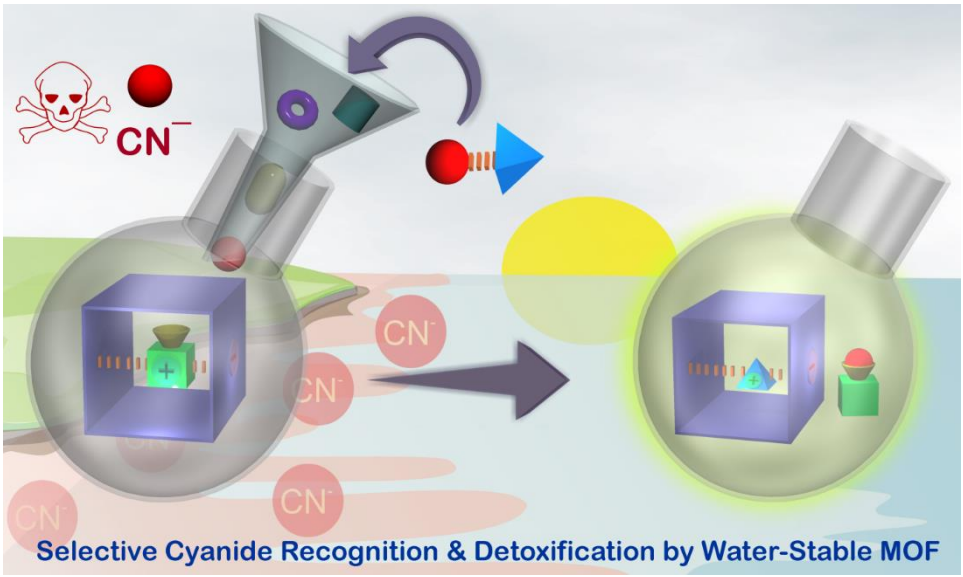

Figure 4: Figure showing selective sensing of CN^- ion by MOF which acts as a molecular reaction flask.

Chapter 6. *Conclusions and Future Outlook*

In summary, the aforementioned four chapters (chapter 2-chapter 5) encompass an ample discussion on four different MOFs which have been utilized for sensing of anions using four different methodologies. While ligand design and choice of metal centres are the key towards development of MOFs as anion sensors, post-synthetic modification and even usage of anionic framework has been found to be efficient in highly selective and sensing of anions. The gradual improvement in the sensing capability of the MOFs and the corresponding efficiency in even detecting toxic anions in human cell lines is one of the significant achievements of my thesis, I believe. This systematic improvement in the sensing performance in MOFs will pave way towards fabricating biosensors for numerous biologically relevant anions and will certainly propel future research in the field of anion sensing by novel materials.

List of Abbreviations

Anal.	Analysis
Calc.	Calculated
CCDC	Cambridge Crystallographic Data Centre
CCD	Charge-coupled device
DMF	N, N-Dimethyl formamide
EtOH	Ethanol
FT-IR	Fourier transform infra-red
gm	Gram
MeOH	Methanol
mg	Milligram
MHz	Megahertz
min	Minutes
mL	Milliliter
mM	Micro molar
mmol	Milli mole
MOF	Metal organic framework
NLO	Non-linear optics
N-donor	Nitrogen donor
PCP	Porous coordination polymer
PXRD	Powder X-Ray Diffraction
RT	Room Temperature
SC-XRD	Single Crystal X-Ray Diffraction
TGA	Thermogravimetric Analysis
THF	Tetrahydrofuran
UV	Ultraviolet
MTT	3-(4,5-dimethylthiazol-2-yl)-2,5-diphenyltetrazolium bromide
UV-Vis	Ultra violet-visible

Research Publications

INCLUDED IN THESIS

1. **Avishek Karmakar**, Biplab Joarder, Abhik Mallick, Partha Samanta, Aamod V. Desai, Sudipta Basu and Sujit Ghosh. Aqueous Phase Sensing of Cyanide Ion Using a Hydrolytically Stable Metal-organic Framework. *Chem. Commun*. **2016**, DOI: 10.1039/C6CC08557A.

2. **Avishek Karmakar**, Naveen Kumar, Partha Samanta, Aamod V. Desai, and Sujit K. Ghosh. A Post-Synthetically Modified MOF for Selective and Sensitive Aqueous-Phase Detection of Highly Toxic Cyanide Ions. *Chem. Eur. J***. 2016**,*22*,864 – 868**.**

3. **Avishek Karmakar**, Aamod V. Desai and Sujit K. Ghosh. Ionic metal-organic frameworks (iMOFs): Design principles and applications. *Coord. Chem. Rev*. **2016**, *307*, 313–341.

4. **Avishek Karmakar**, Aamod V. Desai, Biplab Manna, Biplab Joarder and Sujit K. Ghosh. Amide Functionalized Dynamic Metal-Organic Framework Exhibiting Visual Colorimetric Anion Exchange and Selective uptake of Benzene over Cyclohexane. *Chem. Eur. J.* **2015**, *21*, 7071 – 7076.

5. **Avishek Karmakar**, Biplab Manna, Aamod V. Desai, Biplab Joarder and Sujit K. Ghosh. Dynamic Metal−Organic Framework with Anion-Triggered Luminescence Modulation Behavior. *Inorg. Chem***. 2014**, *53*, 12225-12227.

NOT INCLUDED IN THESIS

6. **Avishek Karmakar**, Rajith Illathvalappil, Bihag Anothumakkool, Arunabha Sen, Partha Samanta, Aamod V. Desai, Sreekumar Kurungot and Sujit K. Ghosh. Hydrogen-Bonded Organic Frameworks: A New Class of Porous Crystalline Proton Conducting Materials. *Angew. Chem. Int. Ed.***2016**, 55, 10667-106713.

7. **Avishek Karmakar**, Amrit Kumar, Abhijeet K. Chaudhari, Partha Samanta , Aamod V. Desai, Rajamani Krishna and Sujit K. Ghosh. Bimodal Functionality in a Porous Covalent triazine framework by Rational Integration of Electron-Rich and –Deficient Pore Surface. *Chem. Eur. J***. 2016,** *22*, 4931 –4937.

8. **Avishek Karmakar**, Partha Samanta, Aamod V. Desai and Sujit Ghosh. Guest Responsive Metal-Organic Frameworks as Scaffolds for Sensing and Separation applications.*Acc. Chem. Res.* **(Special Issue).** (Submitted).

9. **Avishek Karmakar**, Partha Samanta, Arunabha Sen, Aamod V. Desai and Sujit Ghosh. High Proton Conduction in Anionic Frameworks instigated by Cationic Proton Carriers. (*Manuscript Submitted*).

10. Aamod V. Desai, Biplab Manna, **Avishek Karmakar**, Amit Sahu and Sujit K. Ghosh. A Water Stable Cationic Metal-Organic Framework as Dual Adsorbent of Oxo-Anion Pollutants.*Angew. Chem. Int. Ed.* **2016**, *55*, 7811-7815.

11. Biplab Manna, Shweta Singh, **Avishek Karmakar**, Aamod V. Desai and Sujit K. Ghosh. Selective Anion Exchange and Tunable Luminescent Behaviour of MOF based Supramolecular Isomers. *Inorg. Chem.* **2015,** *54***,** 110-116**.**

12. Biplab Manna, Aamod V.Desai, Naveen Kumar, **Avishek Karmakar** and Sujit K.Ghosh. Single-Crystal-to-Single-Crystal Transformation of an Anion Exchangeable Dynamic Metal-Organic Framework. *CrystEngComm* **2015,** *17***,** 8796-8800(Special issue)

13. Biplab Manna, Biplab Joarder, Aamod V. Desai, **Avishek Karmakar** andSujit K.Ghosh. Anion-Responsive Tunable Bulk Phase Homochirality and Luminescence of a Cationic Framework. *Chem. Eur. J.* **2014,** *20***,** 12399-12404.

14**.** Biplab Manna, Abhijeet K. Chaudhari, Biplab Joarder, **Avishek Karmakar** and Sujit K. Ghosh Dynamic Structural Behavior and Anion-Responsive Tunable Luminescence of a Flexible Cationic Metal-Organic Framework. *Angew. Chem. Int. Ed.* **2013,** *52*,998-1002.

15. Partha Samanta, Aamod Desai, Bihag Anothumakkool, **Avishek Karmakar**, Sreekumar Kurungot and Sujit Ghosh, Enhanced Proton Conduction by Post-Synthetic Covalent Modification in a Porous Covalent Framework.*Chem. Mater.* (Under minor revision).

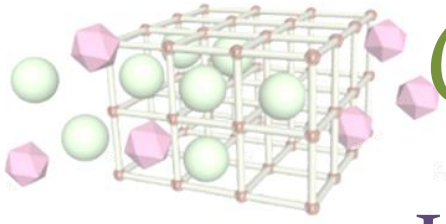

Chapter -1

Introduction

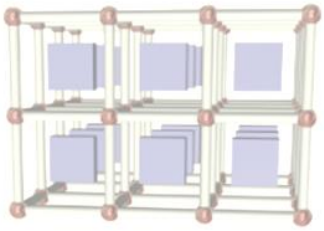

Separation

Sensing

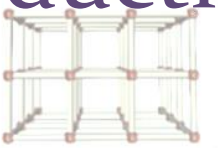

MOFs/PCPs

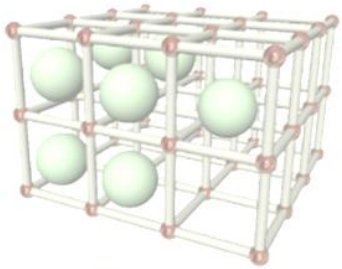

Storage

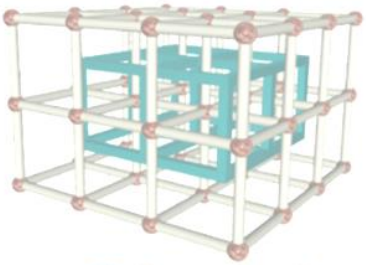

Polymerization

Cover page for Chapter 1

1.1 Anion Sensing/Recognition: A key theme of research

Anion sensing/recognition is one area of research that has gained a considerable amount of interest over the past couple of decades.[1] Since anions find their specific roles in various supramolecular assemblies and myriad of biological processes, it is important to develop artificial receptors which can be used for sensing and even quantifying anions. From the basic element of life i.e. DNA (a polyanion) to the cofactors of various enzymes, anions are ubiquitous. Anion coordination chemistry took a huge leap forward since its birth in the 1960s and various acyclic, macrocyclic, and calixarene, metal complexes and nano-particle based moieties have proven to be excellent host materials for binding of anions, since then.[2] The need for developing novel anion sensors for monitoring the concentration in complicated media such as blood, cells, freshwater, soil, industrial effluents etc. is thus of paramount importance. Systematic designing of anion receptors is challenging because of the varied geometries of the anions, their less charge/size ratio and their sensitivity to different pH ranges, make anions more gruesome to be recognized selectively by a host material.[3] Therefore development of molecular systems where selectivity and sensitivity can be achieved for a particular target anion is desired. For an efficient chemical sensor for anion(s) extensive research has been focused on small single molecules that can suitably identify a single ion in a competitive environment in either a reversible/irreversible manner.[4] The foremost route of anion sensing involves the selective binding of the analyte to the host species resulting in changes in the photo-physical properties of the receptor molecules (**Scheme 1.1**). This primarily involves changes in the absorption or emission wavelengths, fluorescence lifetimes and the quantum yield of the host compound.[5] Quantitative analysis of such changes in turn may lead to determination of the concentration of a particular anion which is essential for real time applications. Selective sensing of a particular analyte is important as the receptor should change their optical properties in response to a sole analyte and therefore chances of false response in minimized.[6] Chromogenic anion sensors i.e. sensors which change their color upon binding/interacting with a particular anion play a pivotal role in terms of identification of such species by visual chroma.[7] Metal based chromogenic hosts involving transition metal ions/ lanthanides and/or π-conjugated coordinated ligands often change their color upon suitable interaction or binding of anion(s).[8] On the other hand, a reaction between the chromogenic host (often non-metal based) and the anion may also result in changes

in the optical properties of the host material and can be realized by visual chroma. On the same line, a chemodosimetric (reaction based) approach of anion sensing can pave way for the fabrication of a suitable sensor with greater selectivity and accuracy.[9] For the design of the perfect host material for sensing of anion it should fulfill the following criteria, a) they should have specific recognition sites for the incoming anions, b) should sense with high degree of selectivity and sensitivity and c) should be thermo-chemically stable for practical applications. Quest for new materials which can fulfill these conditions is the state-of-art and researchers devote significant emphasis on this key theme of research.[10]

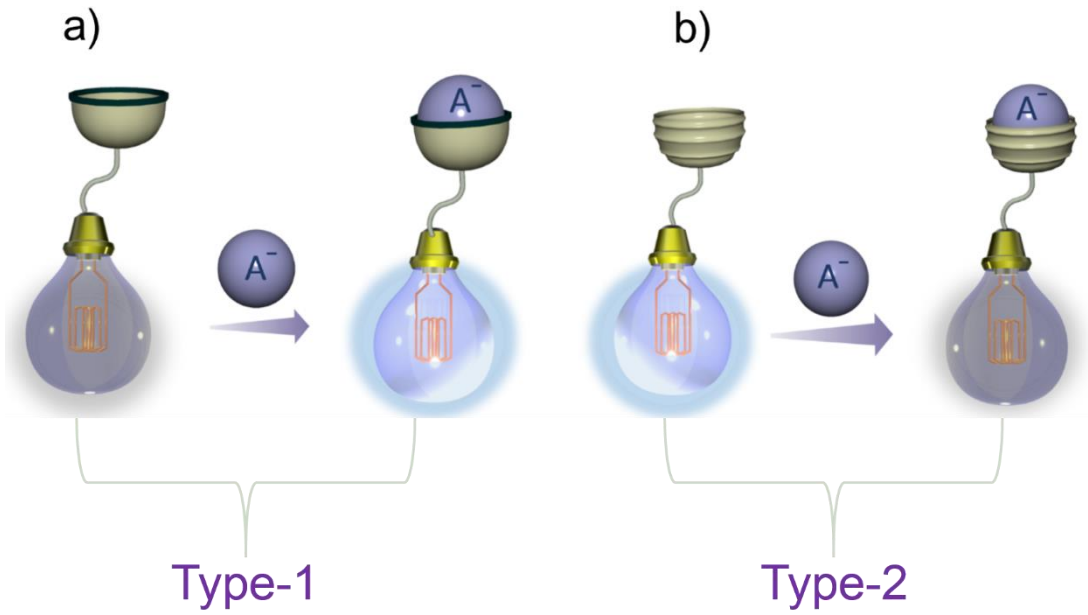

Scheme 1.1*: Schematic overview of optical changes in the receptor after binding to the anions.*

1.2. Metal-organic Frameworks (MOFs): New age smart chemical sensors

Metal-organic frameworks (MOFs) or porous coordination polymers (PCPs) have emerged as one of the most important class of materials simply because of their plethoric applications in the fields of gas storage, separation, catalysis, drug delivery, sensing, conduction, ion-exchange, polymerization, photonics etc.[11] Build from an organic linker and metal node or clusters (**Scheme 1.2**), MOFs give rise to a wide variety of architectures which range from one-dimensional coordination polymers (CPs) to three dimensional (3D) PCPs. The large repertoire

of organic struts available in nature allows for tailor-made syntheses of MOFs which could be used for targeted applications making them one of the most sought materials for chemists and

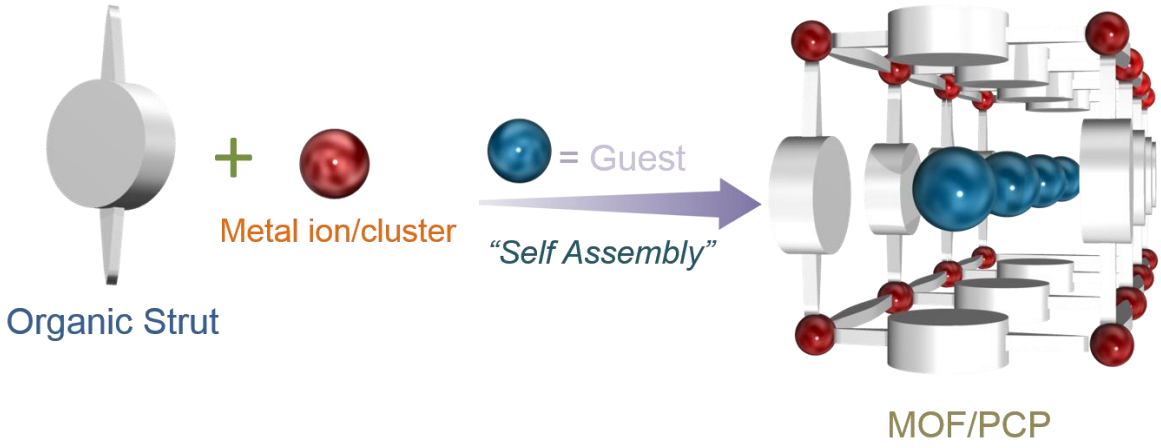

***Scheme 1.2**: Schematic representation of the formation of MOF/PCP via self-assembly process.*

material chemists. The pore structure and shape can be tuned in view of a specific property allowing fabrication of rationally designed MOFs and thus making these materials as an exclusive class of materials which has opened a new domain in the field of research and received huge impetus since the late 90s.[12] Given the wide variety of organic linkers available and the choice of metal centers, the scope of tunability in these ordered architectures are plenty and this allow

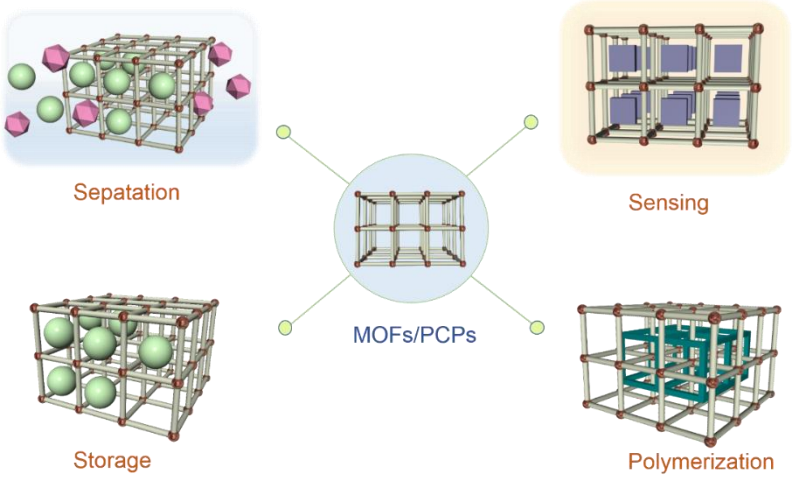

***Scheme 1.3**: Some of the key applications related to MOFs/PCPs known in literature.*

Specific functionalities resulting in diversified applications (**Scheme 1.3**). Also, the suitable incorporation of the signal transduction units inside the MOFs can induce specific changes in the optical signals in response to a particular stimuli.[13] These signal output can be monitored by specific techniques like UV-Vis spectroscopy, fluorescence spectroscopy, localized surface plasmon resonance (LSPR), impedance spectroscopy, cyclic voltammetry, interferometry etc.[14] The extensive catalogue of π-electron rich organic linkers and the wide variety of metal centers (either d-block/f-block) available allow ample scope of constructing luminescent MOFs which can behave differentially to the incoming guest molecules.[15] MOFs sets apart as an efficient class of chemical sensors mostly because of the high degree of selectivity which depends on a number of factors such as a) molecular sieving effect, b) specific interactions like H-bonding, π-π stacking etc., c) specific reactions inside the nano-porous channels of the MOF with the analyte and d) electrostatic interactions of the framework with the incoming guest molecules.[16] In addition, considering the high thermal stability and the possibility of reusability of these type of architectures, MOFs can be fabricated in thin films and selective membranes and thus could lead way to the development of new age smart chemical sensors.

1.3. Choice of MOFs for sensing applications

An important aspect of achieving the sensing applications in MOFs depends of the judicious choice of the building units for the construction of the same. The available metal nodes and numerous number of organic ligands along with combinatorial methods and changes in the reaction parameters can yield almost infinite MOF structures. Also, since the wide library of the MOFs already reported in literature (**Figure 1.1**), a proper screening according to the specific requirements by computation methods or by using Cambridge Crystallographic Data Centre (CCDC), one can even hypothesize the performance of MOFs for sensing of small molecules or even separation of gas molecules. For a MOF to be a perfect material for chemical sensor it has to fulfill the following criteria:

a) It should be luminescent to induce the specific optical signal readout.
b) It should be sufficiently porous for suitable host-guest interactions.
c) Should possess recognition sites for interaction with the incoming analyte molecule.
d) It should be sensitive to the stimuli in the micro-environment.

The performance of the MOF as a sensory material is directly proportional to the concentration of the analyte molecule which can diffuse into the pores (pre-concentration) of the MOF framework and thereby leading to suitable signal. This in turn defines the kinetics of and thermodynamics of the sensing phenomenon. Additionally, presence of secondary functional groups can improve the selectivity factor for enhanced performance. Since the vibrational and the rotational degrees of freedom of the coordinated ligand is much restricted after the formation of the MOF architecture, the MOF shows improved fluorescence properties as compared to the

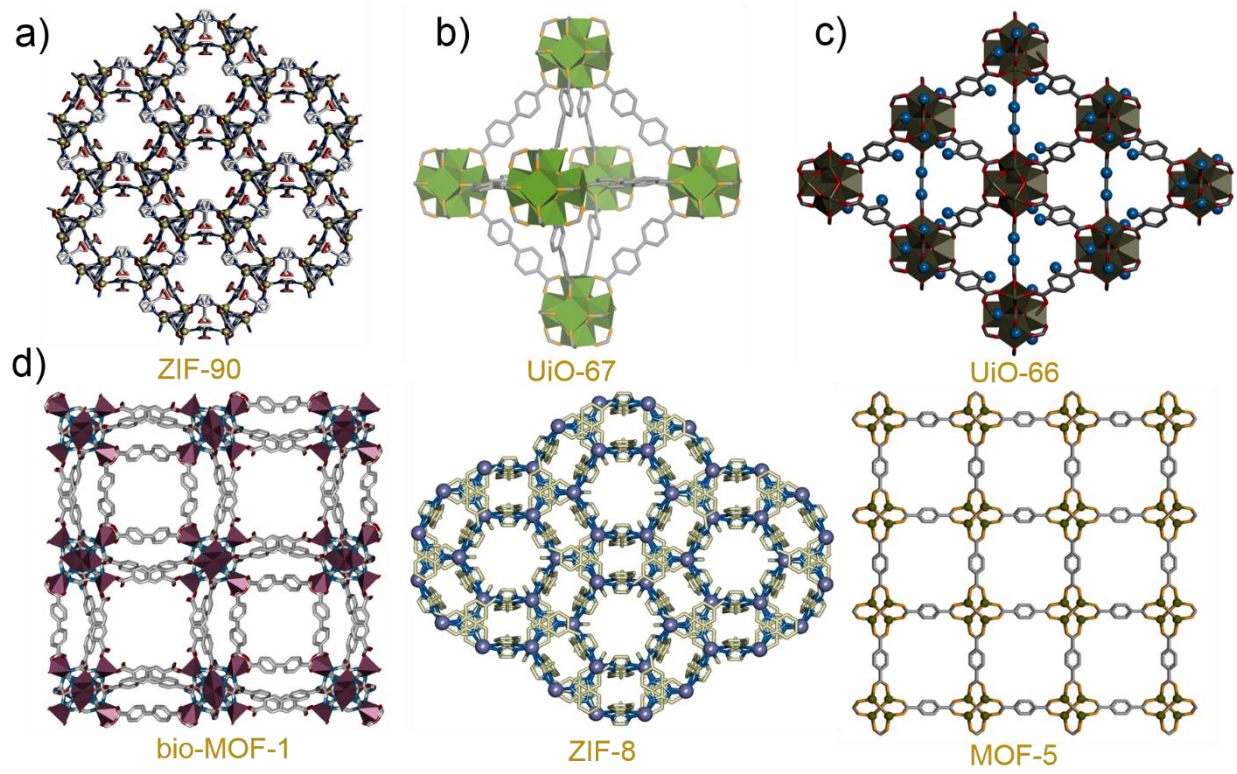

***Figure 1.1**: Representative examples of porous MOFs known for their sensory applications.*[11e-i]

free ligand itself.[17] Also the crystalline nature of the MOFs is essential for the molecular level insight to the sensing mechanism which is also a key advantage that these ordered architecture possesses.[18]

1.4. MOFs as an advanced class of materials for anion sensing applications

The wide choice of metal and ligands used in the synthesis of MOFs bestow ample opportunities to modulate the opto-electronic properties of such porous networked structures. Porous frameworks by design permit the encapsulation of anionic receptors and thereby make it feasible to investigate non-covalent interactions like anion-pi, in confined environments. Most of the MOFs reported till date have utilized the N-H and O-H units of the organic ligand for sensing/recognition of anions.[19] MOFs having luminescence accessory can, therefore, be used as probes for detection of non-polarized molecules upon their interaction with the host framework through physical adsorption or non-covalent interactions. One of the best candidates that manifest the anion recognition/sensing applications are the cationic frameworks where the cationic nature of the backbone results in the necessity of anions (either free or weakly coordinated to the metal center) to neutralize the charge in order to maintain the electrical neutrality.[20] The ions inside such polarized MOFs are often exchanged with other exogenous ions resulting in variable interactions with the framework thus resulting in either selective or multiple anion sensing. The role of metal ions/clusters and the choice of ligands are very important to develop ionicity in a MOF, which will be discussed in the subsequent sections of the thesis. Also, because of charge-induced dipoles created in such a polarized MOF, specific applications which are characteristic of such an ionic framework result, which may be otherwise difficult to obtain in a neutral MOF.[21] Neutral MOFs have also shown to exhibit anion sensing applications by virtue of their specific recognition sites and anion responsive metal centers which result in signal transduction for sensing of anionic species. In one of an interesting report by Chen *et al*. a MOF based on Tb^{3+} and benzene-1,3,5-tricarboxylate resulted in the formation of Tb(BTC)·G (MOF-76) which upon evacuation resulted in the selective sensing of F^- anions.[22] The F^- incorporated MOF, i.e. MOF-76b showed a very high enhancement of photoluminescence intensity due to H-bonding to the MeOH molecules to the F^- ions. The terminal solvent molecules play a crucial role in determining the selectivity and therefore this worked proved that solvent molecules are an important parameter in determining the sensing of anions by MOFs. In an another report by Li and co-workers a tetrazole based ligand was utilized to fabricate a MOF with molecular formula $\{[Cd(\mu_2\text{-}Cl)(\mu_4\text{-}5MT)]_n$ (5MT = 5-methyl-1H-

tetrazole)}for selective recognition of NO_2^- anion due to pore surface and pore size characteristics of the MOF.[23]

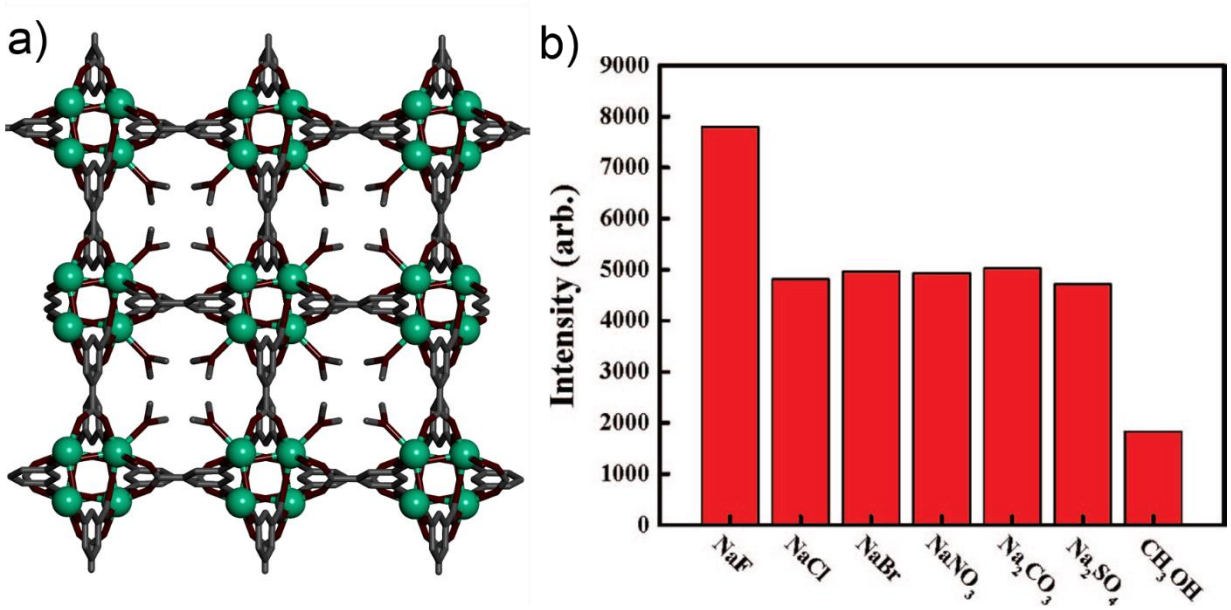

***Figure 1.2**: a) View of the MOF-76b along c axis and b) Optical response of MOF-76b in presence of various anions. (Reproduced with permission from reference 22)*

1.5. Cationic MOFs: Design and synthesis

A cationic MOF is mainly comprised of positively charged frame-work with extra counter anions to balance the charge of the overall framework.[24] The extra anions often lie free in the porous channels of the framework or often are weakly coordinated to the metal center via weak electrostatic attraction. The routes for rational design of a cationic framework are summarized in **Scheme 1.4**. The first method involves the usage of a neutral ligand mostly nitrogen donor ligands (N-donor ligands) for the construction of a MOF resulting in the necessity of extra anions to suffice the net charge of the framework.[25] The most commonly used nitrogen based ligand used for syntheses of cationic MOF is undoubtedly 4-4'-bipyridine (bpy).[26] Pyridyl functionalized ligands therefore represent the most easy and comprehensively used ligand as a part of a strategy to build up a cationic MOF. Robson and co-workers in the early 90's reported the first anion exchange in a Zn based framework in which BF_4^- anions were exchanged with

PF_6^- anions.[24b] In another early report by Yaghi and his group where he demonstrated the construction of a MOF by using bpy ligands to build an interpenetrated 3D MOF in which the free nitrate anions reside in the porous channels of the framework.[26b] Several cationic MOFs have been reported which reports the role of the neutral ligands in the construction of a cationic MOF. Groy and his group workers also synthesized a non-interpenetrated railroad like network consisting of Ni^{2+}cations and bpy ligands in which the free ClO_4^- anions reside in the pores of the framework.[27] Kim and his group members prepared a 2D MOF [28] in which he prepared the N-donor ligand by threading CB[6] with N,N'-bis(3-pyridylmethyl)-1,5-diaminopentane dihydronitrate and thereafter conjunction with $Cu(NO_3)_2$ resulted in the formation of a cationic framework in which the free nitrate anions were post-synthetically exchanged with other anions to study the anion exchange behavior. Rheingold and his group came up with 1,3-bis(4-pyridyl)propane (bpp) ligand to build up two novel cationic MOF with molecular formula [Ag(bpp)]$ClO_4$and [Ag(bpp)]PF_6 in which the anions are free and was studied for further anion exchange behavior.[29] In 2003, Tang reported a series of cationic frame-works using N-pyridyl ligands like 1,3,5-tris(1-imidazolyl)benzene and 1,3-bis(1-imidazolyl)-5-(imidazol-1-ylmethyl)benzene.[30] He explained that the structures obtained using these tripodal ligands were mainly governed by the nature of organic linkers used in the syntheses of MOFs. He also remarked that the counter anions used in the synthetic scheme are responsible in the formation of the frameworks. Lee and co-workers used tripyridyl tri-amides with C_3-symmetry for the construction of 3D hydrogen bonded cationic frameworks.[31] Anion exchange was also studied with these cationic frameworks which exhibited luminescent properties at room temperature. Another set of ligands that are widely used in the construction of cationic frameworks involves the use of cationic imidazolium group in the ligand backbone. This

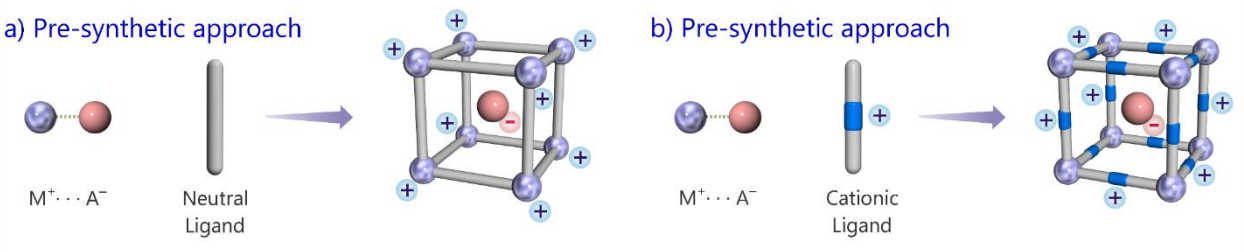

***Scheme 1.4**: Two widely used pre-synthetic approaches for construction of cationic MOFs.*

strategy has been utilized by several groups to generate positively charged framework. In an one such example Hupp and co-workers utilized 1,3-bis(2,6-dimethyl-3,5-dicarboxylphenyl)imidazolium ligand to synthesize cationic framework with molecular formula $[Cu_2(C_{23}H_{17}N_2O_4)\text{-}(DMSO)_2][Cl]$.[32] The structure was made up of paddlewheel $Cu_2(CO_2)_4$clusters and four imidazolium ligands. Wu *et al*. mixed 1,1-methylenebis-(3-(4-carboxyphenyl)-imidazol-3-ium) with $CuCl_2$ to get a paddle wheel structure which contained a net positive charge and therefore requiring the presence of free nitrate anions. Some other examples include the utilization of pyrimidine-2-carboxylate acid to build up a novel cationic frame-work in which free hydroxide anions were present to balance the net charge.

Post synthetically a cationic MOF can be synthesized as explained by Kim and co-workers. A carboxylate based MOF with molecular formula $[Zn_3(\mu_3\text{-}O)(1\text{-}H)_6]\cdot 2H_3O\cdot 12H_2O$ (d-POST-1) was synthesized in which the free pyridyl nitrogen atom were aligned inside the pores of the framework.[33] When a suspension of POST-1 in N,N'-dimethyl formamide (DMF) with stirred in excess iodomethane at room temperature for 2 h results in the formation of the N-alkylated product resulting in the formation of a cationic framework and thereby the free iodide ions were found as the charge balancing anions. Bu *et al*. demonstrated a general method to create a cationic MOF from a neutral framework.[34] In this pioneering work they demonstrated that the differential affinity between distinct metal ions such as Al^{3+} with framework anionic species could strip the anions that are coordinated to the metal center such as the F^- ions in Cr-MIL. $AlCl_3$was used to carry out this post synthetic modification in which the F^- were extracted and subsequently the Cl^- ions were left free inside the pores of the framework allowing facile exchange with other anions like OH^- ions. The major routes for the construction of cationic frameworks by post-synthetic approaches are shown in **Scheme 1.5**.

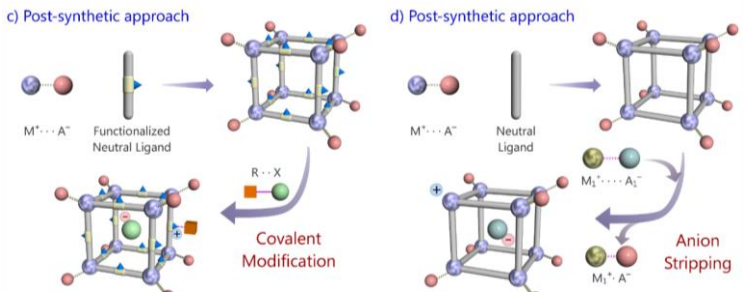

Scheme 1.5*: Two widely used post-synthetic approaches for construction of cationic MOFs.*

1.6. Sensing of anions by cationic MOFs: Luminescence modulation and colorimetric approach

1.6.1. Luminescence based approach for sensing anions:

Among most sensory techniques, photoluminescence has been one of the most sought after owing to sophistication, ease of sampling, high sensitivity and prompt response.[35] In the MOF regime, it has been used kindly owing to ample opportunities of tuning the different metal-ligand based emissions to suit the desired electronic band-gaps. Additionally the wide choices of building units makes MOFs as appropriate candidates for luminescence based transducers for understanding molecular behavior in confined nanospaces.[36] The features of photoluminescence based techniques have been exploited recently in cationic frameworks as a probe for anion capture/exchange processes. Some of them have been discussed herewith. In an early work of exploring luminescence features in a cationic framework, Tzeng and co-workers synthesized a Zn(II) centered amide based cationic coordination polymer.[37] Upon heating the two coordinated water molecules were lost allowing the anions to interact with the metal directly. Phase transformations were observed from a neutral framework bearing coordinated perchlorate ions to a cationic framework upon exposure to moisture. Control single crystal experiments were performed in presence of dry solvents was performed to prove this transformation. Solid state luminescence experiments were performed to monitor this phase transformation (Fig. 24). As a continuation, Oliver and co-workers prepared 3 distinct Cd (II) MOFs from a mixture of anionic and neutral ligands under hydrothermal conditions.[38] Owing to different molar ratios of the reactants 3 dissimilar structures were achieved, with two of them being cationic in nature. The authors attempted to exchange the free organosulfonate ions with nitrate (NO_3^-), permanganate (MnO_4^-), perchlorate (ClO_4^-) and perrhanate (ReO_4^-) anions but found that along with the electrostatic interactions, strong hydrogen bond interaction with the cationic framework precluded any exchange. The separate character of the three compounds was reflected and studied via solid state luminescence measurements. Previously, in a comprehensive work Ghosh and co-workers have shown the utility of a luminescent cationic framework as a probe to sense different anions by a detectable fluorescence signal. A dynamic 1D porous coordination polymer ($1\supset NO_3^-$) constructed from Zn(II) cations and a neutral N-donor ligand had free nitrate anions

in its channels and methanol molecules coordinated to the metal center.[39] Upon air-drying these coordinated solvent molecules were substituted with moisture and correspondingly structural changes were observed. This flexible behavior of the MOF was extended to its anion exchange studies by replacing the NO_3^- anions with guest anions of different coordinating tendencies like N_3^-, $N(CN)_2^-$, SCN^-, ClO_4^- .The compound underwent significant changes in its structure which were attributed to the varied size and geometry of the replacing anion. Competitive ion exchange experiments were performed to understand the affinity order of the chosen ions. The notable differences in the solid state luminescence of the ligand and the MOF propelled them to examine this as the pathway to recognize the anion exchange process (**Figure 1.3**). Thereby, the solid-state luminescence spectra of all the anion exchanged phases were recorded and a remarkable

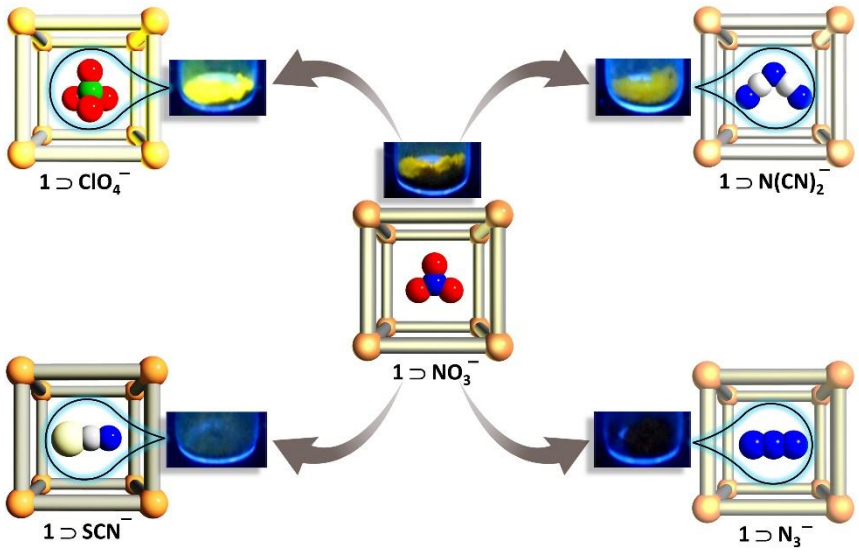

***Figure 1.3**: Tunable luminescence behavior w.r.t different anions in a flexible cationic framework. (Reproduced with permission from reference 39)*

variation was observed. The differences in the observed intensities were correlated to the coordinating attributes of the anions and their interactions with the metal center affecting the inter-ligand transitions. This report demonstrated anion-responsive luminescence in a MOF for the first occasion and serves as a significant juncture in the development of MOF based ion sensors.

1.6.1. Colorimetric anion sensors:

The process of ion recognition can be significantly simpler if the host–guest information is transduced via visual chroma.[40] Cationic networks bearing colored metal ions or photochemically active ligands can be sought as appropriate candidates for such applications. Anion exchange has been recently explored in a few cationic MOFs, but reports of MOFs acting as naked eye sensors have been rare.[41] This part covers the literature reviews of cationic MOFs exhibiting visual post-synthetic anion exchanging changes. In a pioneering work by Dong et al., [42] the efficacy of cationic MOFs as anion receptors in a selective and detectable manner was explored. The authors synthesized a 2D MOF centered on Cu (II) nodes and pillared on a neutral fluorene based ligand which encapsulated nitrate anions in its voids. The free anions were substituted with foreign ions like F^-, Cl^-, Br^-, I^-, SCN^- and N_3^-, the progress of which was characterized by IR, XPS experiments. The authors observed drastic color change (from blue for the pristine sample to different shades of green and brown) with every exchanged anion without perturbing the structural integrity in all the cases. Selectivity experiments were performed to elucidate the ability of the framework to separate anions from a mixture and the results have been attributed to the geometry and coordination affinity of the chosen anions. Zhang and co-workers explored photochromism in a viologen based coordination polymer.[43] A Cd based 1D helical CP was synthesized bearing free perchlorate anions in its coordination space. The authors successfully replaced ClO_4^-ions with foreign anions like I^-, Cl^-, $N_3^-$and SCN^- in a Single crystal–Single crystal (SC-SC) manner in a short time. The initially photochromically inactive compound was found to be photo chemically active after the exchange process, owing to the structural changes occurring upon anion exchange. The different charge transfer (CT) complexes between the electron accepting viologen moieties and pseudohalide ions have been attributed to the multivariate coloration to the various exchanged phases. Upon irradiation, the different phases were found to exhibit different hues originating due to the differential radical generating reactions and this process was found to be reversible. On similar lines to the report by Dong *et al*., Bu and co-workers synthesized a cationic framework bearing free nitrate ions in its channels and utilized the same as a colorimetric probe for several guest anions.[44] A 4-fold novel topological network was synthesized by the in situ reduction of Cu (II) to Cu (I) under crystallization conditions. The occluded methanol molecules were replaced with water molecules

on heating and the resultant phase was found to be air and moisture stable. On exchanging the nitrate ions with different anions (F^-, Cl^-, Br^-, I^-, N_3^-, SCN^-, CO_3^{2-}) in aqueous phase, remarkable visual changes to the color of the parent compound were observed (**Figure 1.4**). Exploiting the luminescence feature bestowed by the metal center, the authors also recorded varying intensities of the different phases by the solid state luminescence experiments.

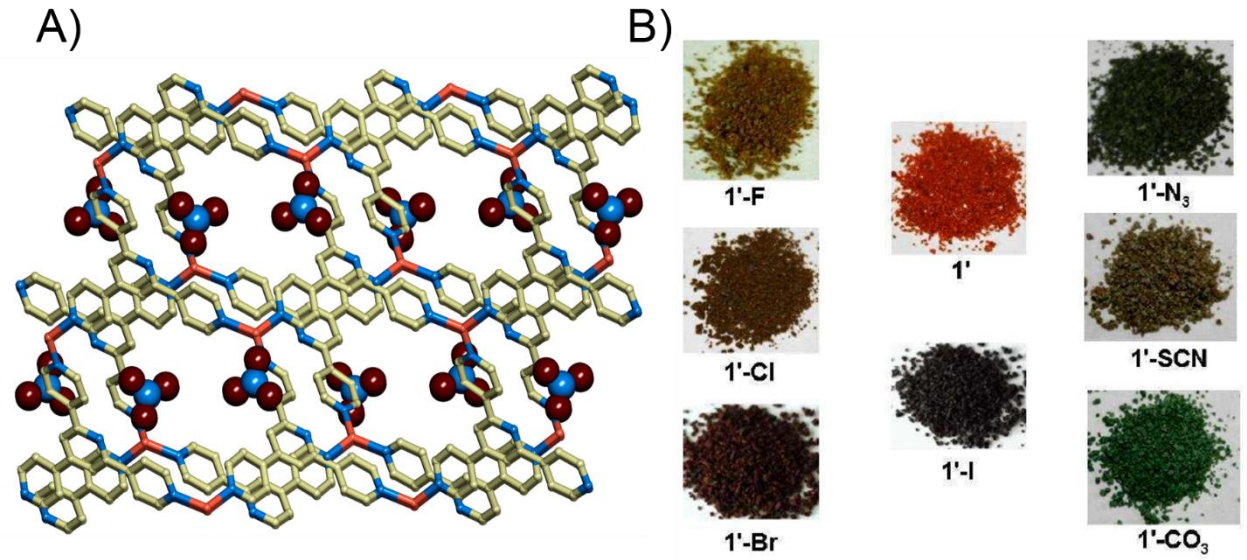

***Figure 1.4**: a) Cu(I) based four fold helical structure containing NO_3^- anions and b) Visual colorimetric changes upon exchanging with different anions. (Reproduced with permission from reference 44)*

1.7. Capture and sensing of toxic anions by cationic MOFs

Heavy oxo-anions like ReO_4^-, CrO_4^{2-}, TcO_4^-, $Cr_2O_7^{2-}$, MnO_4–, AsO_4^{3-}, SeO_3^{2-}, etc. are known to cause serious threats to human health and environment.[45] The U.S. Environmental Protection Agency has listed these metal based oxo-anions in the list of top priority pollutants occurring in nature. The commonly used techniques for separation of such pollutants from waste water involve ion exchange, photocatalytic oxidation and adsorption. However, most of these methods are either cost effective or have accessibility issues. The commonly used ion exchangers are

mainly divided into (i) organic based polymer resins or (ii) inorganic based zeolites or layered double hydroxides (LDHs). But the usage for widespread applications is limited because the poor thermal and chemical stability of the organic polymers and the lack of recyclability and low selectivity for the anions restricts the use of the inorganic based materials. Cationic MOFs play a crucial role in this respect because the readily exchangeable anions which remain free inside the pore can be replaced by these heavy pollutants.[46]

Oilver et al. reported the application of $[Ag_2(4,4'\text{-bipy})_2(O_3SCH_2CH_2SO_3)\cdot 4H_2O]$ (SLUG-21) for the treatment of radioactive waste like permanganate and perrhenate.[47] The cationic unit of Ag-bipy chains, charge balanced by interstitial 1,2-ethanedisulfonate (EDS) anions. Anion exchange performed with aqueous solutions of MnO_4^- showed a trapping of $MnO4^-$ and optical images taken at different time intervals as high as 94% after 48 has confirmed by UV–vis spectroscopy with an adsorption capacity of 283 mg/g which is much higher as compared to the uptake capacity of LDHs (10/150 mg/g). The high performance of SLUG-21 in trapping MnO_4^- was attributed by the authors to the stability of these anions inside the cationic framework upon structural transformation. The extra stability gained upon replacement of the EDS anions by these oxo-anions is the governing factor for such thermodynamic stability. Exchange capacity of SLUG-21 for ReO_4^- was also studied by the authors which revealed an adsorption capacity of high 602 mg/g based on the molecular weight of ReO_4^-. The uncalcined and calcined LDHs are only 37 and 125 mg/g which is much lower than SLUG-21. Thus the authors overcame the problem of low uptake capacity by the hydrotalcites for this two oxo-anions. The exchange rate and capacity of SLUG-21 for other problematic oxo-anions as calculated by the authors follows the order $MnO4^-$> ReO_4^-> ClO_4^-> CrO_4^{2-}> NO_3^-> CO_3^{2-}. In another report by Wang and co-workers[48] a new $[Ag_2\text{-}(btr)_2]\cdot 2ClO_4\cdot 3H_2O$ ($ABT\cdot 2ClO_4$; (btr=4,4'-bis(1,2,4-triazole))which shows capture and separation of $Cr_2O_7^{2-}$in water. This unique MOF composed of distorted octahedral and tetrahedral cages showed contains ClO_4^- anions in the porous cavities which were readily exchanged by dichromate anions. The adsorption capacity of $ABT\cdot 2ClO_4$ for $Cr_2O_7^{2-}$ was calculated to be 0.73 mol/mol after 48 h which precedes the only known lead fluoride material for exchanging dichromate anions. The effect of anion exchange on luminescence was observed as almost complete luminescence quenching was observed after anion exchange detectable even by naked eye. The reason given by the authors was that due to the electron-transfer transitions of

$Cr_2O_7^{2-}$which in turn reduces the energy transfer from the btr ligand to Ag^+ ions by ligand-to-metal charge transfer. A more recent report by Zhang et al. two cationic MOFs, $[Zn_2(Tipa)_2(OH)]\cdot 3NO_3\cdot 12H_2O]$ (FIR-53) and $[Zn(Tipa)]\cdot 2NO_3\cdot DMF\cdot 4H_2O]$ (FIR-54) were synthesized and the exogenous anions, i.e. OH^- and NO_3^- were post synthetically exchanged with $Cr_2O_7^{2-}$.[49] Because of the ease of diffusion of the dichromate anions in FIR-54 showed a high adsorption capacity of 100 mg/g. Both these two compounds trapped the

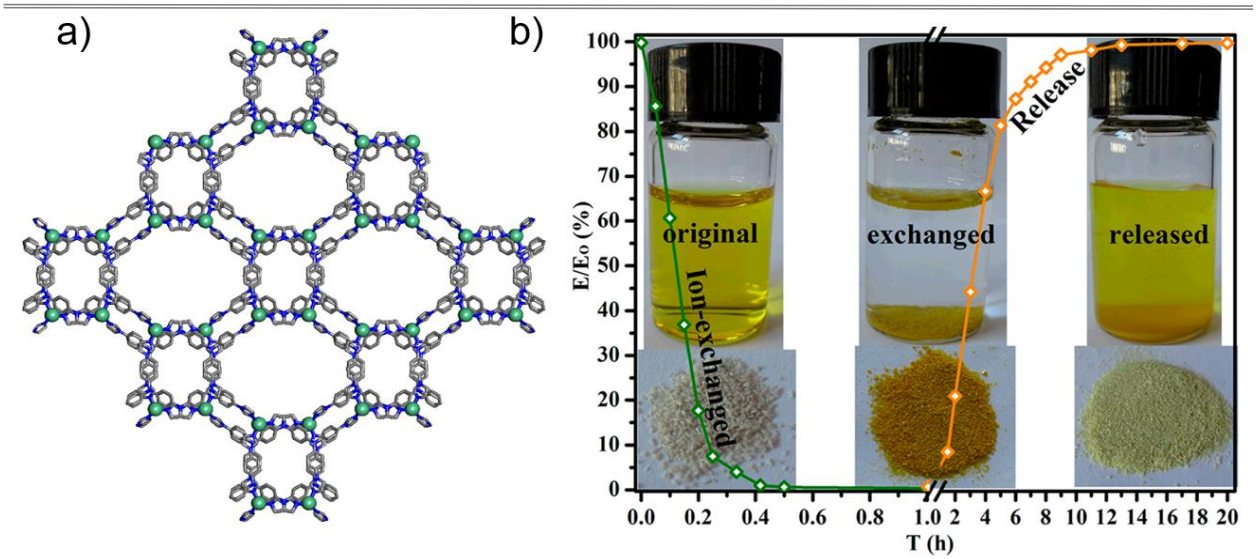

***Figure 1.5**: a) Porous structure of FIR-53 and b) Reversible trapping and release of $Cr_2O_7^{2-}$by by FIR-53. (Reproduced with permission from reference 49)*

incoming anion by SC–SC transformation. In particular, FIR-53 showed unprecedented reversibility behavior without losing its uptake capacity. Zhao et al. synthesized an indium trimer-based cationic framework which could be used as an ion exchange based platform for separation purposes. Various long chain anionic organic dyes like OG_2^- which are otherwise difficult to separate by size exclusion effect were separated by the cation MOF. Moreover molecules within the range ~100 Da < Mw< 1000 Da could be separated depending on the charge and can be used as an suitable material for anion encapsulation and separation. Chen and co-workers fabricated an aminated polymer inside a MOF for facile reversible exchange of $Au(CN)_2^-$ ions in trace amount.[50] Polyvinyl benzyl trimethyl ammonium hydroxide (PVBTAH) captured in ZIF-8 for the very first time demonstrated superior ion exchange dynamics as

compared to the conventional known ion exchange resins like Amberlyst-A26 ion-exchange resin.

1.8. Post-synthetic modification (PSM): An important tool for anion sensing

Post-synthetic modification (PSM) has for long been one of the versatile methods for incorporating the suitable functionality in a MOF. More often than not researchers have employed PSM to achieve diverse applications in the field of storage, separation, catalysis, proton conduction etc.[51] The method of post-functionalization can be a key recognize a particular species due to specific interactions (covalent/non-covalent) with the functionalized MOF (**Scheme 1.6**). Post-functionalization can be achieved in heterogeneous medium and a chemically robust MOF is best suited for it. Ligand functionalization by PSM is one of the widely practiced methods to graft a recognition site in the MOF which in turn can give variable response w.r.t the incoming guest molecules. Since the ordered periodical arrangement of ligands

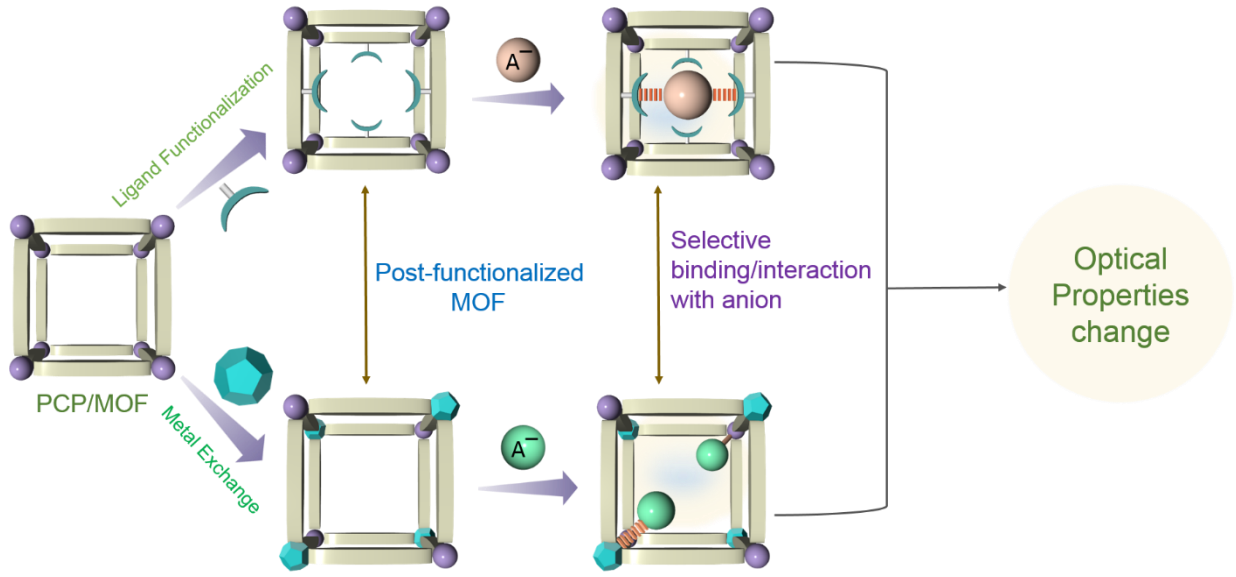

***Scheme 1.6**: Dual PSM strategy for recognition of anions by changes in optical properties.*

play a crucial role in generating a signal output, PSM strategy promises to be one of the suitable techniques to sense an anionic species. Zhang *et al.* fabricated a cationic MOF (ZJU-101) by post

synthetic modification of MOF-867 in which the pyridyl sites were methylated to form N^+–CH_3 units inside the MOF.[52] The free NO_3^- anions were then exchanged by hazardous $Cr_2O_7^{2-}$ anions from water resulting in changes in optical properties. Post-synthetic metalation can also be effective in selective recognition of a particular anion as exhibited by in a recent report by Yan and co-workers. Their group synthesized a lanthanide doped MOF i.e. MIL-125(Ti)-AM-Eu which showed excellent photoluminescence response in presence of PO_4^{3-} anions.[53] Thus judicious strategy of PSM can lead towards development of new MOF based anion sensors with greater selectivity and sensitivity and can be an important tool for anion recognition in heterogeneous phase.

1.9. Application of MOFs for biological assay system

The quantitative and qualitative usage of MOFs for bio-sensing is an active field of research.[54] MOFs have shown tremendous promise in the field of bio-sensing because their structural flexibility, tuneable synthesis and in some cases their bio-compatible nature. The usage of MOFs for sensing of biologically relevant entities like DNA, ssDNA and dsDNA have shown the potential of MOFs to be used for bio-medical applications. For MOFs to be used for in vitro/in vivo sensing applications it must be a) bio-compatible in nature, b) must be non toxic towards cells, c) must be of required size (preferably in nanometric scale) for injection in the cells and b) must be stable at optimum biological conditions. For sensing phenomenon inside the cell lines, a turn on fluorescence output is always desired because in that case visualization and quantification becomes easy. Sensing of toxic anions inside the cells can lead to significant progress in the field of bio-sensing by MOFs and could pave way for designing novel hybridized materials in the field of therapeutics, bio-imaging, drug delivery etc.

1.10. Overview of the thesis:

In chapter 2, I have designed a cationic MOF based on a simple schieff base ligand and Zn^{2+} and the extra framework anions has been utilized for exchange with other foreign anions resulting in anion tunable luminescence modulation behavior.

In the next chapter, I have used a newly designed amide functionalized N-donor ligand with bichelating sites and in conjunction with Cu^{2+}, I have fabricated a one dimensional CP which underwent SC-SC transformation with a foreign anion resulting in visual colorimetric detection.

In 4th chapter, a porous MOF with functional sites has been utilized for PSM to incorporate specific functionalities to sense a toxic anion and this has been realized by fluorescence changes after binding of the anion.

In chapter 5, an anionic CP has been utilized for cationic exchange with a specific dye molecule which acts as sensory unit for CN^{-} anion and the MOF has been utilized as a reaction vessel to achieve detoxification of the same. The sensing properties were found to be effective even *in vitro* studies using human cell lines and the MOF could be recycled for further use also.

In Chapter 6, conclusions and future outlook of the thesis has been briefly discussed.

1.11. References:

1. a) Evans, N. H.; Beer, P. D. *Angew. Chem. Int. Ed.* **2014**, *53*, 11716; b) Wenzel, M.; Hiscock, J. R.; Gale, P. A. *Chem. Soc. Rev.* **2012**, *41*, 480; c) Gale, P. A.; Caltagirone, C. *Chem. Soc. Rev.* **2015**, DOI: 10.1039/C4CS00179F; d) Gunnlaugsson, T.; Glynn, M.; Tocci, G. M.; Kruger, P. E.; Pfeffer, F. M. *Coord. Chem. Rev.* **2006**, *250*, 3094.

2. a) dos Santos, C. M. G.; Harte, A. J.; Quinn, S. J.; Gunnlaugsson, T. *Coord. Chem. Rev.* **2008**, *252*, 2512; (b) Santos-Figueroa, L. E.; Moragues, M. E.; Climent, E.; Agostini, A.; Martıńez-Mañez, R.; Sancenon, F. *Chem. Soc. Rev.* **2013**, *42*, 3489; c) Shang, L.; Jin, L.; Dong, S. *Chem. Commun.* **2009**, *43*, 3077.

3. a) Vance, D.H.; Czamik, A.W. *J. Am. Chem. Soc.* **1994**, *116*, 9397; b) Shannon, R. D.; *Acta Crystallogr. Sect. A.* **1976**, *32*, 751.

4. a) Hu, X.; Huang, J.; Zhang, W.; Li, M.; Tao, C.; Li, G. *Adv. Mater.* **2008**, *20*, 4074−4078; b) b) Tian, D.; Qian, Z.; Xia, Y.; Zhu, C. *Langmuir* **2012**, *28*, 3945; c) Lin, Q.; Zhu, X.; Fu, Y. P.; Zhang, Y. M.; Fang, R.; Yang, L. Z.; Wei, T. B. *Soft Mat.* **2014**, *10*, 5715.

5. a) Xu, Z.; Chen, X.; Kim, H. N.; Yoon, J. *Chem. Soc. Rev.* **2010**, *39*, 127−137; b) Wang, F.; Wang, L.; Chen, X.; Yoon, J. *Chem. Soc. Rev.* **2014**, *43*, 4312−4324; c) d) Yamaguchi, S.; Akiyama, S.; Tamao, K. *J. Am. Chem. Soc.* **2000**, *122*, 6793.

6. a) Guha, S.; Saha, S. *J. Am. Chem. Soc.* **2010**, *132*, 17674−17677; b) Fillaut, J.-L.; Andriès, J.; Perruchon, J.; Desvergne, J.-P.; Toupet, L.; Fadel, L.; Zouchoune, B.; Saillard, J.-Y. *Inorg. Chem.* **2007**, *46*, 5922; c) Hudnall, T. W.; Chiu, C.-W.; Gabbaı¨ F. P. *Acc. Chem. Res.* **2009**, *42*, 388.

7. a) Bhardwaj, V. K.; Hundal, M. S.; Hundal, G. A.*Tetrahedron*, **2009**, *65*, 8556; b) Gotor, R.; Costero, A. M.; Gil, S.; Parra, M.; Martínez-Máñez, R.; Sancenón, F.; Gaviña, P. *Chem. Commun*. **2013**, *49*, 5669; c) Descalzo, A. B.; Rurack, K.; Weisshoff, H.; Martínez-Máñez, R.; Marcos, M. D.; Amorós, P.; Hoffmann, K.; Soto, J. *J. Am. Chem. Soc*. **2005**, *127*, 184.

8. a) Adarsh, N. N.; Kumar, D. K.; Dastidar, P. *CrystEngComm*. **2008**, *10*, 1565; b) Zhou, L. L.; Sun, H.; Li, H. P.; Wang, H.; Zhang, X. H.; Wu, S. K.; Lee, S. T. *Org. Lett*. **2004**, *6*, 1071; c) Zapata, F.; Caballero, A.; Tárraga, A.; Molina, P. *J. Org. Chem*. **2010**, *75*, 162.

9. a) Li, B.; Zhang, C.; Liu, C.; Chen, J.; Wang, X.; Liu, Z.; Yi, F. *RSC Adv*. **2014**, *4*, 46016; b) Kim, S. Y.; Hong, J.-I. *Org. Lett*. **2007**, *9*, 3109; c) Zhang, X.; Li, C.; Cheng, X.; Wang, X.; Zhang, B. *Sens. Actuators, B*: *Chem*. **2008**, *129*, 152.

10. a) Wolfe-Simon, F.; Blum, J. S.; Kulp, T. R.; Gordon, G. W.; Hoeft, S. E.; Pett-Ridge, J.; Stolz, J. F.; Webb, S. M.; Weber, P. K.; Davies P. C. W. *Science*, **2011**, *332*, 1163; b) Gale, P. A.; Busschaert, N.; Haynes, C. J. E.; Karagiannidisa, L. E.; Kirbya, I. L. *Chem. Soc. Rev*., **2014**, *43*, 205.

11. a) Zhou, H. C; Long, J. R; Yaghi, O. M.; *Chem. Rev*. **2012**, *112*, 673 ; b) Horcajada, P.; Gref, C.; Baati, T.; Allan, P. K.; Maurin, G.; Couvreur, P.; Ferey, G.; Morris, R. E.; Serre, C.; *Chem. Rev*. **2012**, *112*, 1232; c) Vittal, J. J.; Coord. *Chem. Re*v. **2007**, *251*, 1781; d) Keeffe, M. O.; Yaghi, O. M., *Chem. Rev*. **2012**, *112*, 67.; d) Li, H.; Eddaoudi, M.; O'Keeffe, M.; Yaghi, O. M. *Nature*. **1999**, *402*, 276; e) Cavka, J. H.; Jakobsen, S.; Olsbye, U.; Guillou, N.; Lamberti, C.; Bordiga, S.; Lillerud, K. P. *J. Am. Chem. Soc*. **2008**, *130*, 13850; f) An, J.; Rosi, N. L. *J. Am. Chem. Soc*., **2010**, *132*, 5578; g) Morris,W.; Doonan, C. J.; Furukawa, H; Banerjee, R.; Yaghi, O.M. *J. Am. Chem. Soc*. **2008**, *130*, 12626; h) Banerjee, R.; Phan, A.; Wang, B.; Knobler, C.; Furukawa, H.; O'Keeffe, M.; Yaghi, O. M. *Science* **2008**, *319*, 939; i) Kandiah, M.; Usseglio, S.; Svelle, S.; Olsbye, U.; Lillerud, K. P.; Tilset, M. *J. Mater. Chem*. **2010**, *20*, 9848−9851.

12. a) Yaghi, O. M.; Li, H. *J. Am. Chem. Soc*. **1995**, *117*, 10401; b) Yaghi, O. M.; Li, H. T. *J. Am. Chem. Soc.* **1996,** *118*, 295; c) Hoskins, B. F.; Robson, R. *J. Am. Chem. Soc*. **1990,** *112*, 1546.

13. a) Li, Y.; Zhang, S.; Song, D.; *Angew. Chem. Int. Ed*. **2013**, 43, 710; b) Lin, R.-B.; Liu, S.-Y.; Ye, J.W.; Li, X. Y.; Z. J.-P. *Adv. Sci*. **2016**, *3*, 1500434.

14. a) Busschaert, N.; Caltagirone, C.; Rossom, W. V.; Gale, P. A. *Chem. Rev*. **2015**, *115*, 8038.

15. a) Cui, Y.; Li, B.; He, H.; Zhou, W.; Chen, B.; Qian, G.; *Acc. Chem. Res*. **2016**, *49*, 483; b) Cui, Y.; Yue, Y.; Qian, G.; Chen, B. *Chem. Rev*. **2012**, *112*, 1126.

16. a) Xiong, W.W.; Athresh, E.U.; Ng, Y.T.; Deng, J. T.; Zhang, Q. *J. Am. Chem. Soc*. **2013**,*135*, 1256; b) Takashima, Y.; Martínez, V. M.; Furukawa, S.; Kondo, M.; Shimomura, S.; Uehara, H.; Nakahama, M.; Sugimoto, K.; Kitagawa, S. *Nat. Commun*. **2011**, *2*, 1.

17. a) Yu, J.; Cui, Y.; Xu, H.; Yang, Y.; Wang, Z.; Chen, B.; Qian, G.; *Nat. Commun*. **2013**, *4*, 2719; b) Xiong, W.W.; Zhang, G.; Zhang, Qi. *Inorg. Chem. Front*. **2014**, *1*, 292–301.

18. a) Farha, O.K.; Spokoyny, A.M.; Mulfort, K.L.; Hawthorne, M.F.; Mirkin, C.A.; Hupp, J.T. *J. Am. Chem. Soc*. **2007**, *129*, 12680; b) Procopio, E.Q.; Fukushima, T.; Barea, E.; Navarro, J.A.R.; Horike, S.; Kitagawa, S. *Chem. Eur. J*. **2012**, *18*, 13117.

19. Custelcean, R.; Moyer, B. A. *Eur. J. Inorg. Chem*. **2007**, *21*, 1321–1340

20. Wang, J.-C.; Liu, Q.-K.; Ma, J.-P.; Huang, F.; Dong, Y.-B. *Inorg. Chem*. **2014**, *53*, 10791.

21. An, J.; Shade, C.M.; Chengelis-Czegan, D.A.; Petoud, S.; Rosi, N. L. *J. Am. Chem. Soc*. **2011**, *133*, 1220.

22. Chen, B.; Wang, L. Zapata, F. Qian, G. L. E. B. *J. Am. Chem. Soc*. **2008**, *130*, 6718.

23. Qiu, Y.; Deng, H.; Mou, J.; Yang, S.; Zeller, M.; Batten, S. R.; Wue, H.; Li, J. *Chem. Commun*., **2009**, 5415.

24. a) Biradha, K.; Hongo, Y.; Fujita, M. *Angew. Chem. Int. Ed*. **2002**, *41*, 3395; b) Hoskins, B. F.; Robson, R. *J. Am. Chem. Soc.* **1990,** *112*, 1546.

25. Yang, Q.-Y.; Li, K.; Luo, J.; Pana, M.; Su, C.Y. *Chem. Commun*. **2011**, *47*, 4234.

26. a) Noro, S.; Kitagawa, S.; Kondo, M.; Seki, K. *Angew. Chem., Int. Ed*. **2000**, *39*, 2082; b) Yaghi, O. M.; Li, H. *J. Am. Chem. Soc.* **1995,** *117*, 10401; c) Noguchi, H.; Kondo, A.; Hattori, Y.; Kajiro, H.; Kanoh, H.; Kaneko, K.; *J. Phys. Chem. C*, **2007**, *111*, 248.

27. Yaghi, O.M.; Li, H.; Groy, T. L.; *Inorg. Chem.* **1997**, *36*, 4292.

28. Lee, E.; Kim, J.; Heo, J.; Whang, D.; Kim, K. *Angew. Chem. Int. Ed*. **2001**, *40*, 399.

29. Pan, L., Woodlock, E. B., Wang, X., Lam, K.-C.; Rheingold, A. L. *Chem. Commun*. **2001**, *32*, 1762.

30. Fan, J.; Gan, L.; Kawaguchi, H.; Sun, W.-Y.; Yu, K.-B.; Tang, W.-X. *Chem. Eur. J*, **2003**, *9*, 3965.

31. Tzeng, B.-C.; Chiu, T.-H.; Chen, B.-S.; Lee, G.-H. *Chem. Eur. J*. **2008**, *14*, 5237.

32. Lee, J.Y.; Roberts, J. M.; Farha, O. K.; Sarjeant, A. A.; Scheidt, K. A.; Hupp, J.T. *Inorg. Chem.* **2009**, *48*, 9971.

33. Seo, J. S.; Whang, D.; Lee, H.; Jun, S.I.; Oh, J.; Jeon, Y. J.; Kim, K. *Nature*, **2000**, *404*, 982.

34. Mao, C.; Kudla, R. A.; Zuo, F.; Zhao, X.; Mueller, L. J.; Bu, X.; Feng, P. *J. Am. Chem. Soc*. **2014**, *136*, 7579.

35. Xin, Y.; Wang, Q.; Liu, T.; Wang, L.; Li, J.; Fang, Y. *Lab Chip*. **2012,** *12*, 4821.

36. a) Wang, P.; Ma, J.-P.; Dong, Y.-B.; Huang, R.-Q.; *J. Am. Chem. Soc.* **2007**, *129*, 10620; b) Liu, Q.-K.; Ma, J.-P.; Dong, Y.-B. *J. Am. Chem. Soc.* **2010**, *132*, 7005.

37. Tzeng, B.-C.; Chang, T.-Yi.; Sheu, H.-S.; *Chem. Eur. J.* **2010**, *16*, 9990.

38. Fei, H.; Oliver, S.R.J. *Dalton Trans.* **2010**, *39*, 11193.

39. Manna, B.; Chaudhari, A. K.; Joarder, B.; Karmakar, A.; Ghosh, S. K. *Angew. Chem. Int. Ed.* **2013**, *52*, 998.

40. Chen, B.; Wang, L.; Zapata, F.; Qian, G.; Lobkovsky, E. B.; *J. Am. Chem. Soc*. **2008**, *130*, 6718–6719.

41. a) Yang, H.Y.; Li, L.K.; Wu, J.; Hou, H.W.; Xiao, B.; Fan, Y.T. *Chem. Eur. J*. **2009**, *15*, 4049; b) Yu, Y.; Zhang, X.-M.; Ma, J.-P.; Liu, Q.-K.; Wang, P.; Dong, Y.-B. *Chem. Commun.* **2014**, *50*, 1444.

42. Ma, J.-P.; Yu, Y.; Dong, Y.-B.; *Chem. Commun*. **2012**, *48*, 2946.

43. Sun, J.-K.; Wang, P.; Yao, Q.-X.; Chen, Y.-J.; Li, Z.-H.; Zhang, Y.-F.; Wu, L.-M.; Zhang, J. *J. Mater. Chem.* **2012**, *22*, 12212.

44. Chen, Y.-Q.; Li, G.-R.; Chang, Z.; Qu, Y.-K.; Zhang, Y.-H.; Bu, X.-H.; *Chem. Sci*. **2013**, *4*, 3678–3682.

45. Izak, P.; Hrma, P.; Arey, B.W.; Plaisted, T. J.; *J. Non-Cryst. Solids.* **2001**, *289*, 17.

46. Custelcean, R.; Bonnesen, P.V.; Duncan, N.C.; Zhang, X.; Watson, L. A.; Berkel, G.V.; Parson, W.B.; Hay, B.P. *J. Am. Chem. Soc.* **2012**, *134*, 8525.

47. Fu, H.-R.; Xu, Z.-X.; Zhang, J. *Chem. Mater*. **2015**, *27*, 205.

48. Li, X.; Xu, H.; Kong, F.; Wang, R. *Angew. Chem. Int. Ed*. **2013**, *52*, 13769–13773.

49. Fu, H.-R.; Xu, Z.-X.; Zhang, J. *Chem. Mater*. **2015,** *27*, 205.

50. Gao, L.; Li, C.-Y.V.; Chan, K.-Y.; Chen, Z.-N. *J. Am. Chem. Soc*. **2014,** *136* , 7209.

51. Cohen, S. M.; *Chem. Rev*.**2012**, *112*, 970.

52. Zhang, Q.; Yu, J.; Cai, J.; Zhang, L.; Cui, Y.; Yang, Y.; Chen, B. and Qian, G., *Chem. Commun.* **2015**, 51. 321.

53. Lian, X.; Yan, B. *Dalton Trans.*, **2016**, *45*, 18668.

54. Keskin, S.; Kızılel, S. *Ind. Eng. Chem. Res.*, **2011**, *50*, 1799.

Chapter -2

Dynamic Metal–Organic Framework with Anion-Triggered Luminescence Modulation Behavior

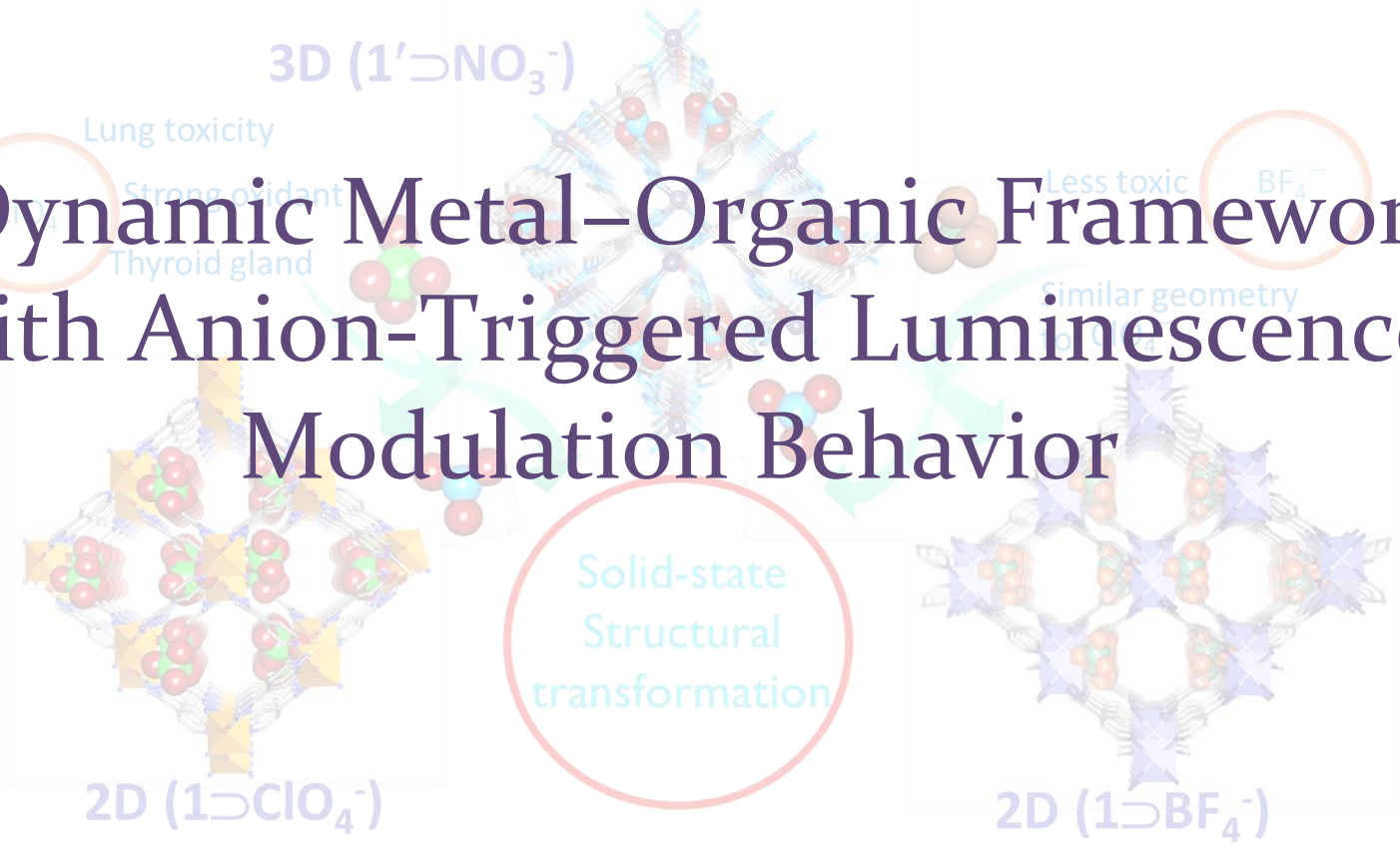

Cover page for Chapter 2

2.1. Introduction:

Porous coordination polymers or metal−organic frameworks (MOFs) with tunable properties have emerged as an exciting class of multifunctional materials because of their applications over a wide range.[1] In particular, "soft porous frameworks" have attracted much attention in recent years because of their highly ordered network along with structural flexibility.[2] They score over the conventional rigid porous frameworks in a way that they respond to a specific guest molecule and change their micro-cavities into those that match the shape and affinity of the incoming guest molecule. These materials undergo solid-state structural transformation when a guest molecule comes in or goes out of the framework. Such guest-responsive tailorable behavior along with enzyme-like specificity makes it a stimulus-responsive smart host material, thereby triggering a manifold increase in the host-guest interactions.[2,3] Combinations of a neutral flexible ligand and metal ions generally give rise to cationic frameworks.[4] These frameworks usually harbor solvents as guests in their porous cavities. Upon drying, these loosely trapped guests escape, thus leading to structural transformations.[5] These guest-driven structural transformations often find a way to build up a dynamic framework.[4b] In addition, these cationic MOFs have extra counter anions to neutralize the overall charge of the framework, which usually weakly coordinates to the metal ions or sometimes remains free in the framework lattice.[6] The incorporation of a d^{10} metal ion in complexation with a nitrogen-donor ligand at room temperature often provides luminescent cationic frameworks.[7] Variation of the counter anions in a luminescent cationic framework by other foreign anions of different size, shape, and geometry may often regulate the framework functionalities.[8] Especially, the anion-switchable fluorescence of a luminescent cationic framework has been one of the most investigated topics in this regard because it finds very useful application such as chemical sensors and anion receptors, paving the way for a concoction of new materials.[4b,7,9] In spite of a lot of reports on dynamic frameworks, anion/guest-switchable fluorescence tuning of a MOF mixed with its inherent framework flexibility is not so common.[10,4b.]

Herein, in this chapter a three-dimensional (3D) cationic luminescent framework built from a newly designed nitrogen donor ligand [(E)-N-[1-(pyridin-4-yl)ethyidene]hydrazine carbohydrazide; Scheme S1 in the Supporting Information (SI)] with a flexible skeleton (Figure 2.1.a) with multiple coordinating sites in combination with zinc(II). The framework shows guest-

driven structural dynamics in a reversible way. The air-dried phase of the compound exhibits size-dependent anion exchange behavior, and this is well demonstrated by single crystal-to-single crystal (SCSC) structural transformation experiments along with other spectroscopic techniques. The cationic framework shows interesting anion-responsive tunable luminescent behavior (Scheme 2.1).

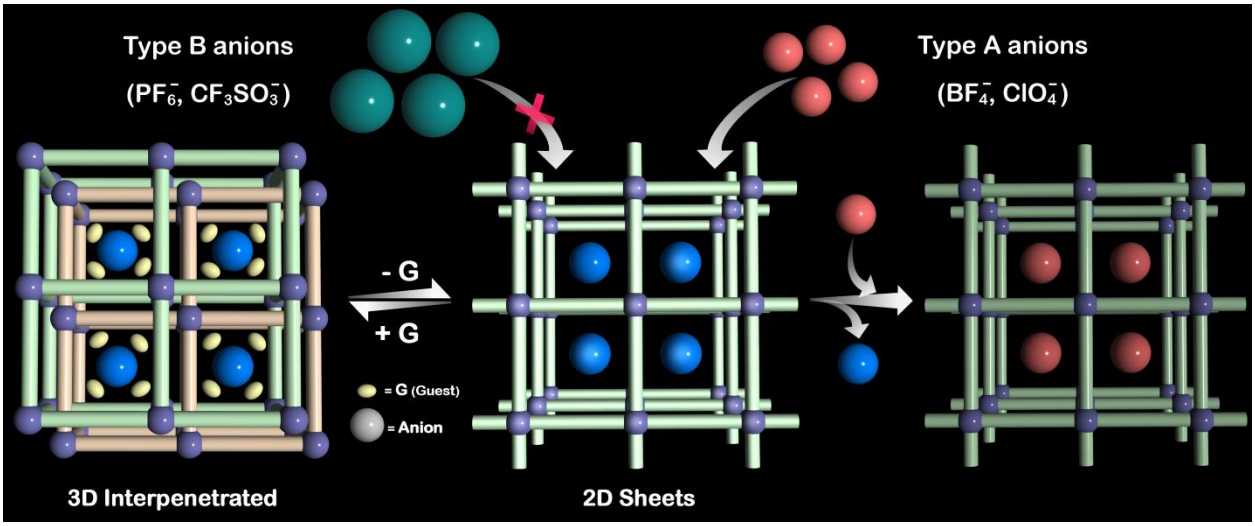

Scheme 2.1. *Schematic Representation of a Guest and Anion-Responsive Dynamic Framework.*

2.2. Experimental Section:

2.2.1. General remarks:

2.2.1.1. Materials: All the reagents and solvents were commercially available and used without further purification.

2.2.1.2. Physical measurements: Powder X-ray diffraction (PXRD) patterns were measured on Bruker D8 Advanced X-Ray diffractometer at room temperature using Cu-Kα radiation (λ= 1.5406 Å) with a scan speed of 0.5° min^{-1} and a step size of 0.01° in 2 *theta*. Thermogravimetric analysis was recorded on Perkin-Elmer STA 6000, TGA analyzer under N_2 atmosphere with heating rate of 10° C/min. FT-IR spectra were recorded on NICOLET 6700 FT-IR Spectrophotometer using KBr Pellets.

2.2.1.3. X-ray Structural Studies: Single-crystal X-ray data of compound **1′⊃NO_3^- , 1⊃ClO_4^-** and **1⊃BF_4^-** were collected at 200 K on a Bruker KAPPA APEX II CCD Duo diffractometer (operated at 1500 W power: 50 kV, 30 mA) using graphite-monochromatic Mo Kα radiation (λ = 0.71073 Å). Crystal was on nylon Cryo Loops (Hampton Research) with Paraton-N (Hampton Research). The data integration and reduction were processed with SAINT[11] software. A multi-scan absorption correction was applied to the collected reflections. The structure was solved by the direct method using SHELXTL[12]and was refined on *F2* by full-matrix least-squares technique using the SHELXL-97[13] program package within the WINGX[14] programme. All non-hydrogen atoms were refined anisotropically. All hydrogen atoms were located in successive difference Fourier maps and they were treated as riding atoms using SHELXL default parameters. The structures were examined using the *Adsym* subroutine of PLATON[15] to assure that no additional symmetry could be applied to the models. PLATON SQUEEZE programme was used to omit the diffused electron density associated with disordered solvent molecules outside the coordination sphere to improve the % of R. **Appendix 2.1**, **2.2** and **2.3** contains crystallographic data for 1′⊃NO_3^-, 1⊃ClO_4^-& 1⊃BF_4^- respectively. Crystallographic data for the structural analysis have been deposited with the Cambridge Crystallographic data Centre. CCDC 1001339 (**1′⊃NO_3^-**) , CCDC 1001338 (**1⊃ClO_4^-**) and CCDC 1001417 (**1⊃BF_4^-**) . Copies of the data can be obtained free of charge at www.ccdc.cam.ac.uk/conts/retrieving. html .

2.2.1.4. Sorption Measurements: Solvent sorption measurements were performed using BelSorpmax (Bel Japan). All of the solvents used were of 99.99% purity. The desolvated samples was obtained by heating sample at 100 °C under vacuum for 3 hrs. and the dehydration was confirmed by TGA and PXRD. Prior to adsorption measurement the desolvated sample was pre-treated at 100 °C under vacuum for 3 hrs.

using BelPrepvacII and purged with N_2 on cooling.

2.2.2. Synthesis:

2.2.2. a Synthesis of Ligand: ((E)-N′-(1-(Pyridin-4-yl) ethyidene) hydrazine carbohydrazide): To a solution of Carbohydrazide (1gm, 11.1mmol) in 30 ml MeOH, 4-acetyl pyridine (1.47 gm, 12.1 mmol) was added in presence of catalytic amount of Acetic acid1 (1 ml) to increase the electrophilicity of the carbonyl group of 4-acetyl pyridine and refluxed in an ice cold condition at 80oC for about 5-6 hrs. in an oil bath . White ppt. formed was filtered off and subsequently washed with MeOH and EtOH and then dried under vacuum to give 1.65 gm of L. Yield: 1.65 gm., 95% **(Scheme 2.2)**. The ligand was characterized by ^{1}H-NMR **(Appendix 2.4)**.

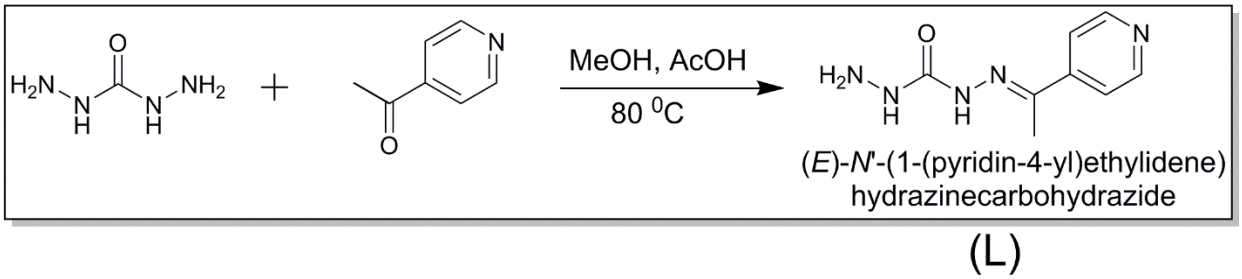

Scheme 2.2: *Schematic representation of ligand (L).*

2.2.2. b Synthesis of Compound (1′⊃NO_3^-): DCM/MeOH solution of the ligand (19 mg, 0.1 mmol) was taken in a layering tube and to it a mixture of chlorobenzene and methanolic solution of Zn $(NO_3)_2$ (29.74 mg, 0.1 mmol) was carefully layered. Transparent rod like crystals of **1′⊃NO_3^-** suitable for X-ray studies were obtained after 2 days in 60 % yield. When parent crystals were taken out from the mother liquor and kept in open air for about 1-6 hrs, it gives rise to another type crystals compound **1⊃NO_3^-**.

2.2.3 Anion exchange study: Crystals of compound **1⊃NO_3^-** was slowly stirred in MeOH solution (0.5 mmol/5 mL H_2O) of $NaClO_4$, $NaBF_4$, respectively for about 5 days at r.t. giving rise to the anion exchange product, characterized by FT-IR, XPRD, TGA, solid- state UV & solid-state emission spectra.

2.2.3. a Synthesis of Compound 1⊃ClO_4^-: Crystals of compound **1⊃NO_3^-** dipped into MeOH solution (0.5mmol/10 mL MeOH) of NaClO4 for about 5 days to get compound **1⊃ClO_4^-** $[\{Zn(L)_2\}(ClO_4)_2 \cdot xG]_n$, Confirmed from SCXRD study.

Elemental analysis of **1⊃ClO_4^-** (%) calculated (squeezed form) C_{16} H_{22} N_{10} O_{10} Cl_2 Zn: C 29.53, H 3.41, N21.53 Found (desolvated phase): C 31.22, H 3.57 N 22.43.

2.2.3. b Synthesis of Compound 1⊃BF_4^-: Crystals of compound **1⊃NO_3^-** dipped into MeOH solution (0.5mmol/5 mL MeOH) of $NaBF_4$ for about 5 days to get compound **1⊃BF_4^-** $[\{Zn(L)_2\}(BF_4)_2 \cdot xG\}]$confirmed from SCXRD study.

Elemental analysis of **1⊃BF_4^-** (%): calculated C_{16} H_{22} N_{10} O_2 B_2 F_8 Zn: C 30.73, H 3.55, N 22.40 Found (desolvated phase): C 29.77, H 3.45, N 22.

2.2.3. Reversibility test: Each solid powder of the exchanged compounds stirred very slowly in methanolic solution (5 mL) of tetra butyl ammonium nitrate (0.75 mmol) separately for about 5 days at r.t. , filtered off, washed with MeOH several times and characterized by FT-IR.

2.3. Result and discussions: The combination of L with zinc (II) in a solvent system of methanol/dichloromethane/chlorobenzene at room temperature yielded transparent block-shaped crystals of the compound $[\{Zn(L)_2\}(NO_3)_2 \cdot xG]_n$ (1′⊃NO_3^-; G is a disordered guest molecule). Single-crystal X-ray diffraction (SCXRD) analysis of 1′⊃NO_3^- showed that it crystallized in a monoclinic system with space group *C2/c*. The asymmetric unit contains two ligands, one zinc(II) ion and two non-coordinated nitrate (NO_3^-) anions. Each zinc (II) ion displays distorted

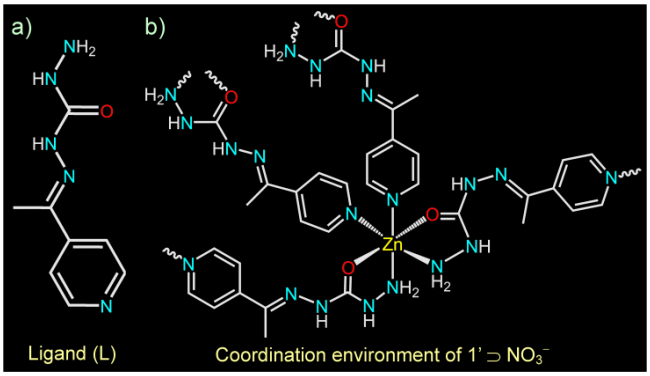

***Figure 2.1**: a) Chemical diagram of ligand (L) and b) Coordination environment around the zinc centre in 1′⊃NO_3^-.*

octahedral geometry with a N_4O_2 donor set from four ligands (**Appendix 2.6 a**). Two ligands bind in a bidentate fashion through amine nitrogen and carbonyl oxygen, and the other two connect the same zinc (II) node via pyridyl nitrogen, thus extending into a 3D structure, as shown in **Figure 2.1** and **Appendix 2.6 b**. 2-fold interpenetration creates large one-dimensional tube like channels along the *b* axis, in which disordered solvent molecules and nitrate anions were located (**Figure 2.2**).

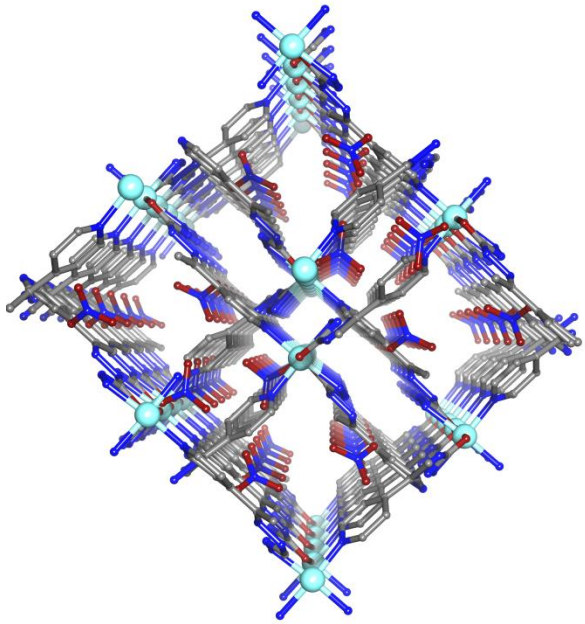

***Figure 2.2**: Figure showing porous channel with free NO_3^- in 1′⊃NO_3^- along b axis .*

A noteworthy feature of the compound is that when 1′⊃NO_3^- was kept out of the mother liquor at room temperature and air dried for about 24 h, it showed a drastic structural change and is transformed to a new phase, which was evidenced from the time dependent powder X-ray diffraction (PXRD) pattern (**Figure 2.3a**). PXRD patterns at various time intervals and in the presence of a small amount of mother liquor indicate that the structural integrity is initially maintained. However, after about 1−6 h, the PXRD pattern showed a drastic structural change and converted to a new phase, 1⊃NO_3^-, which demonstrates the dynamic nature of compound 1′⊃NO_3^- (**Figure 2.3b)**. Furthermore, when 1⊃NO_3^- was immersed in the mother liquor, compound 1⊃NO_3^- reverts back to compound 1′⊃NO_3^-, as shown by the PXRD pattern (**Appendix 2.5**), indicating the reversible nature of the framework. Because of the weak crystalline nature of 1⊃NO_3^-, the structure could not be obtained even after several attempts.

Because 1′⊃NO_3^-showed structural transformation at room temperature, we performed anion-exchange experiments with the air-stable phase 1⊃NO_3^-, which also contains the framework

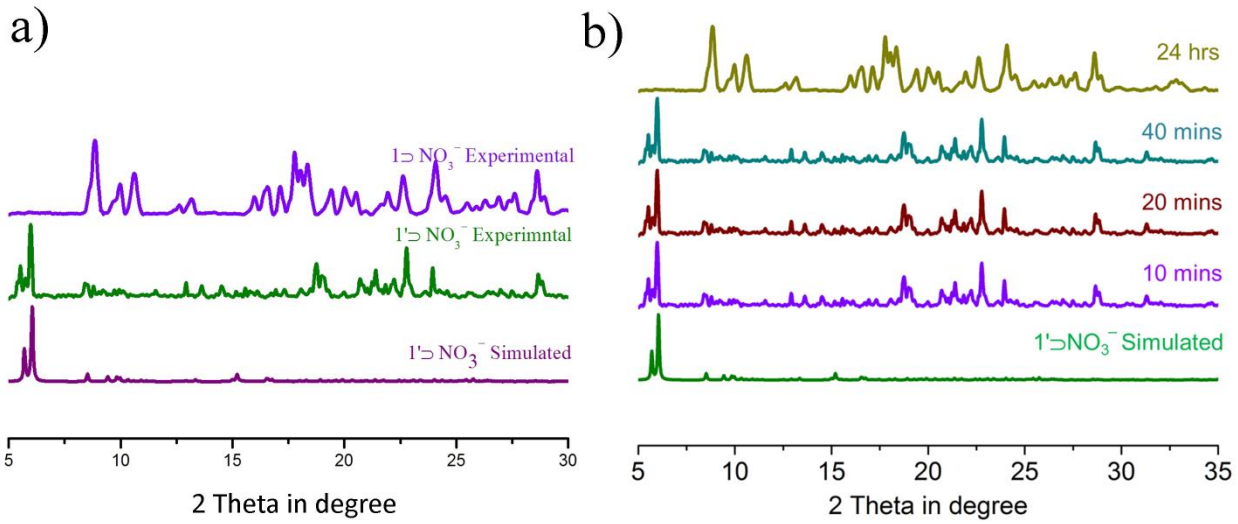

***Figure 2.3**: a) PXRD patterns of compound 1′⊃$NO_3^-$and 1⊃$NO_3^-$and b) Time dependent PXRD patterns of 1′⊃NO_3^-.*

NO_3^- anions [confirmed by IR]. Anion induced structural changes were observed when attempts were made to exchange 1⊃$NO_3^-$with other anions. Anion exchange completion was monitored by dipping the crystals of 1⊃NO_3^- in separate methanolic solutions of $NaClO_4$, $NaBF_4$, KPF_6, $KSbF_6$, and $NaCF_3SO_3$ and thereafter characterized by FT-IR spectra and CHNS data after about 4−5 days. FT-IR spectra of the anion-exchanged products showed strong bands that were characteristic of the exchanged anions. For compound 1⊃NO_3^- with NO_3^-anions, inside the channels, a characteristic band at 1380 cm^{-1} is observed as a result of the nitrate anion. However, the ligand (L) shows a characteristic band around the same region as that of the NO_3^-anion due to C−C aromatic stretch. Therefore, although the intensity of this band is unchanged in the exchanged products, new peaks at 1080 cm^{-1} (1⊃ClO_4^-) and 1034 cm^{-1} (1⊃BF_4^-) were observed in the respective exchanged compounds (**Figure 2.4a**). For PF_6^-, SbF_6^-, and $CF_3SO_3^-$, because of larger size, these anions could not be exchanged and therefore show no characteristic peak in IR spectra even after 5−10 days.

Selective anion exchange, i.e., separation of anions based on similar shape and size, is one of the intriguing aspects of such dynamic anion exchange processes. In a typical experiment, crystals of

$1\supset NO_3^-$ were immersed in a methanolic solution of mixed anions (BF_4^-/ClO_4^-) having equimolar concentration. Selective anion exchange by the framework was observed in which NO_3^- was quantitatively exchanged with BF_4^- (**Figure 2.4 b**). Reversibility could not be attained when I tried to exchange both ClO_4^- and BF_4^- with excess NO_3^- because of the stronger hydrogen-bonding interaction of ClO_4^- and BF_4^- with the framework lattice (**Appendix 2.9**).

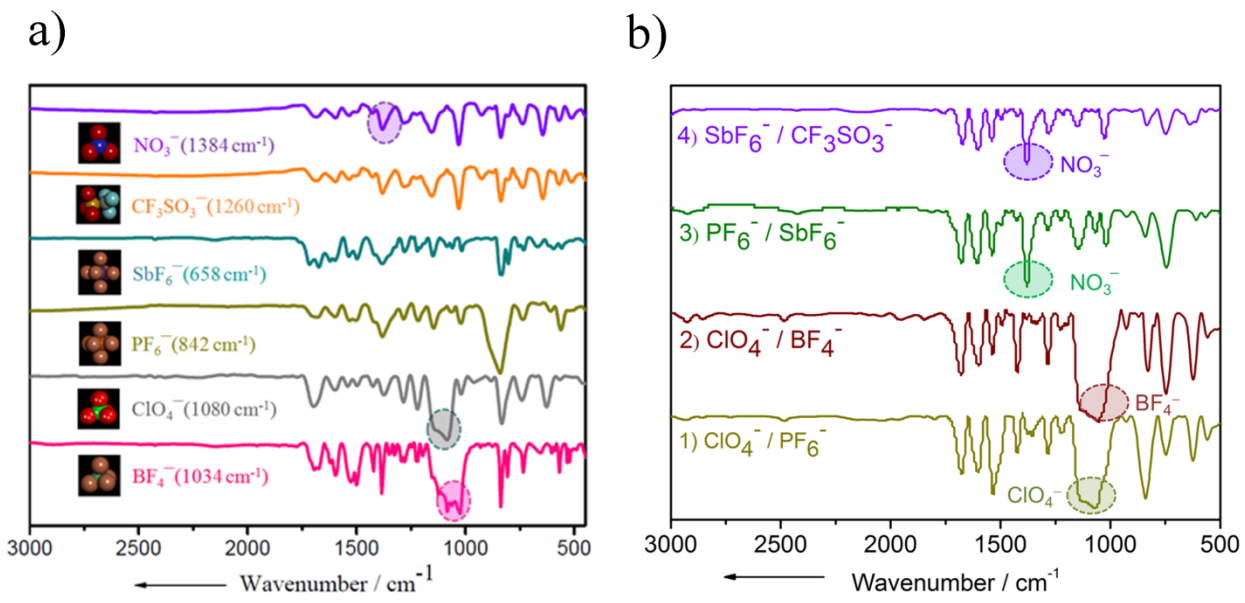

***Figure 2.4**: a) FT-IR spectra of $1'\supset NO_3^-$ and different anion exchanged compounds showing highlighted bands for corresponding anions and b) FT-IR spectra of different binary combinations showing selective anion exchange.*

During the anion-exchange process, X-ray-quality single crystals were obtained for $1\supset ClO_4^-$ (**Figure 2.5**) and $1\supset BF_4^-$, respectively (**Appendix 2.8**). Single-crystal analysis of compound $1\supset ClO_4^-$ and $1\supset BF_4^-$ revealed that both compounds $[\{Zn(L)_2\}(ClO_4)_2\cdot xG]_n$ ($1\supset ClO_4^-$) and $[\{Zn(L)_2\}(BF_4)_2\cdot xG\}]_n$ ($1\supset BF_4^-$) crystallized in a monoclinic system and were isostructural. The asymmetric unit of compound $1\supset ClO_4^-$ contains half of a zinc ion, one ligand, and one non-coordinated ClO_4^- anion. The zinc (II) ion displays perfect octahedral geometry, with the N_4O_2 donor set having the same coordination environment as that in the case of $1'\supset NO_3^-$, forming two-dimensional (2D) network (**Appendix 2.7**). Interestingly, close examination of all of the structures revealed that during structural transformation the $L{-}Zn^{II}{-}L$ angle for the compounds

is quite different from 106.22° (1′⊃NO_3^-) compared to 112.17° (1⊃ClO_4^-) and 66.49° (1⊃BF_4^-; **Appendix 2.14**). This is probably due the cooperative effect of ligand flexibility and the loss of low-boiling solvents from the lattice voids, which leads to the drastic change in the overall network with Zn−N bond rearrangements, thereby resulting in the formation of these more stable 2D structures. Single-crystal structural analysis showed complete exchange of NO_3^- in 1⊃NO_3^- by incursive anions in the exchanged compounds, whereas the bulk powder FT-IR analysis and CHNS data revealed ~98% exchange of the same. The PXRD patterns of compounds 1⊃ClO_4^- and 1⊃BF_4^-match exactly with their respective simulated patterns, and this proves the phase purity of the bulk sample after anion exchange. As observed, compound 1′⊃NO_3^-upon air drying transforms to a stable phase (1⊃NO_3^-), which thereby undergoes SCSC transformation after

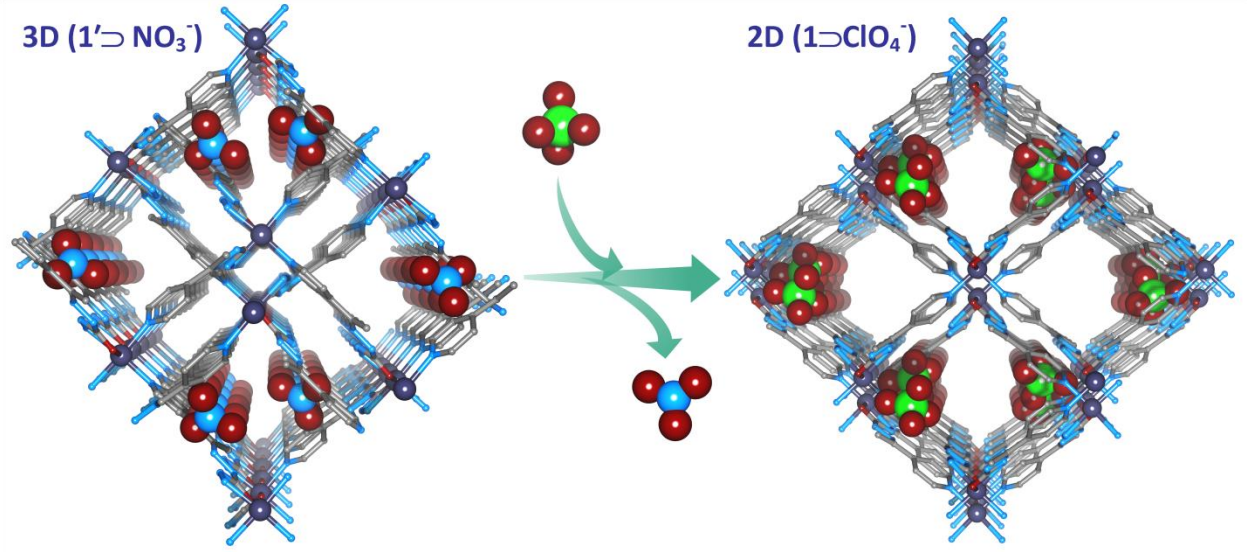

Figure 2.5: *Perspective view of Solid state structural transformation from* ***1′****⊃NO_3^- to* ***1****⊃ClO_4^- showing overall packing of both phases.*

anion exchange to form structures 1⊃ClO_4^- and 1⊃BF_4^-. More interestingly, the PXRD pattern of 1⊃ClO_4^- was also quite similar to the experimental PXRD pattern of compound 1⊃NO_3^-, thereby indicating that compound 1⊃NO_3^-probably was isostructural with 1⊃ClO_4^- and 1⊃BF_4^- (**Figure 2.6**). Thermogravimetric analysis (TGA) of compounds 1⊃NO_3^-, 1⊃ClO_4^-, and 1⊃BF_4^- demonstrated that the compounds were thermally stable up to ~225 °C with an

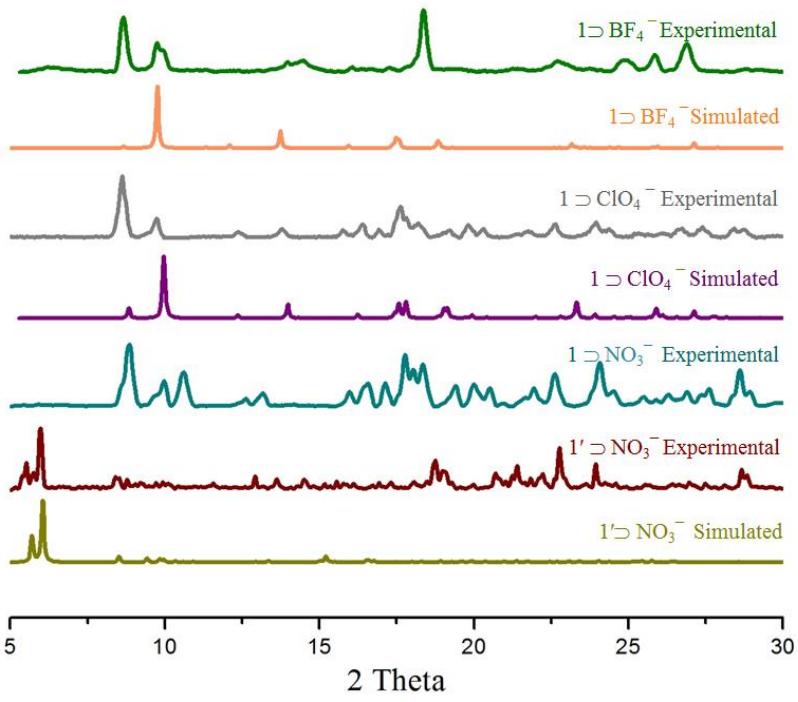

Figure 2.6: *PXRD patterns of 1⊃NO_3^-, 1⊃$NO_3^-$and various anion exchanged compounds.*

initial loss because of lattice solvent molecules (**Appendix 2.10-2.12**). Guest-inclusion behavior for compounds 1⊃NO_3^-, 1⊃ClO_4^-, and 1⊃BF_4^-were examined by solvent sorption measurements at 298 K. The ethanol sorption profile for compound 1⊃NO_3^- showed a typical hysteretic gate-opening nature (P/P_0 = 0.78) of dynamic frameworks and an uptake amount of about 152 mL g^{-1} (6.82 mmol g^{-1}). For anion-exchanged compounds 1⊃ClO_4^- and 1⊃BF_4^-, the uptake amounts were 135 mL g^{-1} (6.035 mmol g^{-1}) and 173 mL g^{-1} (7.74 mmol g^{-1}) (**Figure 2.7**) with similar sorption patterns. The difference is the sorption amount with similar sorption patterns is due to the differential interaction of guest with similar frameworks but containing anions of different shape, size, and electronic nature.

UV absorptions were measured in order to check the absorption profile for anion-exchanged compounds. Compound 1⊃NO_3^- and anion-exchanged compounds show similar nature in the absorption curves (**Figure 2.8a**). Also, solid-state emission spectra were investigated for

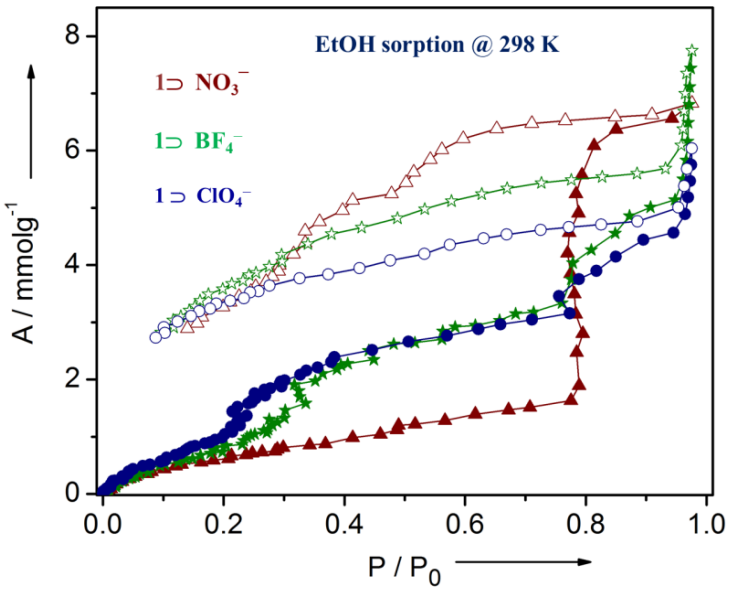

Figure 2.7: *Ethanol sorption of $1\supset NO_3^-$, $1\supset ClO_4^-$ and $1\supset BF_4^-$ at 298K.*

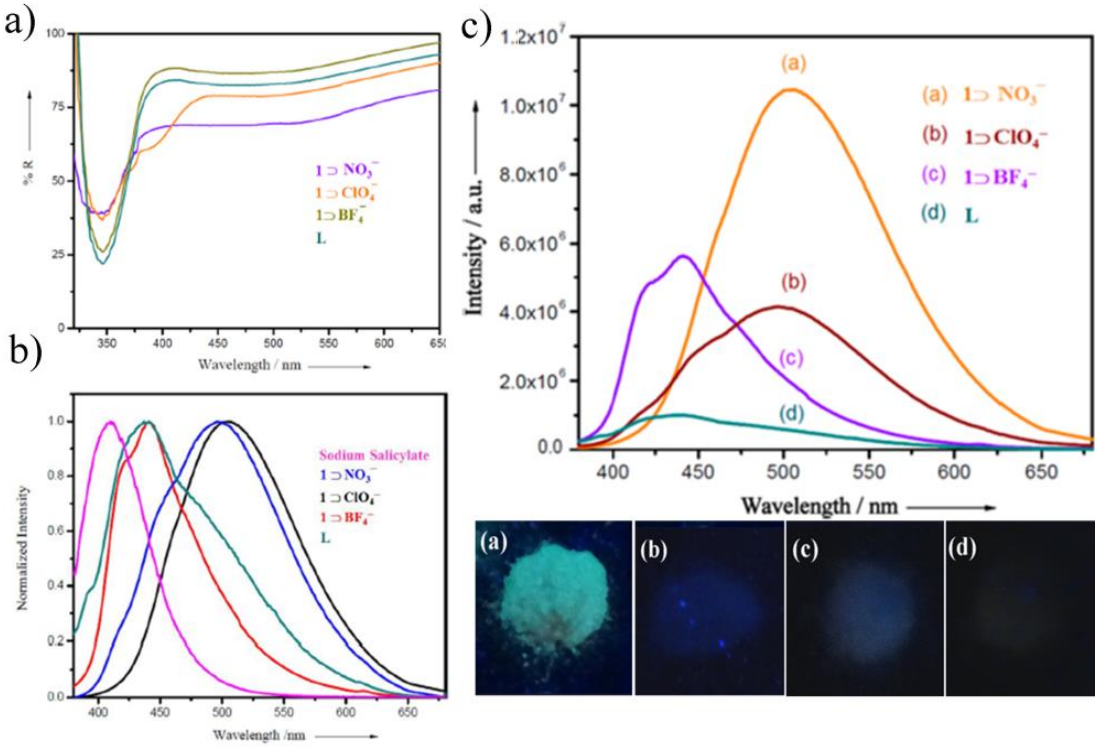

Figure 2.8: *a) Diffused reflectance spectra $1\supset NO_3^-$ and other anion exchanged compounds, b) Solid- state luminescence spectra of $1\supset NO_3^-$ and other anion exchanged compounds (Normalized intensity plot) and c) Solid state emission spectra of **1**$\supset NO_3^-$, free ligand and anion exchanged compounds (left) and optical micrographs of the same compounds under UV light (right).*

for powdered samples of L, desolvated compounds of both 1⊃NO_3^- and other anion exchanged samples at room temperature. Upon photo-excitation at 350−400 nm, L displays a weak fluorescence and, consequently, emission maxima at 440 nm. Compound 1⊃NO_3^-showed an intense broad band at 505 nm exhibiting a significant red shift compared to L. This can be attributed to π*−π intraligand transitions, metal-to-ligand charge transfer, or the effect of coordination of the ligand to the metal center. 1⊃$ClO_4^-$and 1⊃BF_4^-displayed broad peaks with intensity maxima at 442 and 497 nm, respectively (**Figure 2.8 c**). Both exchanged compounds showed a blue shift with respect to emission of 1⊃NO_3^- (**Figure 2.8 b**). The emission intensity of exchanged compounds showed very drastic differences compared to 1⊃NO_3^-, which may be due to the differential interaction of anions with the framework lattice. The quantum yields were measured for 1⊃$NO_3^-$and anion-exchanged compounds in the solid state at room temperature according to Bril and De Jager-Veenis.[16] The calculated quantum yield values of 1⊃NO_3^-, 1⊃ClO_4^-, and 1⊃BF_4^- were 0.873, 0.0583, and 0.0337, respectively, which supported the corresponding emission profiles of the respective compounds.

In conclusion, we have synthesized a luminescent cationic porous framework using a newly designed flexible chelating nitrogen-donor ligand. The framework showed guest-driven structural dynamics in a reversible manner. The framework contains free anions in its lattice voids. These anions can be exchanged easily by other anions of different shape and size. These anion-exchange experiments were well demonstrated by SCSC structural transformation and other spectroscopic techniques. Furthermore, selective anion-exchange results prove the affinity of the host framework toward anions of similar nature and can be an efficient system for ion separation. Also, anion-exchanged compounds show anion-dependent tunable luminescence and therefore have potential to develop as smart materials for chemical sensors, light-emitting devices, and other optoelectronic design strategies.

2.4. References:

1. a) Zhou, H. C.; Long, J. R.; Yaghi, O. M. *Chem. Rev*. **2012**, *112*, 673 – 674; b) Park, I. H.; Chanthapally, A.; Zhang, Z.; Lee, S. S.; Zaworotko, M. J.; Vittal, J. J. *Angew. Chem. Int. Ed*. **2014**, *53*, 414–419; c) Das, M. C; Bharadwaj, P. K. *J. Am. Chem. Soc*.**2009**, *131*, 10942–10949; d) Cui, Y.; Xu, H.; Yue Y.; Guo, Z.; Yu, J.; Chen, Z.; Gao, J.; Yang, Y.; Qian, G.; Chen, B. *J. Am. Chem. Soc*. **2012**, *134*, 3979 – 3982; e) Ohba, M.; Yoneda, K.;Agustí, G.; Muñoz, M. C.; Gaspar, A. B.; Real, J. A.; Yamasaki, M.;Ando, H.; Nakao, Y.; Sakaki, S.; Kitagawa, S. *Angew. Chem., Int. Ed*. **2009**, *48*, 4767.

2. a) Horike, S.; Shimomura, S.; Kitagawa, S. *Nat. Chem*. **2009**, *1*, 695 – 704; b) Yanai, N.; Kitayama, K.; Hijikata, Y.; Sato, H.; Matsuda, R.; Kubota, Y.; Takata,M.; Mizuno, M.;Uemura, T.; Kitagawa, S.*Nat. Mater*.**2011**, *10*, 787-793; c) Schneemann, A.; Bon, V.; Schwedler, I.; Senkovska, I.; Kaskel, S.; Fischer, R.A. *Chem. Soc. Rev*. **2014**, 43, 6062-6096; d) Henke, S.; Schneemann, A.; Wütscher,A.; Fischer, R.A. *J. Am. Chem. Soc*. **2012**, , 134, 9464−9474.

3. Kitayama, N. K.; Hijikata, Y.; Sato, H.; Matsuda, R.; Kubota, Y.;Takata, M.; Mizuno, M.; Uemura, T.; Kitagawa, S. *Nat.Mater*. **2011**, *10*, 787 – 793.

4. a) Wang, J. H.; Li, M.; Li, D. *Chem sci.* **2013**,*4*, 1793-1801; b) Manna, B.; Chaudhari, A. K.; Joarder, B.; Karmakar, A.; Ghosh, S. K. *Angew. Chem. Int. Ed*. **2013**, *52*, 998 – 1002; c) Halper, S. R.; Do, L.; Stork, J. R.; Cohen, S. M. *J. Am. Chem. Soc.* **2006,** *128*, 15255-15268.

5. a) Biradha, K.; Fujita, M. *Angew. Chem. Int. Ed*. **2002**, *41*, 3392-3395; b) Lun, D. J.; Waterhouse, G. I. N.; Telfer, S. G. *J. Am. Chem. Soc.* **2011**, *133*, 5806-5809.

6. a) Li, X.; Xu, H.; Kong, F.; Wang, R. *Angew. Chem. Int. Ed*. **2013**,*52*, 13769 –13773; b) Min, K. S.; Suh, M. P. *J. Am. Chem. Soc.* **2000**, *122*, 6834 – 6840; c) Yang, Q.Y.; Li, K.; Luo, J.; Pana, M. Su, C.Y. *Chem. Commun*. **2011**, *47*, 4234 – 4236.

7. a) Hou, S.; Liu, Q. K.; Ma, J. P.; Dong, Y. B. *Inorg. Chem.* **2013**, *52*, 3225– 3235; b) Chen, Y. Q.; Li, G. R.; Chang, Z.; Qu,Y. K.; Zhang Y. H.; Bu, X. H. *Chem. Sci.* **2013**, *4*, 3678-3682.

8. a) Maji, T. K.; Matsuda, R.; Kitagawa, S. *Nat. Mater*. **2007**, *6*, 142- 148; b) Ma, J. P.; Yu, Y.; Dong, Y. B. *Chem. Commun*.**2012**, *48*, 2946 – 2948.

9. a) Chen, B.; Wang, L.; Zapata, F.; Qian, G.; Lobkovsky, E. B. *J. Am. Chem. Soc*. **2008**, *130*, 6718 – 6719; b) Furman, J. D.; Warner, A. Y.; Teat, S. J.; Mikhailovsky, A. A.; Cheetham, A. K. *Chem. Mater.***2010**, *22*, 2255–2260.

10. Takashima, Y.; Martinez, V. M.; Furukawa, S.; Kondo, M.; Shimomura, S.; Uehara, H.; Nakahama, M.; Sugimoto K.; Kitagawa, S. *Nat. Commun*. **2011**, *2*, 168.

11. *SAINT Plus*, (Version 7.03); Bruker AXS Inc.: Madison, WI, **2004**.

12. G. M. Sheldrick, *Acta Crystallogr*. *Sect.A* **2008**, 112 –122.

13. G. M. Sheldrick, SHELXTL, Reference Manual: version 5.1: Bruker AXS; Madison, WI, 1997.

14. *WINGX* version 1.80.05 Louis Farrugia, University of Glasgow.

15. A. L. Spek, (2005) PLATON, A Multipurpose Crystallographic Tool, Utrecht University, Utrecht, The Netherlands.

16. Bril, A.; De Jager-Veenis, A.W. *J. Res. Natl. Bur. Stand. Sect.A* **1976**, *80A*, 401 – 407.

Appendix:

Appendix 2.1: *Crystal data and structure refinement for compound* ***1′⊃NO₃⁻***.

Identification code	**Compound 1 ⊃NO_3^-**	
Identification code	Compound 1′⊃NO_3^-	
Empirical formula	C_{16} H_{22} N_{12} O_8 Zn	
Formula weight	575.82	
Temperature	200(2) K	
Wavelength	0.71069 Å	
Crystal system	Monoclinic	
Space group	*C 2/c*	
Unit cell dimensions	a = 27.511(5) Å	α= 90.000(5)°.
	b = 23.284(5) Å	β= 131.079(5)°.
	c = 18.752(5) Å	γ = 90.000(5)°.
Volume	9055(4) $Å^3$	
Z	8	
Density (calculated)	0.845 Mg/m^3	
Absorption coefficient	0.579 mm^{-1}	
F(000)	2368	
Crystal size	0.120 x 0.110 x 0.100 mm^3	
Theta range for data collection	1.395 to 18.393°.	
Index ranges	-24<=h<=24, -20<=k<=20, -16<=l<=16	
Reflections collected	16616	
Independent reflections	3320 [R(int) = 0.0582]	
Absorption correction	Semi-empirical from equivalents	
Max. and min. transmission	0.9444 and 0.9338	
Refinement method	Full-matrix least-squares on F2	
Data / restraints / parameters	3320 / 12 / 334	
Goodness-of-fit on F2	1.095	
Final R indices [I>2sigma(I)]	R1 = 0.0645, wR2 = 0.1771	
R indices (all data)	R1 = 0.0801, wR2 = 0.1859	
Largest diff. peak and hole	0.502 and -0.410 $e.Å^{-3}$	

Appendix 2.2: *Crystal data and structure refinement for compound* ***1⊃ClO₄⁻***

Identification code	**Compound 1 ⊃ClO_4^-**	
Identification code	Compound 1⊃ClO_4^-	
Empirical formula	C_{16} H_{22} Cl_2 N_{10} O_{10} Zn	
Formula weight	650.70	
Temperature	200(2) K	
Wavelength	0.71073 Å	
Crystal system	Monoclinic	
Space group	*C 2/c*	
Unit cell dimensions	a = 18.740(4) Å	α= 90°.
	b = 12.600(2) Å	β= 105.597(4)°.
	c = 15.198(3) Å	γ = 90°.
Volume	3456.5(12) $Å^3$	
Z	4	
Density (calculated)	1.250 Mg/m^3	
Absorption coefficient	0.918 mm^{-1}	
F(000)	1328	
Crystal size	0.120 x 0.120 x 0.110 mm^3	
Theta range for data collection	1.971 to 26.225°.	
Index ranges	-23<=h<=23, -15<=k<=15, -18<=l<=18	
Reflections collected	14263	
Independent reflections	3470 [R(int) = 0.0190]	
Absorption correction	Semi-empirical from equivalents	
Max. and min. transmission	0.9058 and 0.8978	
Refinement method	Full-matrix least-squares on F^2	
Data / restraints / parameters	3470 / 0 / 178	
Goodness-of-fit on F2	1.042	
Final R indices [I>2sigma(I)]	R1 = 0.0661, wR2 = 0.1765	
R indices (all data)	R1 = 0.0717, wR2 = 0.1813	
Largest diff. peak and hole	1.921 and -1.457 e.$Å^{-3}$	

Appendix 2.3: *Crystal data and structure refinement for compound* ***1⊃BF$_4^-$***

Identification code	**Compound 1⊃BF$_4^-$**	
Identification code	Compound 1⊃BF$_4^-$	
Empirical formula	C_{16} H_{22} B_2 F_8 N_{10} O_2 Zn	
Formula weight	625.42	
Temperature	200(2) K	
Wavelength	0.71073 Å	
Crystal system	Monoclinic	
Space group	*C 2/c*	
Unit cell dimensions	a = 18.834(5) Å	α= 90.000(5)°.
	b = 12.345(5) Å	β= 106.163(5)°.
	c = 15.224(5) Å	γ = 90.000(5)°.
Volume	3400(2) Å3	
Z	4	
Density (calculated)	1.222 Mg/m^3	
Absorption coefficient	0.793 mm^{-1}	
F(000)	1264	
Crystal size	0.140 x 0.110 x 0.100 mm^3	
Theta range for data collection	2.249 to 20.013°.	
Index ranges	-18<=h<=16, -11<=k<=11, -14<=l<=14	
Reflections collected	6124	
Independent reflections	1543 [R(int) = 0.0434]	
Absorption correction	Semi-empirical from equivalents	
Max. and min. transmission	0.9249 and 0.8970	
Refinement method	Full-matrix least-squares on F^2	
Data / restraints / parameters	1543 / 0 / 186	
Goodness-of-fit on F2	1.096	
Final R indices [I>2sigma(I)]	R1 = 0.0540, wR2 = 0.1247	
R indices (all data)	R1 = 0.0608, wR2 = 0.1276	
Largest diff. peak and hole	0.359 and -0.333 e.Å^{-3}	

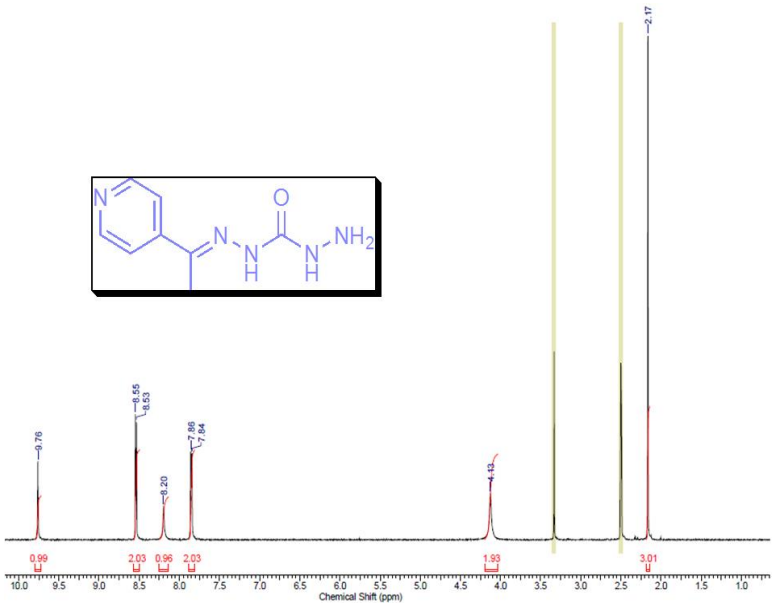

***Appendix 2.4**: [1]H-NMR of Ligand (L).*

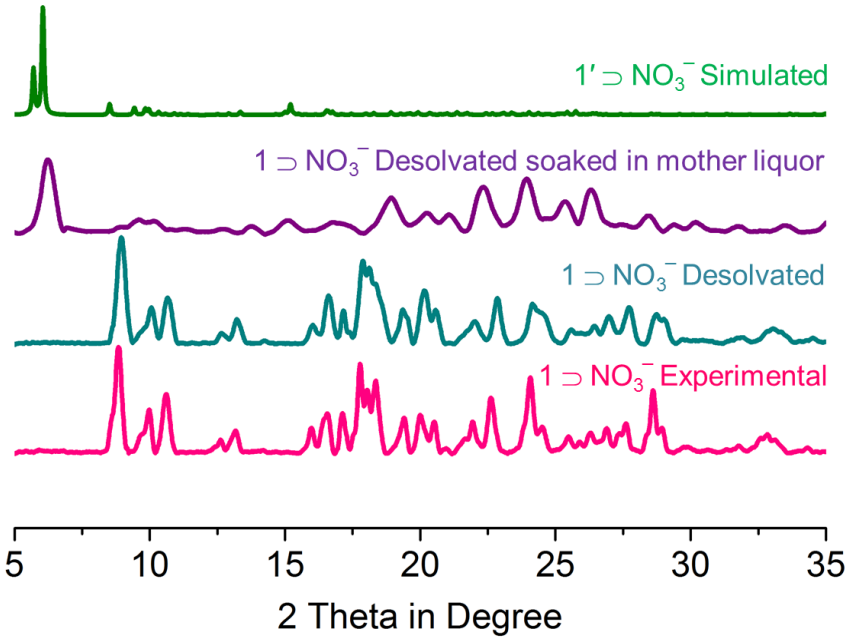

***Appendix 2.5:** PXRD patterns of compound **1′⊃NO₃⁻** and **1⊃NO₃⁻** showing reversibility.*

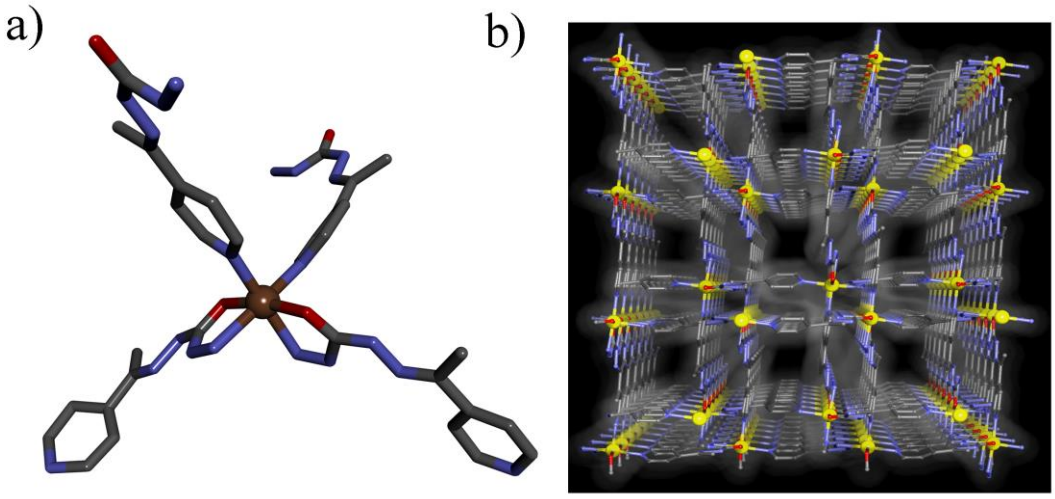

Appendix 2.6: *Coordination environment around the metal center in* ***1⊃ NO_3^-*** *. (Colour code; Carbon: gray, oxygen: red, nitrogen: blue, zinc: brown) and b) Overall packing of* ***1⊃ NO_3^-*** *.*

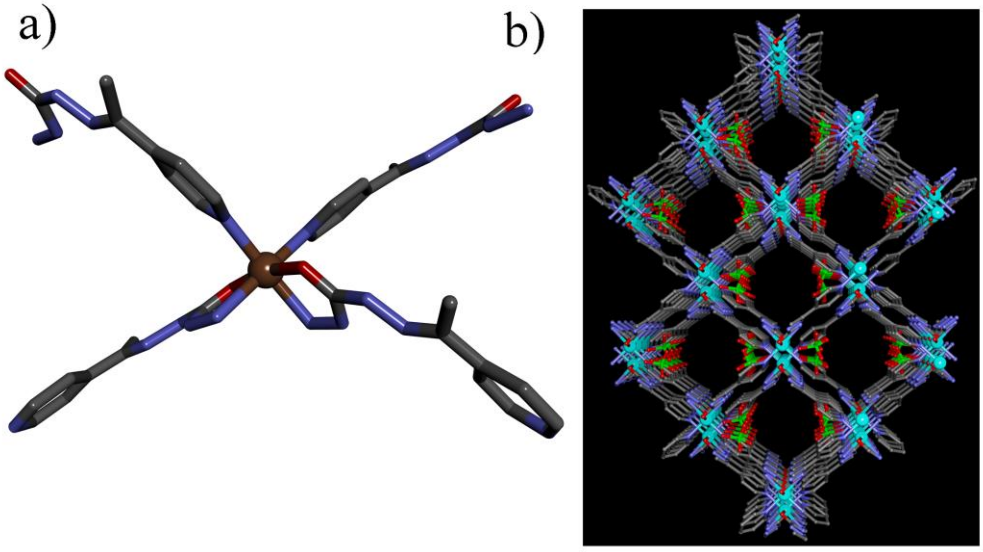

Appendix 2.7: *) Coordination environment around the metal center in* ***1⊃ ClO_4^-*** *. Hydrogen atoms have been deleted for clarity****.*** *(Colour code; Carbon: gray, oxygen: red, nitrogen: blue, zinc: brown) and b) Overall packing of* ***1⊃ ClO_4^-*** *showing free* ***ClO_4^-*** *anions in the interstitial position.*

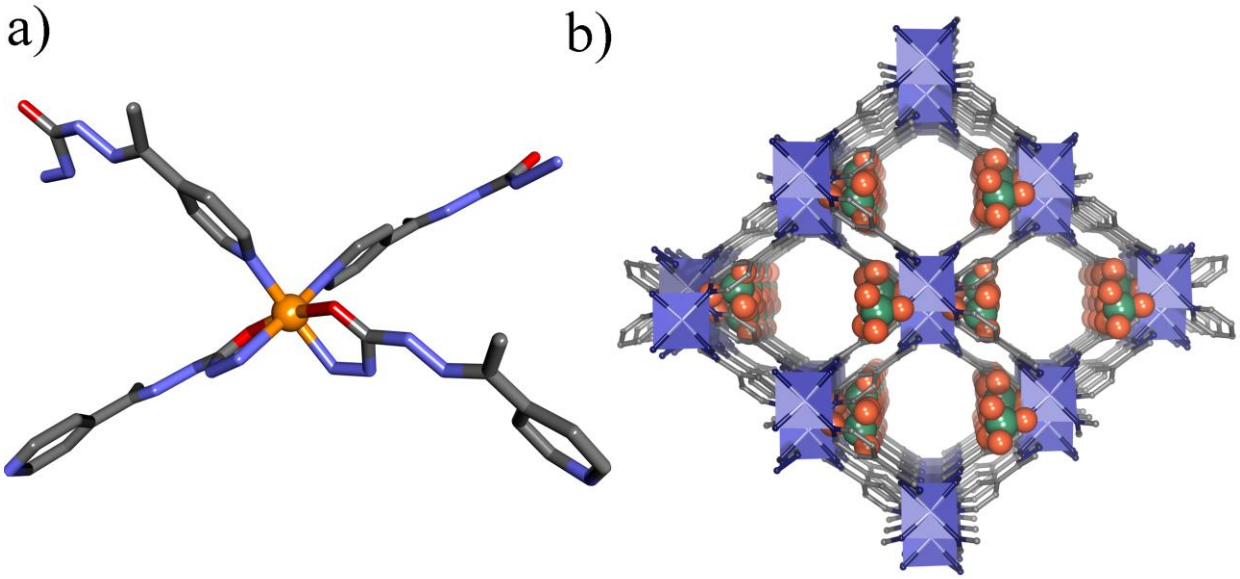

***Appendix 2.8**: a) Coordination environment around the metal center in **1⊃ BF_4^-**. Hydrogen atoms have been deleted for clarity. (Colour code; Carbon: gray, oxygen: red, nitrogen: blue, zinc: orange) and b) Overall packing of **1⊃ BF_4^-** showing free **BF_4^-** anions in the interstitial position.*

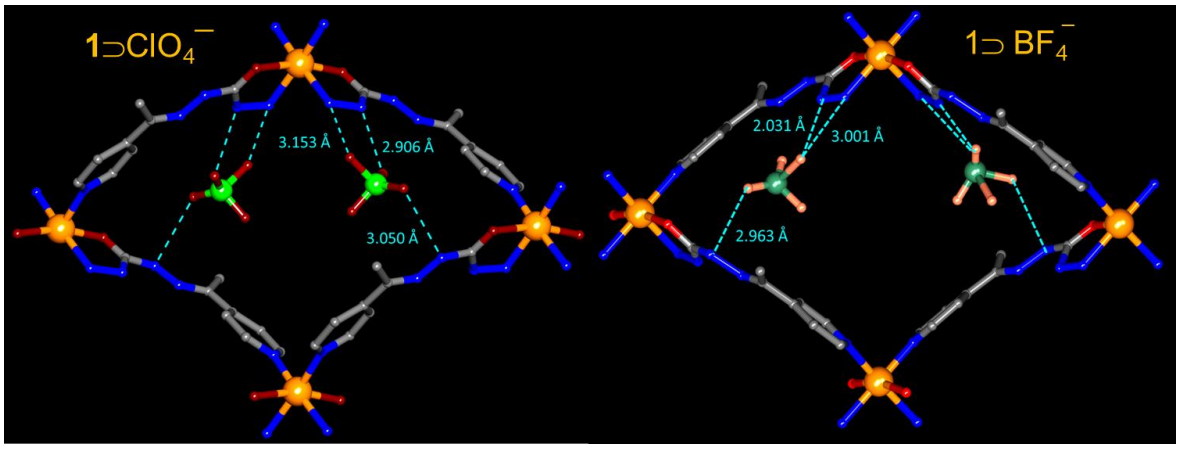

***Appendix 2.9**: Hydrogen bonding interaction and distances of free **ClO_4^-** and free **BF_4^-** in **1⊃ ClO_4^-** and **1⊃ BF_4^-** respectively.*

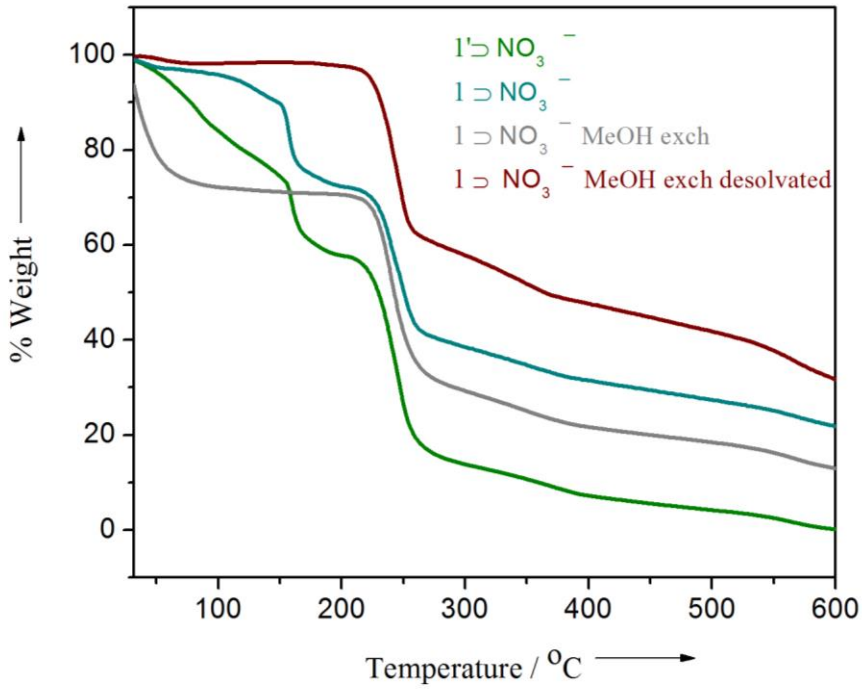

***Appendix 2.10**: TGA of **1'⊃NO3¯ 1⊃ NO3¯** solvent exchanged **1⊃ NO3¯** and desolvated compounds.*

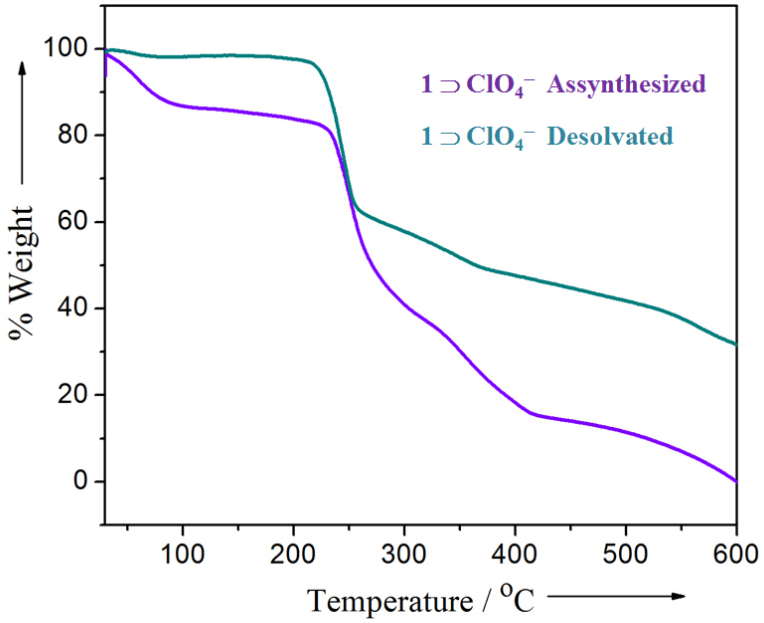

***Appendix 2.11:** TGA of **1⊃ ClO4¯**: as synthesized and desolvated compounds.*

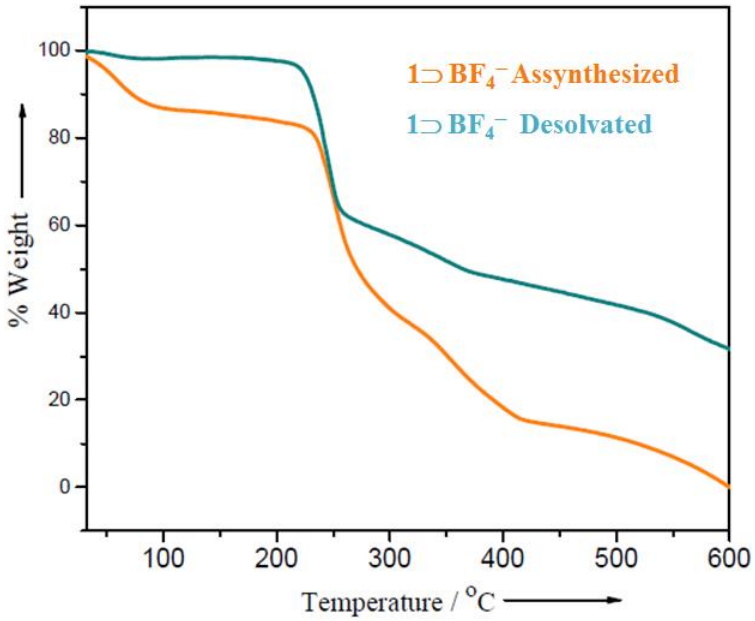

***Appendix 2.12**: TGA of **1⊃BF$_4^-$**: as synthesized and desolvated compounds.*

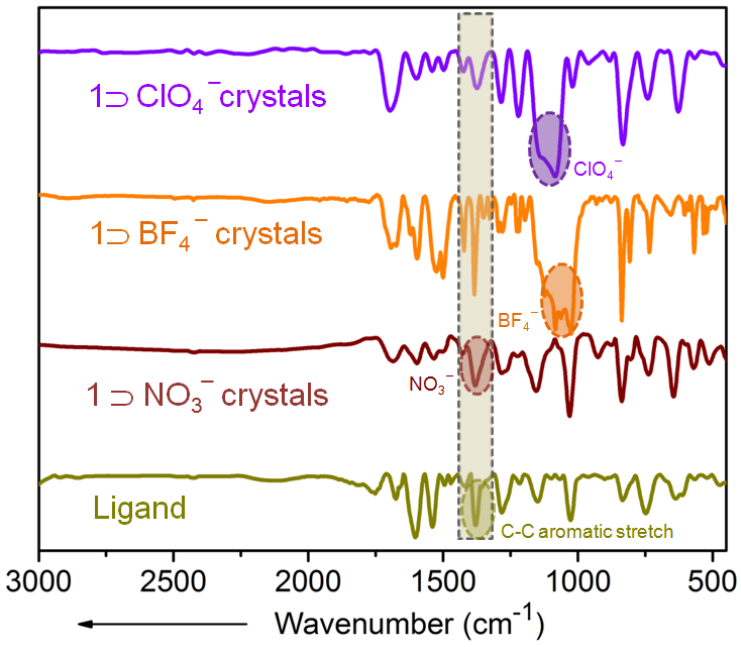

***Appendix 2.13**: FT-IR spectra of free ligand, **1⊃NO$_3^-$** and anion exchanged compounds.*

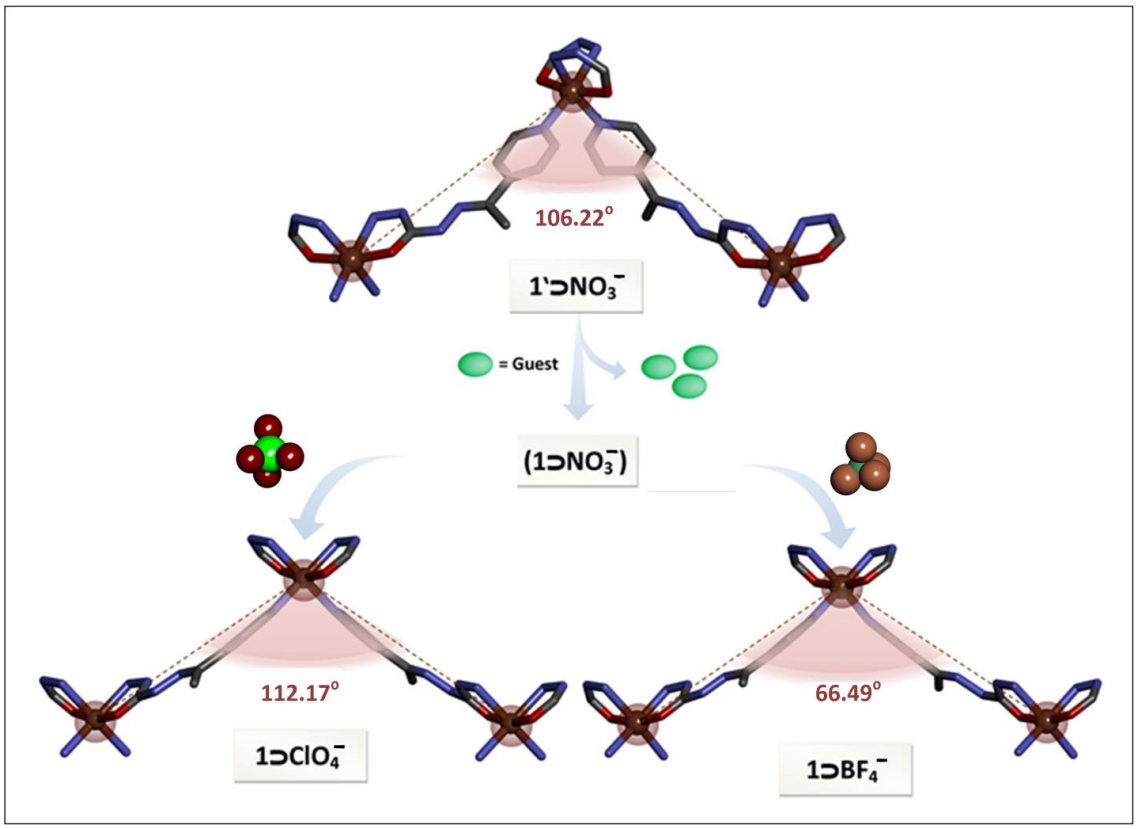

***Appendix 2.14**: Changes in M-M-M angle of 1'⊃NO_3^- during structural transformations.*

Chapter -3

An Amide-Functionalized Dynamic Metal–Organic Framework Exhibiting Visual Colorimetric Anion Exchange and Selective Uptake of Benzene over Cyclohexane

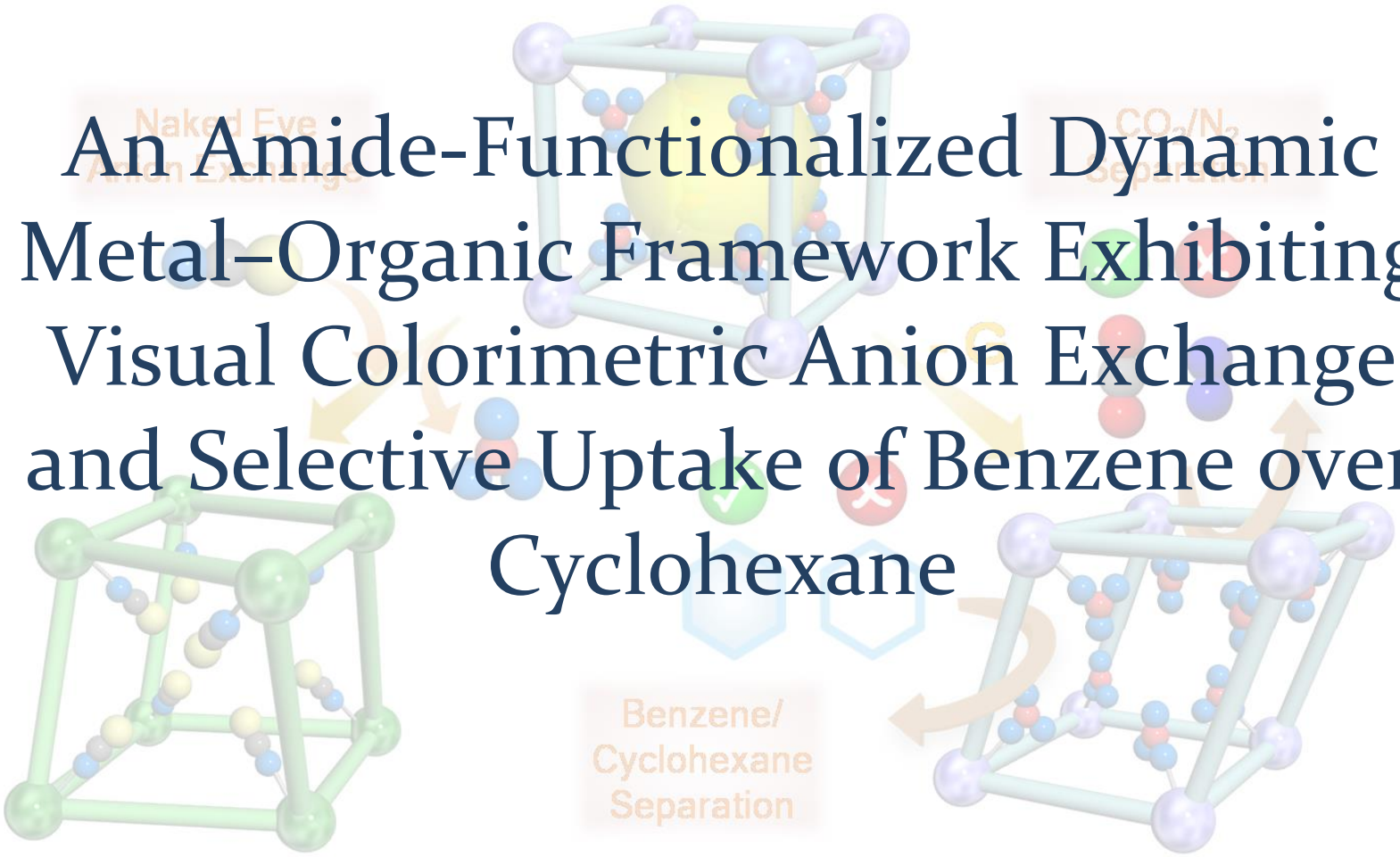

Cover page for Chapter 3

3.1 Introduction:

Metal–organic frameworks (MOFs) are an important class of materials that have shown astounding applications in conventional proof-of-concept usage in separation, storage of gases, sensing, catalysis, ion-exchange, and fuel cells.[1] The serviceability of such ordered crystalline networks often depends on the incorporation of various functionalities within it, and development of such MOFs that can truly act as a multifunctional material [2] is the demand of the current state of art. In this regard, dynamic/flexible MOFs in which the structures and properties can be tuned in response to an external stimulus are of significant interest.[3]Their structural dynamism can indeed be the key principle for the concoction of diversified functionalities within the MOFs. The major challenges in chemical industries are development of materials which can address the issues concerning separation and environmental pollution.[4]The conventional separation techniques which can effectively separate two small molecules are often expensive and require processes that are highly energy-demanding. [5] Cyclohexane, which is generally produced by the hydrogenation of benzene in industry, has unreacted benzene in the mixture, and separation of these two components is of considerable significance. In particular, because of the similarity in the boiling points (benzene, 80.1˚C and cyclohexane, 80.7˚C) and comparable Lennard–Jones collision diameters of these two components, conventional techniques often face a serious impediment in such separation procedures. [6] The current methods of separation of these two species involve the removal of residues from the distillate and are often gruesome. MOFs, owing their designable architecture and structural dynamism, score over the other conventional materials in this aspect, because by the virtue of their sieving effect, [7] they can selectively act as an efficient adsorbent for a particular adsorbate over others, such as benzene over cyclohexane, or even among other hydrocarbon congeners. [8] Also, one of the intriguing features of MOFs is the wide variety of organic ligands available for the construction allows syntheses of tailor-made materials for specific interactions with the incoming guest molecules. For instance, an amide-functionalized MOF can form favorable hydrogen-bonding interactions or sometimes because of the inherent basicity of the amide group [2d] can even interact differentially with the C-H protons of benzene and cyclohexane. An amide integrated framework can also discriminate between polar gas molecules such as CO_2 and other nonpolar gases owing to strong dipole–quadrupole interactions with CO_2 and can be an important candidate for carbon dioxide storage and

separation. [9, 2d] In addition to this, sensing and separation of small anions by cationic/neutral MOFs is one of the important area in the realm of the field of MOFs. [10] Most of the anion exchange/sensing properties of MOFs reported so far are either dependent on fluorescence based methods of detection or by other spectroscopic techniques. Development of anion receptors that can sense anions by visual chroma are of great current interest as the anion recognition can consequently be realized by the naked eye. [11] Copper (II)-based MOFs are one of the well-known systems for such colorimetric anion sensors. [12] They are known to exhibit Jahn–Teller distortions in which the axial bonds which are usually coordinated by anions are significantly weakened. Anion exchange reactions at these axial sites in such MOFs may often result in visual color change and are getting immense importance in the field of sensors and actuators.[13] Integration of such multiple functionalities such as CO_2 separation/storage, separation of commercially important cyclic C_6 hydrocarbon congeners, and anion sensing by MOFs are rare, and development of such MOFs in a targeted fashion are of considerable importance.

In our endeavor to incorporate multifarious functionality in a MOF, in this chapter I synthesized a novel coordination polymer with molecular formula $[\{CuL_2(NO_3)_2\}\cdot$o-xylene$\cdot DMF]_n$ ($1\supset NO_3^-$) by solvothermal reaction of $Cu(NO_3)_2\cdot 6H_2O$ and a newly designed amide functionalized N-donor ligand L (**Figure 3.1 a**) in a solvent combination of 1:1 DMF/o-xylene (see the Supporting Information). The compound $1\supset NO_3^-$transforms to a new phase $1'\supset NO_3^-$ upon desolvation. The desolvated compound shows a preferential uptake of benzene over cyclohexane at room temperature by the virtue of favorable interaction with the benzene molecules. The compound $1'\supset NO_3^-$ also showed a strong affinity for CO_2 over other gases at low temperature. Moreover, the parent Copper (II)-based compound, that is $1\supset NO_3^-$, exhibited a visual colorimetric detection of SCN^- anion through an anion-exchange process, which was monitored by a solid state structural transformation process (**Scheme 3.1**).

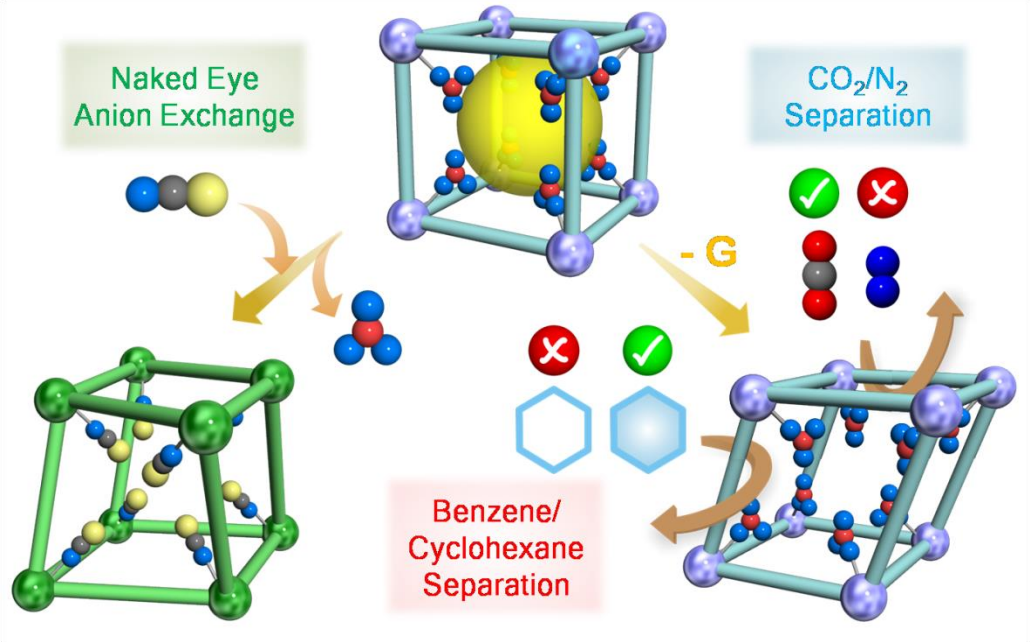

Scheme 3.1:*Schematic representation showing multifunctional behaviour of compound 1⊃NO_3^-.*

3.2 Experimental Section:

3.2.1. General remarks:

3.2.1.1. Materials: All the reagents and solvents were commercially available and used without further purification.

3.2.1.2. Physical measurements: Powder X-ray diffraction (PXRD) patterns were measured on Bruker D8 Advanced X-Ray diffractometer at room temperature using Cu-Kα radiation (λ= 1.5406 Å) with a scan speed of 0.5° min^{-1} and a step size of 0.01° in 2 *theta*. Thermogravimetric analysis was recorded on Perkin-Elmer STA 6000, TGA analyzer under N_2 atmosphere with heating rate of 10° C/min. FT-IR spectra were recorded on NICOLET 6700 FT-IR Spectrophotometer using KBr Pellets.

3.2.1.3. X-ray Structural Studies: Single-crystal X-ray data of compound 1⊃NO_3^-, 1D⊃$NO_3^-$and 1⊃SCN^- were collected at 200 K on a Bruker KAPPA APEX II CCD Duo diffractometer (operated at 1500 W power: 50 kV, 30 mA) using graphite-monochromatic Mo Kα radiation (λ = 0.71073 Å). The data integration and reduction were processed with SAINT[14] software. A multi-scan absorption correction was applied to the collected reflections. The

structure was solved by the direct method using SHELXTL[15] and was refined on F^2 by full-matrix least-squares technique using the SHELXL-97[16] program package within the WINGX[17] programme. All non-hydrogen atoms were refined anisotropically. All hydrogen atoms were located in successive difference .The structures were examined using the Adsym subroutine of PLATON[18] to assure that no additional symmetry could be applied to the models. PLATON SQUEEZE programme was used to omit the diffused electron density associated with disordered solvent molecules outside the coordination sphere to improve the % of R. **Appendix3.1**, **3.2** and **3.3** contains crystallographic data for the 1⊃NO_3^-, 1D⊃$NO_3^-$and 1⊃SCN^-respectively.

3.2.1.3 Sorption Measurements: Low pressure gas and solvent sorption measurements were performed using BelSorpmax (Bel Japan). The sorption-recyclability experiments were recorded in BelAqua (Bel Japan). All the gases used were of 99.999% purity. The desolvated samples was obtained by heating sample at 100 °C under vacuum for 3h and the desolvation was confirmed by TGA and PXRD. Prior to adsorption measurement the desolvated sample was pre-treated at 100 °C under vacuum for 4h using BelPrepvacII and purged with N_2 on cooling. Low pressure gas sorption measurements were performed using BelSorpmax (Bel Japan). All of the gases used were of 99.999% purity.

3.2.2. Synthesis:

3.2.2. a Synthesis of Ligand (L): The solution 4-Aminopyridine in DMF (13.2mmol) was added to the solution of 5-*tert*-Butylisophthalic acid in DMF (4.4 mmol) under ice cold conditions (**Scheme 3.2**). The mixture was treated with DCC (11.2mmol) and HOBt (11.2mmol). The reaction mixture was stirred for about 12 h at room temperature and the completion of the reaction was monitored by TLC. After completion of the reaction, the reaction mixture was diluted with EtOAc (100 mL) and DCU was filtered through the sintered funnel. The EtOAc layer was washed with brine (3 × 50 mL) followed by 5% aq. HCl (3 × 50 mL), 10% aq. Na_2CO_3 (1 × 50 mL), brine (3 × 50 mL) and dried over anhydrous Na_2SO_4. The crude product was purified by column chromatography using MeOH/DCM to get the pure product. Yield 2.6 gm., 82%. The Ligand was characterized by ^{1}H-NMR (**Appendix3.4**).

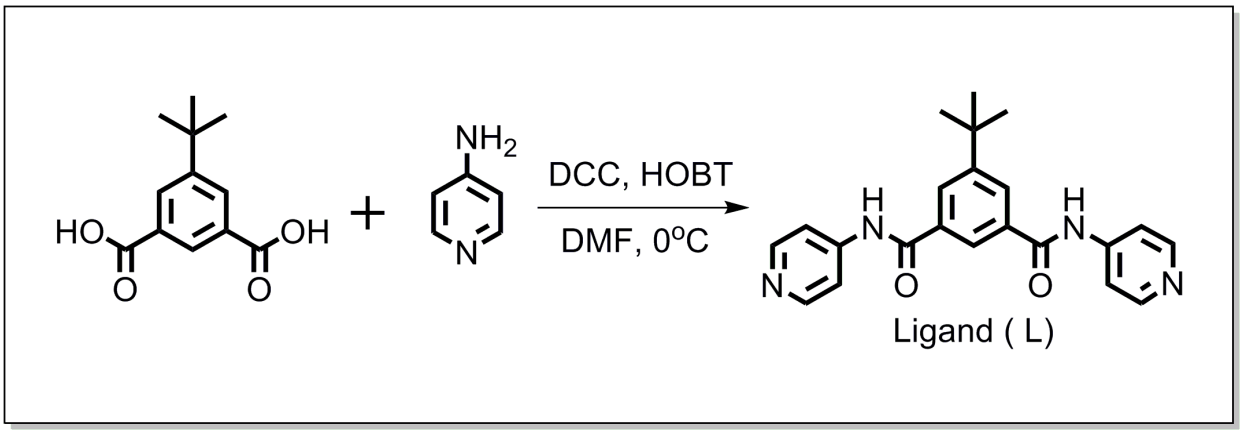

Scheme 3.2:*Schematic representation of the synthesis of ligand (L).*

3.2.2. b Synthesis of Compound ($1\supset NO_3^-$): 0.1mmol of L (0.0374gm) and 0.1 mmol of Cu(NO3)2 were taken in a glass vial containing 1 ml DMF and 1 ml o-xylene. The resulting solution was heated at 90˚C for two days. After cooling dark blue crystals of compound crystals compound $1\supset NO_3^-$were formed in about ~70% yield. $([CuL_2 (NO_3)_2].o\text{-}Xylene.DMF)_n$.

3.2.2. c Synthesis of Compound $1D\supset NO_3^-$: When compound $1\supset NO_3^-$was exchanged in acetone for 6-7 days and then heated at 50˚C for 5hrs it gave another type of crystal $1D\supset NO_3^-$ (Characterized by SC-XRD study).The bulk sample of $1D\supset NO_3^-$[Elemental analysis (%):Calculated C_{88} H_{87} Cu_2 $N_{20}O_{12}$:C 55.99 H 4.65 N14.64] loses the coordinated water molecule readily and transforms to the new phase i.e. $1'\supset NO_3^-$[Found C56.45 H 4.10 N 14.92].

3.2.2. d Synthesis of Compound $1\supset SCN^-$: Crystals of compound $1\supset NO_3^-$dipped into MeOH solution (0.5mmol/10 mL MeOH) of KSCN for about 5hrs to get compound $1\supset SCN^-$ $[\{CuL(SCN)_2\}.xG]_n$. Confirmed from SCXRD study.

Elemental analysis of $1\supset SCN^-$ (%): calculated (squeezed form) : C 59.56, H 4.67, N 15.10 S 6.91 Found (desolvated phase): C 57.53, H 5.12 N15.45 S 7.07.

3.3. NMR study of Guest-included phases: Compound 1′⊃$NO_3^-$was exposed to vapors of different guests, digested with DCl and then extracted with $CDCl_3$ and D_2O. The organic extract was then characterized by 1H and ^{13}C NMR experiments.

3.4. Result and discussions: Single crystal X-ray diffraction analysis of compound 1⊃NO_3^-revealed that the compound crystallized in Monoclinic system with space group *P2/c*.The asymmetric unit contains one Cu(II), one L, one coordinated nitrate (NO_3^-) anion, one DMF molecule and half *o*-xylene molecule. The Cu(II) center is coordinated byfour nitrogen atoms from four L and two coordinated NO_3^- to furnish an octahedral geometry (**Figure 3.1**). In complex 1⊃NO_3^- the ligand L exhibits a cis-conformation. The N-H protons of the ligands are hydrogen bonded to the oxygen atoms of the solvent DMF molecules and the oxygen atoms of the coordinated nitrate anion to form a hydrogen bonded structure.The dihedral angles between its phenyl ring and two pyridine rings are 42 and 40.5 respectively. Two ligands connect the Cu(II) nodes forming an infinite dimeric chain of copper resulting in overall 1D porous framework along crystallographic *a* axis(**Figure 3.2 and Appendix 3.5-3.6**).

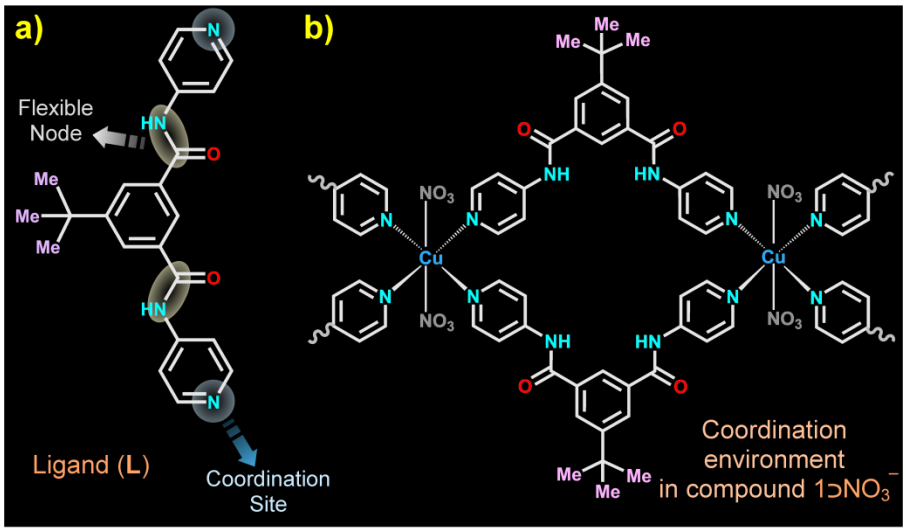

Figure 3.1:*a) Chemical diagram of ligand (L) and b) Coordination environment around the copper centre in 1⊃NO_3^-.*

Powder X-ray diffraction analysis of bulk sample of 1⊃NO_3^-showed considerable difference from the simulated pattern (**Figure 3.3 a**) which prompted us to believe that the compound

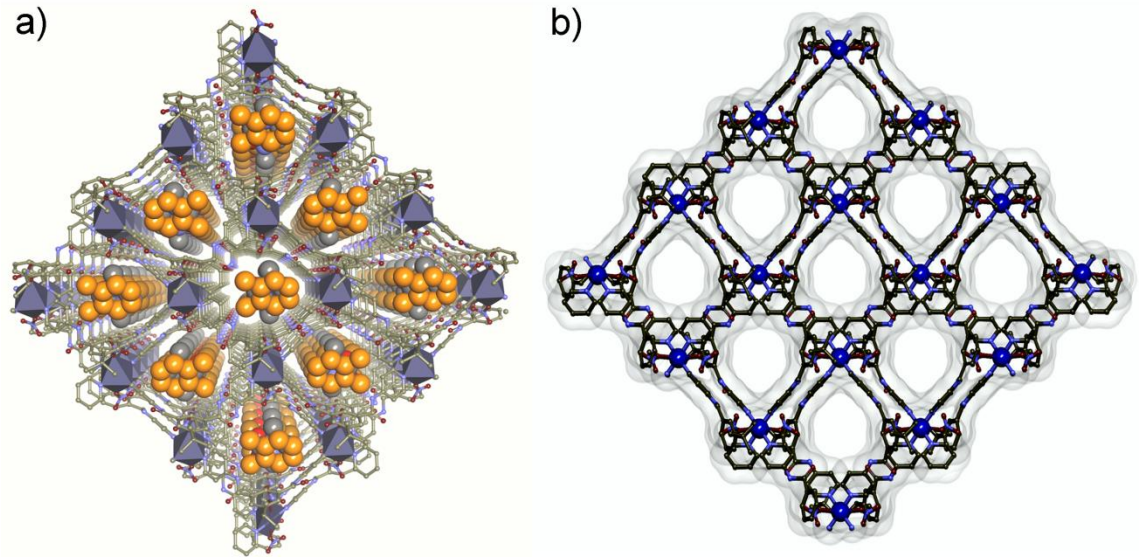

Figure 3.2: *a) Porous view of compound 1⊃NO_3^- with solvent molecules and b) Porous view of compound 1⊃NO_3^- along a axis.*

1⊃NO_3^- underwent structural changes when brought out of mother liquor, indicative of the structural dynamism of the compound. Thermogravimetric analysis (TGA) performed under N_2 revealed that the compound 1⊃NO_3^- showed an initial loss of about 22% which corresponds to the DMF and *o*-xylene molecules (**Figure 3.3 b**) after which the compound is stable upto ~280˚C with no further

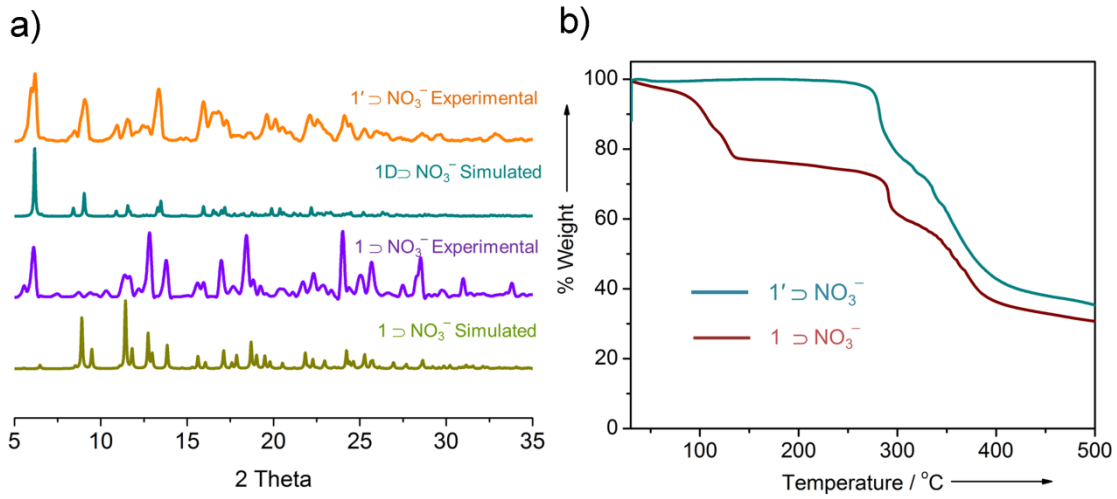

Figure 3.3: *a) PXRD patterns of 1⊃NO_3^-,1D⊃NO_3^- and 1 ⊅NO_3^- and b) TGA profile of 1⊃NO_3^- and 1 ⊅NO_3^-.*

weight loss. In our attempt to obtain the air dried phase or the desolvated phase of compound 1⊃NO_3^-I performed solvent exchange experiment with the compound by dipping the single crystals of 1⊃NO_3^-in acetone for about 6-7 days and then heating the compound at 50˚C under vacuum to get the guest solvent free phase of compound 1D⊃NO_3^-(**Figure 3.4**). Single crystal X-ray analysis of compound 1D⊃NO_3^-revealed that it belonged to Monoclinic system with space group *P21/c* with molecular formula $[Cu_2L_4(NO_3)_4(H_2O)]_n$. The asymmetric unit of compound contains two nonequivalent copper centers, four ligands, one coordinated water molecule, two nitrate anions coordinated to one copper centre in one case and one coordinated nitrate anion and one free nitrate anion in the other case. The ligand though adopts a cis- conformation as in 1⊃$NO_3^-$is sufficiently deviated from the parent compound and connects the nearby copper node .This results in breaking of the metal to ligand bond and the overall packing of the compound therefore changes drastically from the parent compound i.e.1⊃NO_3^-resulting in the

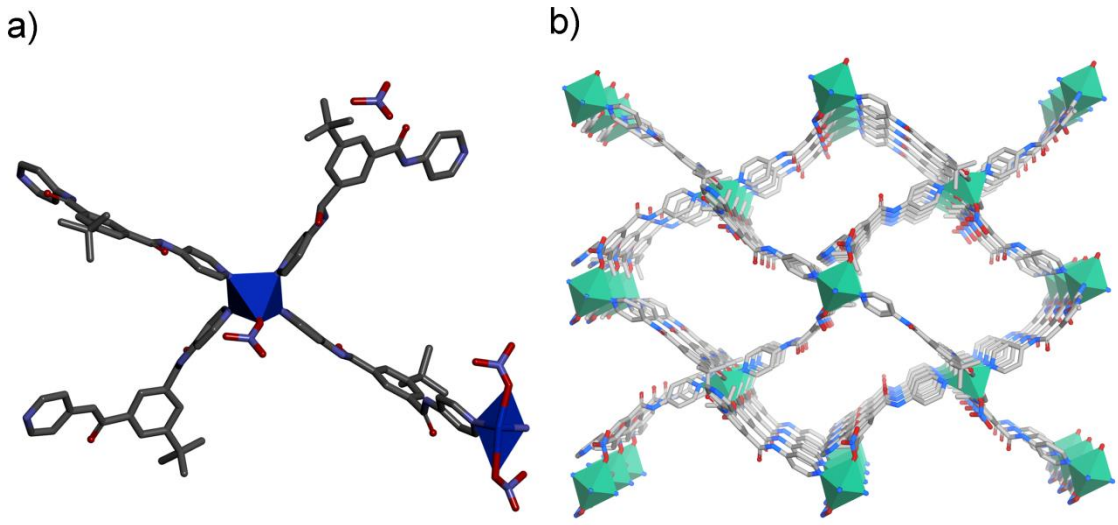

Figure 3.4 *a) Asymmetric unit of 1D⊃NO_3^-. Metals are shown in dark blue polyhedra and b) Single net of 1D⊃NO_3^- in perspective view. Metals are shown in dark green polyhedra.*

formation of non-porous 2D structure in 1D⊃NO_3^-in which the N-H protons of the ligand are hydrogen bonded to the oxygen atom of the coordinated nitrate anion (**Appendix 3.7**). Such structural changes in 1D coordination polymers upon desolvation have been vividly explained by Vittal and co-workers.[19] Although the compound 1D⊃NO_3^-has one coordinated water molecule the TGA pattern of the bulk sample shows no loss even at high temperature thereby confirming

that the compound loses the water molecule and our assumption is that free pyridyl nitrogen from the adjacent sheet coordinates to the copper centre. This may often happen because of air drying of the single crystals which results in the loss of the coordinated water molecules evenat ambient temperature. The PXRD pattern of the simulated pattern of the single crystal compound $1D\supset NO_3^-$and of the bulk sample $1'\supset NO_3^-$(after replacement of water molecule by pyridyl group) almost matches thereby confirming there is not much structural changes (2D structure is maintained) in the bulk sample after the loss of the water molecule from the copper node.As evidenced from X-ray data in as-synthesized compound $1\supset NO_3^-$the axial bonds containing coordinated NO_3^- are much elongated than the equatorial bonds and are consequently weakened due J-T distortion. In this view , I tried to perform anion exchange experiments with coordinating anions like SCN^-, N_3^-, Cl^-, Br^-, $I^-$and F^-ions in compound $1\supset NO_3^-$. While in all the other cases I observed the loss of crystallinity after anion exchange processes crystallinity were maintained in the case of SCN^- anions. Interestingly such anion exchange process could be monitored in a naked eye manner as the blue compound of $1\supset NO_3^-$transformed into dark green colour (**Figure 3.4 a**). Single crystals were obtained for compound $1\supset SCN^-$during anion exchangeprocess which revealed that the compoundbelonged to Monoclinic

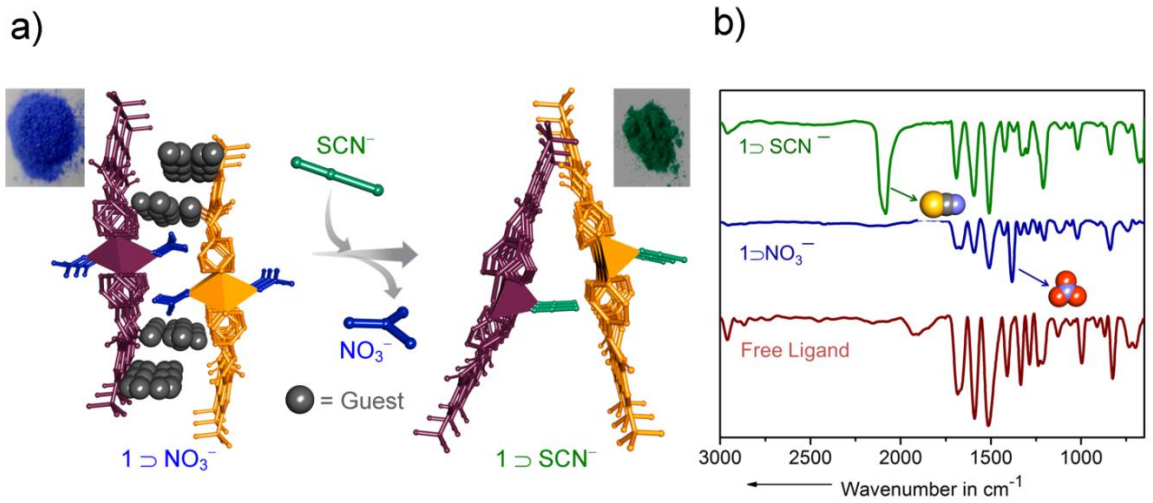

Figure 3.5: *a) Single-crystal to single-crystal structural transformation from $1\supset NO_3^-$ to $1\supset SCN^-$, resulting in a color change from blue to green. and b) FT-IR spectra of free ligand, $1\supset NO_3^-$, and $1\supset SCN^-$.*

system with space group *P21/n* and molecular formula $[\{CuL(SCN)_2\}\bullet xG]_n$. (G=disordered guest molecules). The asymmetric unit of compound $1\supset SCN^-$contains one copper, two ligands, one coordinated SCN^- anion and one free SCN^-anion. Each copper centre is coordinated to four pyridyl nitrogen of the four ligands and one coordinated SCN^-which replaced the NO_3^- anions from the axial position in $1\supset NO_3^-$to furnish a square pyramidal geometry (**Figure 3.6**).The two cooper centers are connected by two strands of ligands and results in a one- dimensional ribbonlike structure (**Appendix 3.8**). The two different one dimensional strands are notparallel as in the case of $1\supset NO_3^-$due to the loss of the o-xylene guest molecules during anion exchange process. This results in a complete non- porous structure of compound $1\supset SCN^-$. The change in the structure of

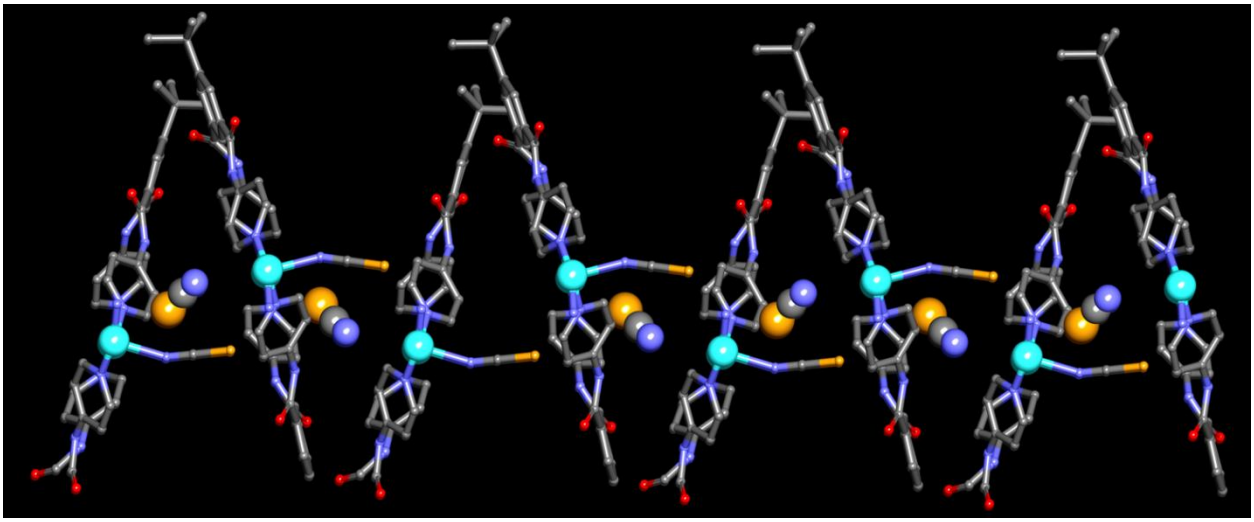

Figure 3.6:*Two different dimensional chains in* $1\supset SCN^-$*. Metal centers and anions are shown in space fill model.*

the compound upon anion exchange was also supported by PXRD data which shows a definite difference in the patterns of the two compounds ($1\supset NO_3^-$and $1\supset SCN^-$) which demonstrates the dynamic anion exchange properties of $1\supset NO_3^-$(**Appendix 3.10**). The anion exchange completion was monitored by FT-IR and whereas bulk sample purity was confirmed by PXRD (**Appendix 3.9**) and CHNS results. The IR spectra of the compound $1\supset NO_3^-$and $1\supset SCN^-$shows disappearance of the peak for NO_3^-anion and emergence of new peak of SCN^- around

~2071cm^{-1}(**Figure 3.5 b**) whereas CHN results confirm quantitative exchange (~95%) exchange of NO_3^- by SCN^- anions. Also such an anion exchange process was found to be irreversible in nature. SCN^- anions are known to be present in blood plasma because of its source from foods, car exhausts and cigarettes and therefore have a biological impact.[20] Therefore selective sensing of SCN^- anions by visual colorimetric anion exchange behavior in MOFs are important and have been reported very rarely in literature.

To investigate the structural dynamism and the effect of amide functionality of the non-porous framework 1′⊃NO_3^-sorption measurements were carried out for various gases and solvent vapors. Gas adsorption measurements were carried out at lowtemperatures for various gases like CO_2, N_2, H_2, Ar and CH_4. For CO_2 measurement at 195 K the compound shows a uptake of around 84mL/g whereas for other gases (N_2, H_2, Ar and CH_4) the compound shows negligible uptake (**Figure 3.7**). Such selectivity of CO_2 and corresponding transformation from the nonporous phase to microporous phase of compound 1′⊃NO_3^-can be ascribed to the strong dipole quadrupolar interaction of the CONH groups with the incoming CO_2 molecules. This results in strong host

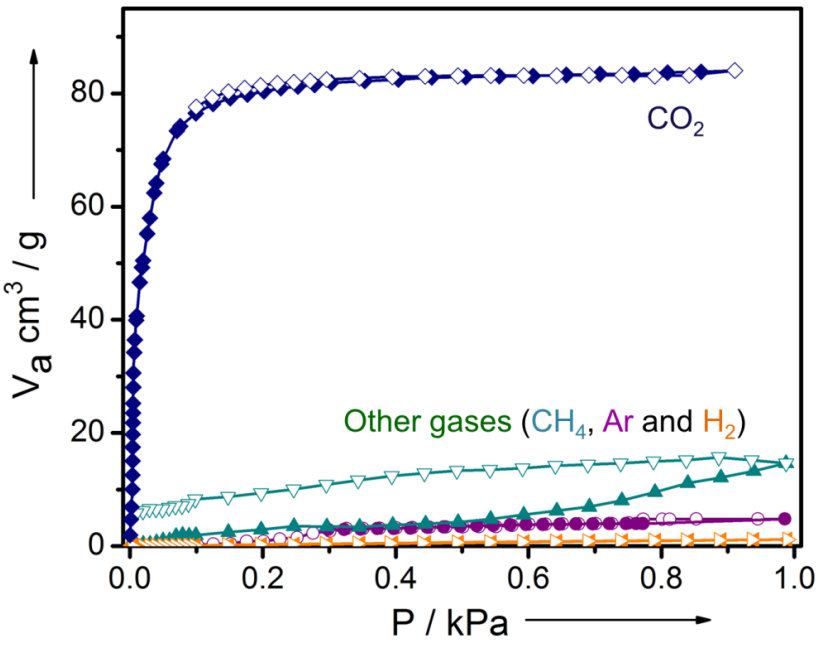

Figure 3.7: *Gas adsorption isotherms of CO_2 and other gases (H_2, Ar and CH_4) at low temperatures in 1⊃NO_3^- showing clear separation.*

guest interaction due to confinement effect and therefore results in such preferential uptake. Solvent sorption measurements were carried out at 298K to confirm the dynamic nature of the compound. Hydrophilic solvents like EtOH, PrOH, BuOH and H_2O show a very high uptake amount with a typical hysteretic nature at low P/P_0 pressures. This type of behavior is consistent with the dynamic nature of the compound 1′ↄNO_3^-which results due to structural changes in the host framework. The favorable attractive hydrogen bonding interactions of the -OH groups of the incoming guest molecules with the pendent amide groups result in opening of the host framework consequently giving rise to such high uptake (**Figure 3.8**). Also, such uptake amount is size dependent which confirms the size effect in such adsorption process. In order to confirm the structural dynamism as evidenced from the sorption results PXRD experiment was performed with the vapor exposed sample of 1′ↄ$NO_3^-$with various hydrophilic solvents. From the PXRD pattern it is evident that upon exposure to solvents like EtOH, PrOH, BuOH the host framework undergoes subtle structural changes which may be due the dynamic nature of the compound and/or may be also because of inclusion of solvents of different sizes (**Figure 3.9 b**).

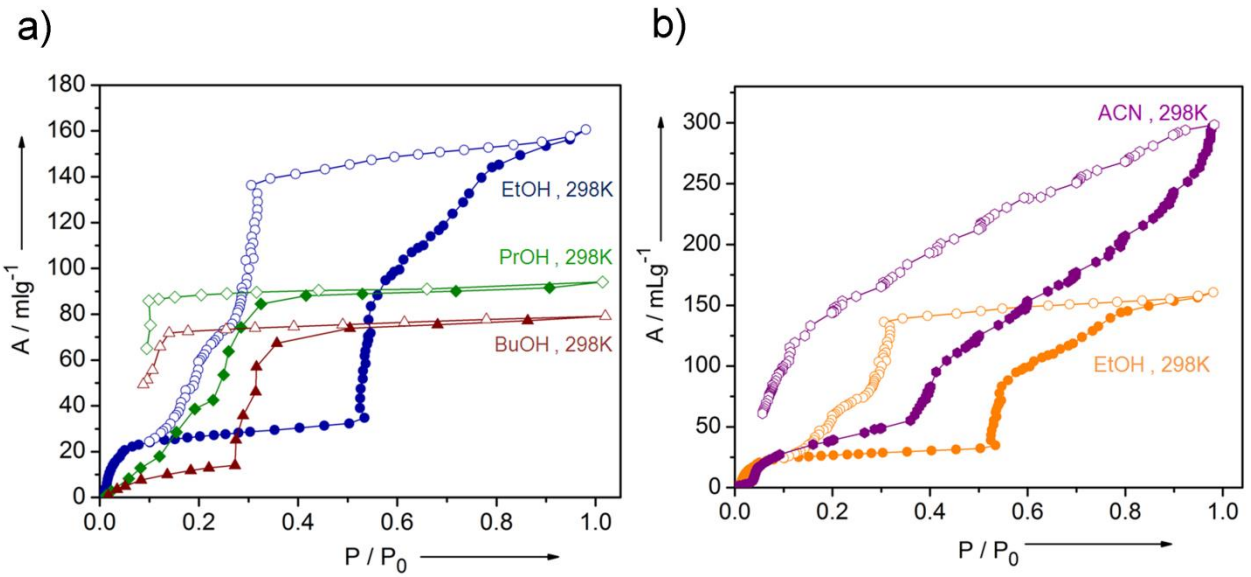

Figure 3.8: *a) Sorption profile showing size dependent uptake of alcohols for compound 1ↄNO_3^- at 298K and b) adsorption profile comparison of ethanol and acetonitrile for compound 1ↄNO_3^-.*

As discussed earlier separation of benzene and cyclohexane requires significant attention because of their similarities in physical properties resulting in difficulties in their separation in petrochemical industries. Although non-porous, compound 1′⊃$NO_3^-$was found to be structurally flexible in nature and I speculated that the amide functionality with basic sites[21] could be utilized for separation of benzene and cyclohexane. In this regard, I performed sorption measurements with these two species at 298K. Sorption results show a considerably high uptake amount of benzene (~2 molecules per formula unit) whereas negligible uptake amount in the case of cyclohexane (**Figure 3.9 a**). This may be because acidity of C-H proton in benzene is

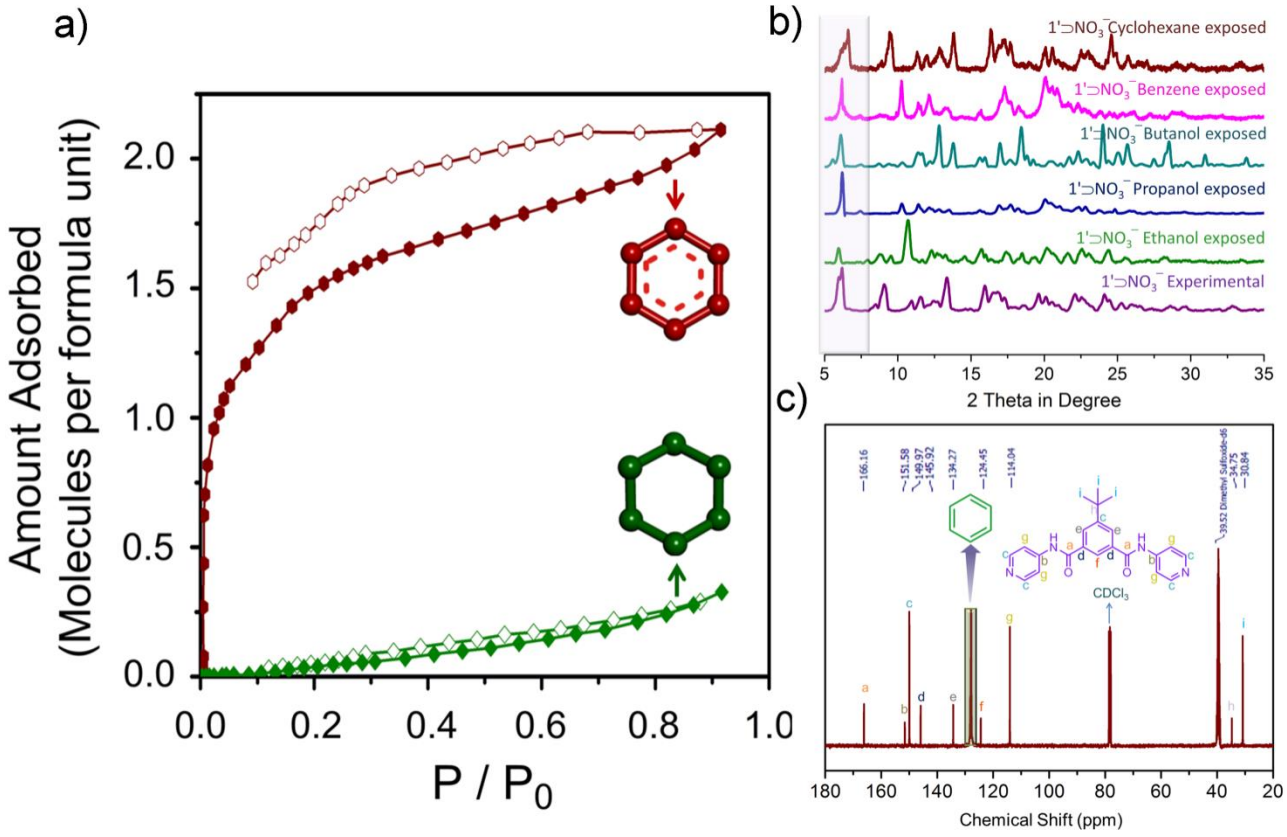

Figure 3.9: *a) Benzene and cyclohexane adsorption profile of compound 1⊃NO_3^- at 298 K, b) PXRD patterns of 1⊃NO_3^- and other solvent exposed samples and c) ^{13}C- NMR spectra of digested sample of 1⊃NO_3^- exposed to 1:1 mixture of benzene and cyclohexane vapors.*

comparatively more than cyclohexane C-H proton due the hydrogen atom in benzene is located in the sp^2 hybridized orbital as compared to the sp^3 hybridized orbital of the hydrogens of

cyclohexane.[22]As a result the interaction of benzene is much more with basic amide functionality in the framework. Moreover, due to π–π interactions or C–H/π interactions between the adsorbed molecules and the aromatic rings of the framework the preferential uptake of benzene is favored. All these factors combined, 1′ↄNO_3^-can efficiently act as a suitable adsorbate for selective uptake of benzene over cyclohexane. The selectivity achieved in this case is comparable to the selectivity of Benzene/Cyclohexane by MOFs reported in literature (**Appendix 3.13**). The PXRD pattern of the benzene and cyclohexane vapor exposed samples of 1′ↄNO_3^-shows that in case of cyclohexane exposed samples there are not much changes in the PXRD pattern of the compound. However, in case of benzene exposed samples a slight variation in PXRD pattern is observed which may be attributed to the interaction of the benzene molecules with the framework.To further corroborate this fact the compound 1′ↄ$NO_3^-$was exposed to vapors of 1:1 mixture containing benzene and cyclohexane and thereafter digested with DCl and extracted with $CDCl_3$ and D_2O afterwhich the sample was characterized by ^{13}C-NMR. The ^{13}C NMR spectra shows a prominent peak of benzene along with the ligand which conclusively proves that the compound 1′ↄNO_3^-selectively takes benzene even from a mixture of benzene and cyclohexane (**Figure 3.9 c**). UV-VIS reflectance spectra of 1′ↄNO_3^-, benzene and cyclohexane exposed sample were recorded at 298K. The UV spectra shows that the benzene exposed sample shows a prominent shift whereas the cyclohexane exposed sample shows no remarkable shift with respect to compound 1′ↄNO_3^-(**Appendix 3.12**).

In conclusion, I synthesized a novel 1D metal-organic framework base on a flexible neutral amide based N donor ligand. The framework underwent interesting structural transformation upon desolvation and this guest free phase could be utilized for separation of CO_2 and other non-polar gases like N_2, H_2, and CH_4 at low temperatures. Moreover, the combination of structural flexibility and guest responsive enzymatic behavior has been used to address one of the important challenges of chemical industries i.e. separation of benzene and cyclohexane. In view of achieving further versatility visual colorimetric detection of SCN^-anions has also been studied via anion exchange process which is rarely reported in literature. Such incorporation of multi-functionalities in MOFs is an important aspect and if achieved in an economical fashion could be the most sought material in chemical industries for the future.

3.5. References:

1. a) Keeffe, M. O.;Yaghi, O. M.,*Chem. Rev*. **2012**, *112*, 675; b) Wang, C.; Zhang, T.;Lin, W.;*Chem. Rev*. **2012**, *112*, 1084; c) Zhou, H. C;Long, J. R;Yaghi, O. M.; *Chem. Rev*. **2012**, *112*, 673 ; d) Nagarkar, S. S.;Joarder, B.;Chaudhari, A. K.;Mukherjee, S.;Ghosh, S. K.;*Angew. Chem., Int. Ed*. **2013**, *52*, 2881; e) Horcajada, P.;Gref, C.; Baati, T.;Allan,P. K.;Maurin, G.;Couvreur, P.;Ferey, G.;Morris, R. E.;Serre, C.;*Chem. Rev*. **2012**, *112*, 1232; f) Vittal, J. J.; Coord. *Chem. Rev*. **2007**, *251*, 1781; g) Ohba, M.;Yoneda, K.; Agustí, G.;Muñoz, M. C.;Gaspar, A. B.;Real, J. A.;Yamasaki, M.;Ando, H.;Nakao, Y.;Sakaki, S.;Kitagawa, S. *Angew. Chem. Int. Ed*. **2009**, *48*, 4767; h) Reinsch, H.;Kruger, M.;Marrot, J.;Stock, N. *Inorg. Chem*. **2013**, *52*, 1854;

2. a) Guo, Z.;Cao, R.;Wang, X.;Li, H.;Yuan, W.;Wu, G. H.;Li, J. *J. Am. Chem. Soc*. **2009**, *131*, 6894; b) Fang, Q. R.;Zhu, G. S.;Jin, Z.;Xue, M.;Wei, X.;Wang, D.;Qiu, S.L. *Angew. Chem. Int. Ed*. **2006**, *45*, 6126 ; c) Park, I. H.;Chanthapally, A.;Zhang, Z.;Lee, S. S.;Zaworotko, M. J.;Vittal, J. J.; *Angew. Chem. Int. Ed*. **2014**, *53*, 414; d) Hasegawa, S.;Horike, S.;Matsuda, R.;Furukawa, S.; Mochizuki, K.;Kinoshita, Y.;Kitagawa S. *J. Am. Chem. Soc*. **2007**, *129*, 2607.

3. a) Horike, S.;Shimomura, S.;Kitagawa, S. *Nat. Chem*. **2009**, *1*, 695; b) Ghosh, S. K.;Bureekaew, S.;Kitagawa, S.;*Angew. Chem. Int. Ed*. **2008**, *47*, 3403; c) Henke, S.;Schneemann, A.;Wütscher, A.;Fischer, R.A. *J. Am. Chem. Soc*. **2012**, *134*, 9464. d) Schneemann, A.;Bon, V.; Schwedler, I.;Senkovska, I.;Kaskel, S.;Fischer, R.A. *Chem. Soc. Rev*. **2014**, *43*, 6062; d) Lun, D. J.;Waterhouse, G. I. N.;Telfer, S. G. *J. Am. Chem. Soc*. **2011**, *133*, 5806. e) Manna, B.;Chaudhari, A. K.; Joarder, B.;Karmakar, A.;Ghosh, S. *Angew. Chem. Int. Ed*. **2013**, *52*, 998 ; f) Yanai, N.;Kitayama, K.;Hijikata, Y.;Sato, H.;Matsuda, R.;Kubota, Y.;Takata, M.;Mizuno, M.;Uemura, T.;Kitagawa, S. *Nat. Mater*. **2011**, *10*, 787;
4. a) Khan, N.A.;Hasan, Z.; Jhung, S. H. *J. Haz. Mat*. **2013**, *244*, 444; b) Farha, O. K.;Spokoyny, A. M.;Mulfort, K. L.; Hawthorne, M. F.;Mirkin, C. A.;Hupp, J. T. *J. Am.*

Chem. Soc. **2007**, *129*, 12680; c) Vincenzo, G. D.;Ferenc, F.;Donald, H.;Jiří, J. K. *J. Cl. Prod*. **2009**, *17*, 889; d) Li, S. L.;Xu, Q.*Energy Environ. Sci*. **2013**, 6, 1656.

5. a) Villaluenga, J. P. Garcia;Tabe-Mohammadi, A. *J. Membr. Sci*., **2000**,*169*, 159; b) Uemasu, I.;Kushiyama, S. *Fuel Process. Technol*. **2004**, *85*, 1519; c) Qin, J. W.;Ye, Q.;Xiong, X. J.;Li, N. *Ind. Eng. Chem. Res*. **2013**, *52*, 10754.

6. a) Hijikata, Y.;Horike, S.;Sugimoto, M.;Sato, H.;Matsuda, R.;Kitagawa, S. *Chem. Eur. J*. (DOI: 10.1002/chem.201003734); b) Gade, S. K.;Tuan, V. A.;Gump, C. J.;Noble, R. D.;Falconer, J. L. *Chem. Commun*. **2001**, 601; c) Shimomura, S.;Horike, S.;Matsuda, R.;Kitagawa, S. *J. Am. Chem. Soc*., **2007**, *129*, 10990; d) Bai, Y. X.;Qian, J. W.;Zhao, Q.;Xu, Y.;Ye, S. R. *J. Appl. Polym. Sci*. **2006**, *102*, 2832.

7. a) Peralta, D.;Chaplais, G.;Masseron, A. S.;Barthelet, K.;Chizallet, C.;Quoineaud, A. A.;Pirngruber, G. D.;*J. Am. Chem. Soc*. **2012**, *134*, 8115; b) Y. He, W. Zhou, R. Krishna, B. Chen. *Chem. Commun*. **2012**, *48*, 11813.

8. a) Liu, Q. K.;Ma, J. P.;Dong, Y. B. *Chem. Eur. J*. **2009**, *15*, 10364; b) Mukherjee, S.;Joarder, B.;Manna, B.;Desai, A. V.;Chaudhari, A. K.;Ghosh, S. K. *Sci. Rep*. DOI: 10.1038/srep05761; c) Joarder, B.; Mukherjee, S.; Chaudhari, A. K.;Desai, A.V.;Manna, B.; Ghosh, S. K. *Chem. Eur. J*. **2014**, *20*, 15303.

9. a) Xiong, S.;He, Y.;Krishna, R.;Chen, B.;Wang, Z. *Cryst. Growth Des*. **2013**, *3*, 2670.

10. (a) Wang, J. H.;Li, M.;Li, D. *Chem. Sci*. **2013**,*4*, 1793; (b) Manna, B.;Chaudhari, A. K.;Joarder, B.;Karmakar, A.;Ghosh, S. K. *Angew. Chem. Int. Ed*. **2013**, *52*, 998; (c) Halper, S. R.;Do, L.;Stork, J. R.;Cohen, S. M. *J. Am. Chem. Soc*. **2006**,*128*, 15255; d) Hou, S.;Liu, Q. K.;Ma,J. P.;Dong, Y. B. *Inorg. Chem*. **2013**, *52*, 3225; e) Maji, T. K.;Matsuda, R.;Kitagawa, S. *Nat. Mater*. **2007**, *6*, 142; f) Karmakar, A.;Manna, B.; Desai, A.V.; Joarder, B.;Ghosh, S.K. *Inorg. Chem*. DOI: 10.1021/ic501477u; g) Manna, B.; Joarder, B.;Desai, A. V.;Karmakar, A.;Ghosh, S. K. *Chem. Eur. J*. **2014**, *20*, 12399.

11. a) Chen, B.;Wang, L.;Zapata, F. G. Qian, E. Lobkovsky, B. *J. Am. Chem. Soc*. **2008**, *130*, 6718; b) Bauer, C. A.;Timofeeva, T. V.;Settersten, T. B.;Patterson, B. D.;Liu, V. H.;Simmons, B. A.;Allendorf, M. D. *J. Am. Chem. Soc*. **2007**, *129*, 7136; c) Gong, Y.;Qin, J. B.;Wu, T.;Li, J. H.;Yang, L.;Cao, R. *Dalton Trans*. **2012**, *41*, 1961; d) Palacios, M. A.;Nishiyabu, R.;Marquez, M.;Anzenbacher,P. *J. Am.Chem. Soc*. **2007**, *129*, 7538; (e) Lavigne, J. J.;Anslyn, E. V.;*Angew.Chem., Int. Ed*. **1999**, *38*, 3666.

12. a) Ma, J. P.;Yu, Y.;Dong, Y. B. *Chem. Commun*. **2012**, *48*, 2946; b) Chen, Y.-Q.;Li, G.-R.;Chang, Z.;Qu, Y.-K.;Zhang, Y.H.; Bu, X. H. *Chem. sci*. 2013, *4*, 3678.

13. a) Kreno, L. E. et al. *Chem.Rev*. **2012**, *112*, 1105; b) Kreno, L. E.;Leong, K.;Farha, O. K.;Allendorf, M.; R.P. Duyne,V.;Hupp, J. T. *Chem. Rev*. **2012**, *112*, 1105.

14. a) Leong, W. L.;Vittal, J. J. *Chem. Rev*. **2011**, *111*, 688; b) Nagarathinam, M.;Vittal, J. J. *Chem. Commun*., **2008**, 438–440; c) Nagarathinam, M.;Vittal, J.J. *Angew. Chem. Int. Ed*. **2006**, *45*, 4337.

15. a) Hipps, K. W.; Mazur, U.*J. Phys. Chem*., **1992**, 96 , 1160; b) Tanaka,A.; K. Deguchi, Deguchi, T. *Anal. Chimi. Acta*, **1992**, 261, 281.

16. Streitwieser Jr., A.;Caldwell, R. A.;Young,W. R.;*J. Am. Chem. Soc*., **1969**, 91 , 529.

Appendix:

Appendix 3.1: *Crystal data and structure refinement for compound* ***1⊃NO₃⁻***.

Identification code	**Compound 1⊃NO_3^-**	
Identification code	Compound 1⊃NO_3^-	
Empirical formula	C_{58} H_{64} Cu N_{12} O_{12}	
Formula weight	1184.75	
Temperature	200(2) K	
Wavelength	0.71073 Å	
Crystal system	Monoclinic	
Space group	*P 2/c*	
Unit cell dimensions	a = 16.6868(19) Å	α= 90°.
	b = 13.6318(16) Å	β= 107.420(2)°.
	c = 15.1712(18) Å	γ = 90°.
Volume	3292.7(7) Å3	
Z	2	
Density (calculated)	1.195 Mg/m^3	
Absorption coefficient	0.396 mm^{-1}	
F(000)	1242	
Theta range for data collection	1.279 to 28.323°.	
Index ranges	-22<=h<=21, -18<=k<=18, -20<=l<=20	
Reflections collected	33031	
Independent reflections	8151 [R(int) = 0.0546]	
Completeness to theta = 25.242°	99.9 %	
Refinement method	Full-matrix least-squares on F^2	
Data / restraints / parameters	8151 / 0 / 381	
Goodness-of-fit on F2	1.260	
Final R indices [I>2sigma(I)]	R1 = 0.0683, wR2 = 0.1955	
R indices (all data)	R1 = 0.0955, wR2 = 0.2082	
Extinction coefficient	n/a	
Largest diff. peak and hole	1.402 and -1.137 $e.Å^{-3}$	

Appendix 3.2: *Crystal data and structure refinement for compound* ***1D⊃NO₃⁻***

Identification code	**Compound 1D⊃NO_3^-**	
Identification code	Compound 1D⊃NO_3^-	
Empirical formula	C_{88} H_{90} Cu_2 N_{20} O_{21}	
Formula weight	1890.87	
Temperature	293(2) K	
Wavelength	0.71069 Å	
Crystal system	Monoclinic	
Space group	P 21/c	
Unit cell dimensions	a = 26.374(5) Å	α= 90.000(5)°.
	b = 15.514(5) Å	β= 109.561(5)°.
	c = 23.053(5) Å	γ = 90.000(5)°.
Volume	8888(4) Å3	
Z	4	
Density (calculated)	1.413 Mg/m^3	
Absorption coefficient	0.563 mm^{-1}	
F(000)	3936	
Theta range for data collection	0.819 to 22.284°.	
Index ranges	-19<=h<=27, -16<=k<=16, -24<=l<=23	
Reflections collected	74975	
Independent reflections	10923 [R(int) = 0.3244]	
Completeness to theta = 25.240°	67.9 %	
Refinement method	Full-matrix least-squares on F^2	
Data / restraints / parameters	10923 / 42 / 1144	
Goodness-of-fit on F2	0.998	
Final R indices [I>2sigma(I)]	R1 = 0.1228, wR2 = 0.2814	
R indices (all data)	R1 = 0.3148, wR2 = 0.3955	
Extinction coefficient	n/a	
Largest diff. peak and hole	1.561 and -0.629 $e.Å^{-3}$	

\

Appendix 3.3: *Crystal data and structure refinement for compound* ***1⊃SCN⁻***

Identification code	**Compound 1⊃SCN⁻**	
Identification code	Compound 1⊃SCN⁻	
Empirical formula	C_{46} H_{43} Cu N_{10} O_4 S_2	
Formula weight	927.56	
Temperature	200(2) K	
Wavelength	0.71073 Å	
Crystal system	Monoclinic	
Space group	*P 21/n*	
Unit cell dimensions	a = 12.3742(14) Å	α= 90°.
	b = 29.549(3) Å	β= 97.083(2)°.
	c = 14.0120(16) Å	γ = 90°.
Volume	5084.3(10) Å3	
Z	4	
Density (calculated)	1.212 Mg/m^3	
Absorption coefficient	0.561 mm^{-1}	
F(000)	1928	
Theta range for data collection	1.378 to 26.718°.	
Index ranges	-13<=h<=15, -25<=k<=37, -17<=l<=17	
Reflections collected	81491	
Independent reflections	10679 [R(int) = 0.0961]	
Completeness to theta = 25.242°	100.0 %	
Refinement method	Full-matrix least-squares on F^2	
Data / restraints / parameters	10679 / 12 / 574	
Goodness-of-fit on F^2	1.187	
Final R indices [I>2sigma(I)]	R1 = 0.0688, wR2 = 0.1845	
R indices (all data)	R1 = 0.1018, wR2 = 0.1974	
Extinction coefficient	n/a	
Largest diff. peak and hole	1.643 and -0.927 $e.Å^{-3}$	

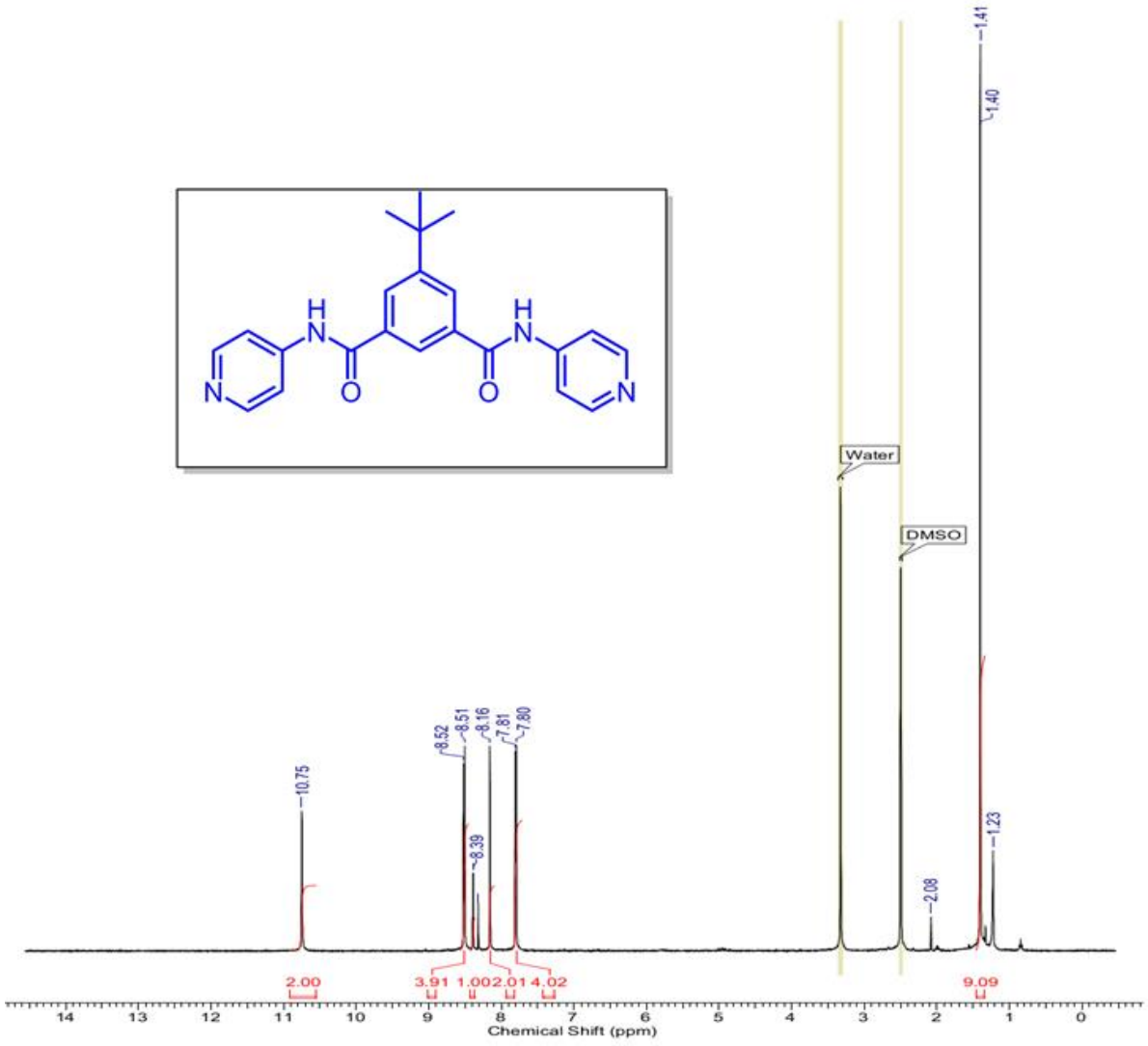

***Appendix 3.4**: [1]H-NMR of Ligand (L).*

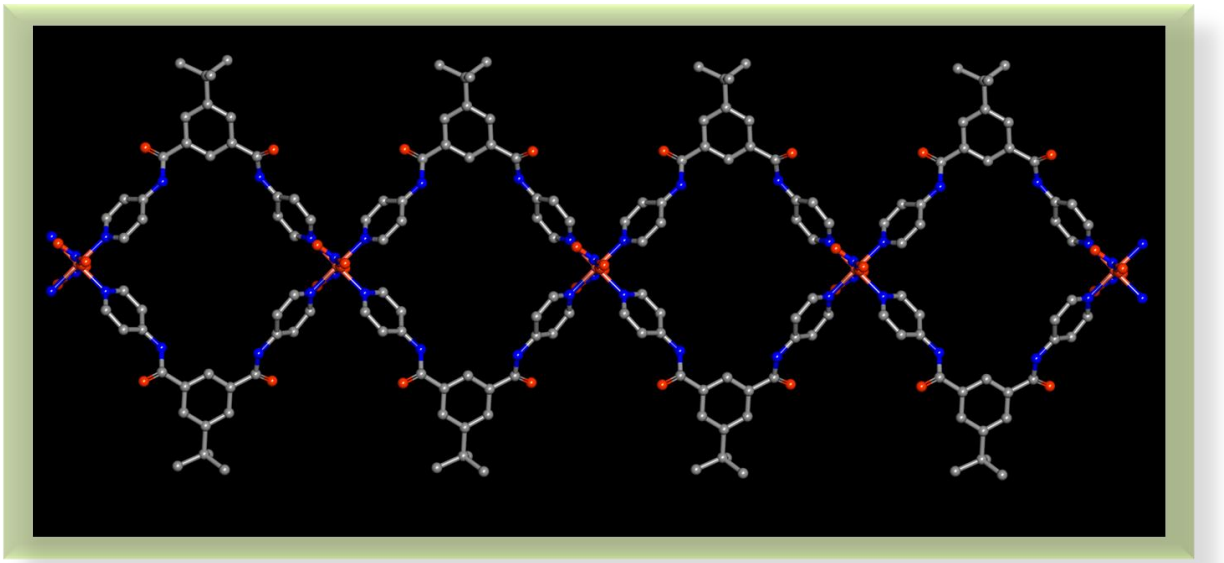

Appendix 3.5: *Coordination environment around the metal centre showing octahedral geometry around Cu centre in 1⊃NO_3^-. Hydrogen atoms have been deleted for clarity. (Color code; Carbon: gray, oxygen: red, nitrogen: blue, zinc: brown).*

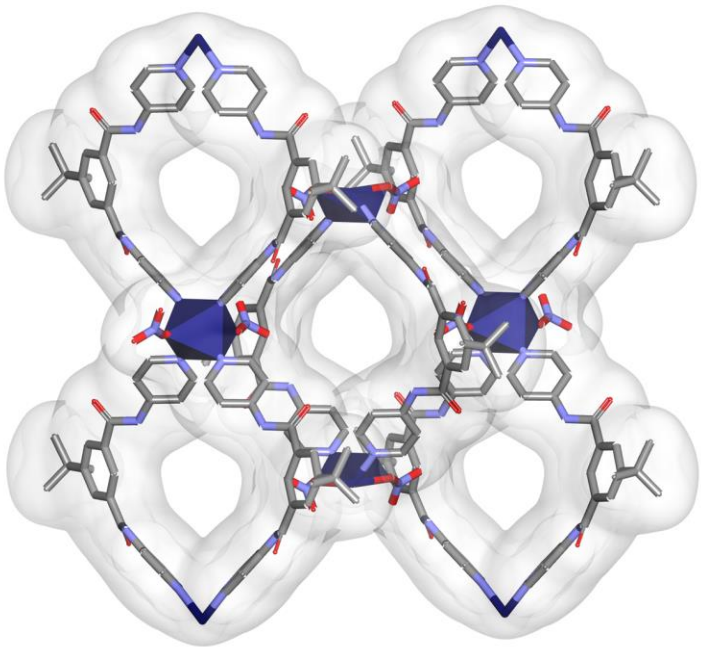

Appendix 3.6: *Surface view of 1⊃NO_3^-. Metals are shown in blue polyhedra.*

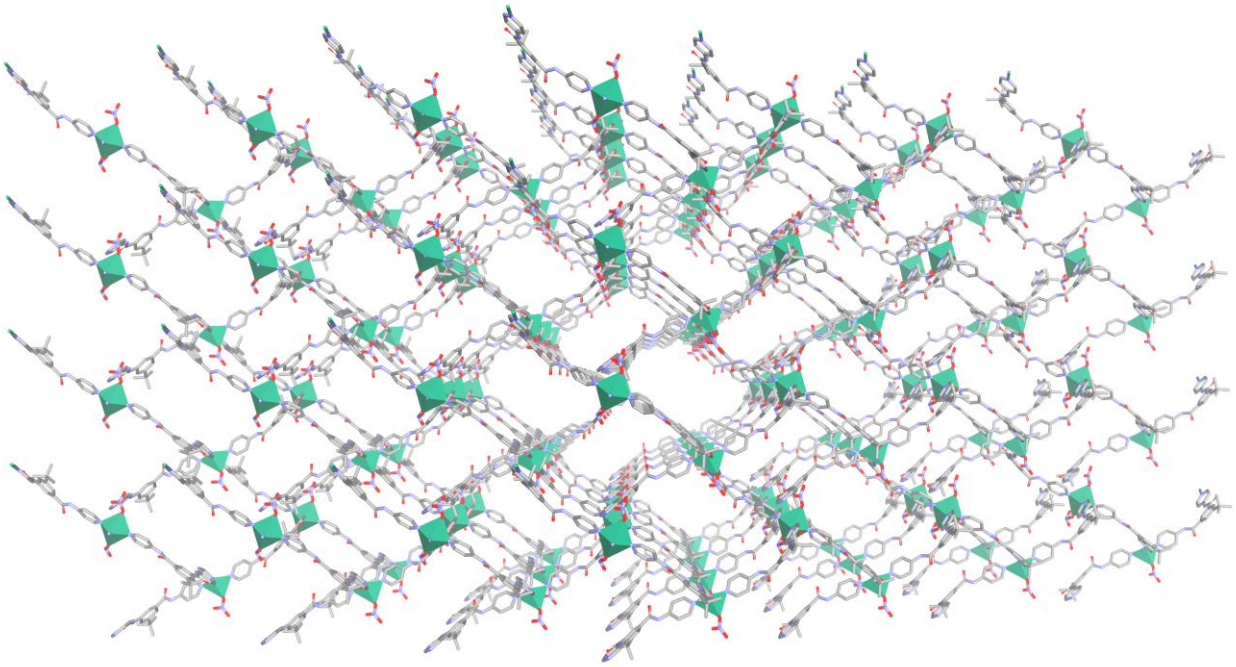

Appendix 3.7: *Single net of 1D⊃NO_3^- in perspective view. Metals are shown in dark green polyhedra.*

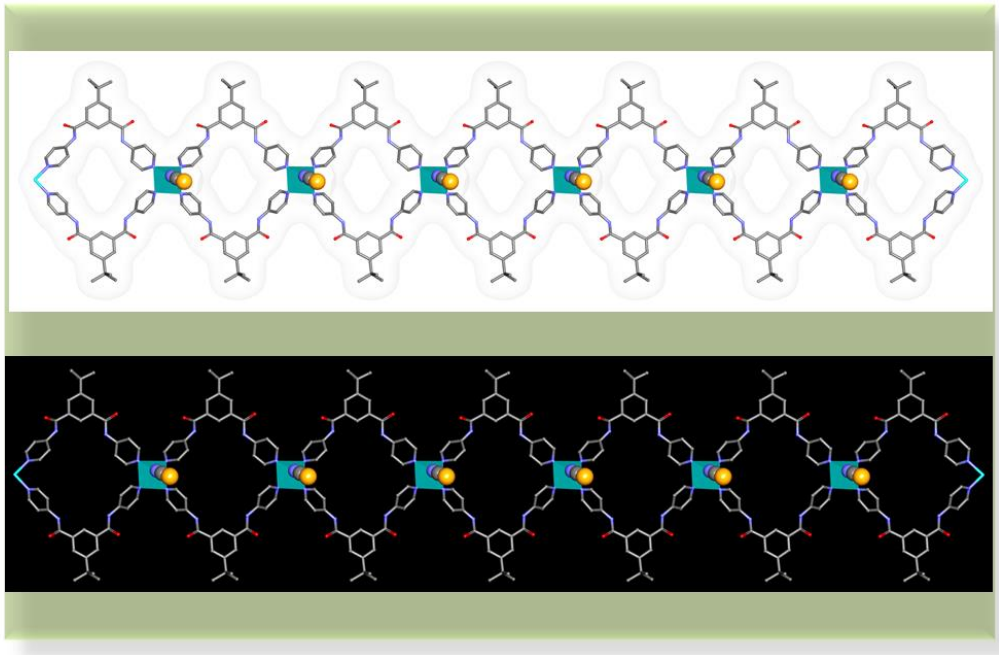

Appendix 3.8*: Ribbon like one dimensional chain in 1⊃SCN^-.*

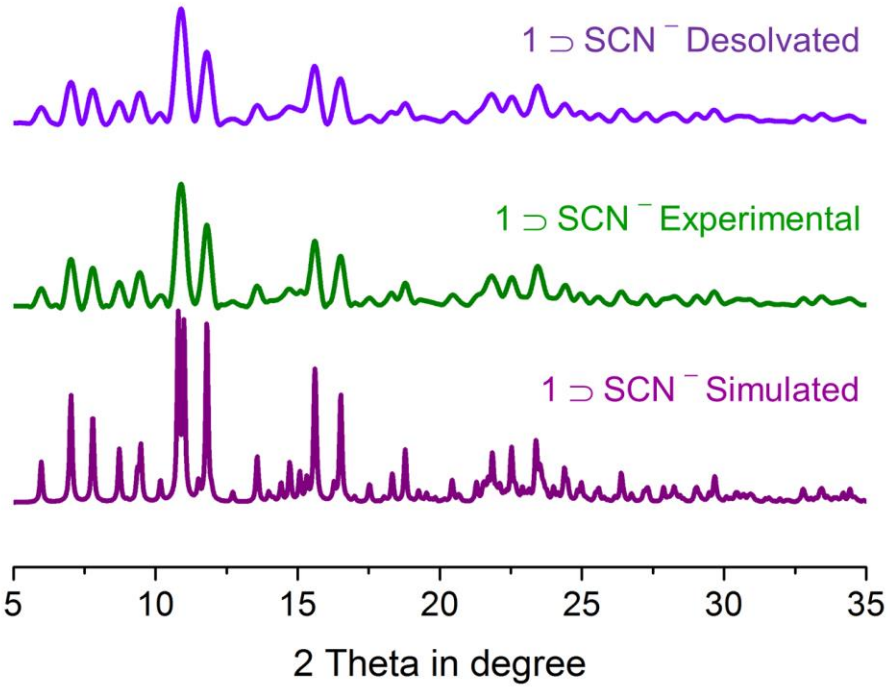

***Appendix 3.9**: PXRD patterns of compound 1⊃SCN^- simulated, assynthesized and desolvated.*

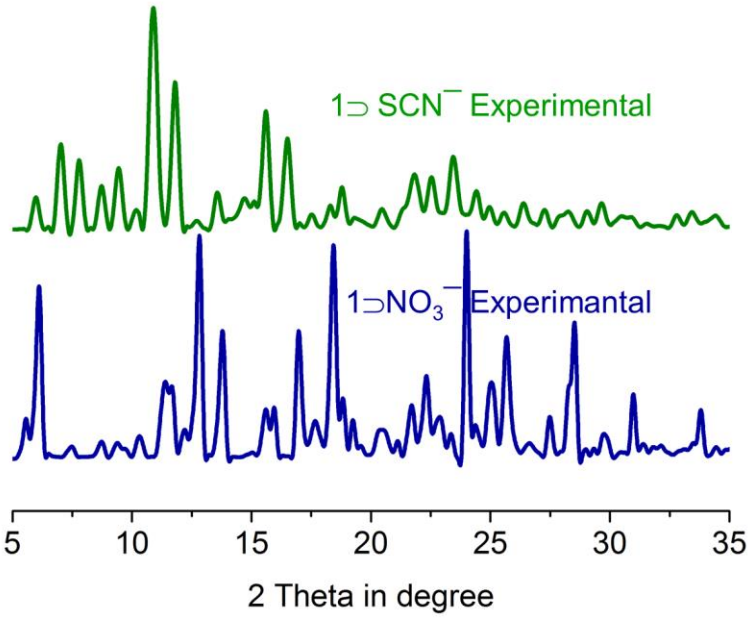

***Appendix 3.10**: Comparison of PXRD patterns of compound 1⊃SCN^- (Experimental) and compound 1⊃NO_3^- (Experimental).*

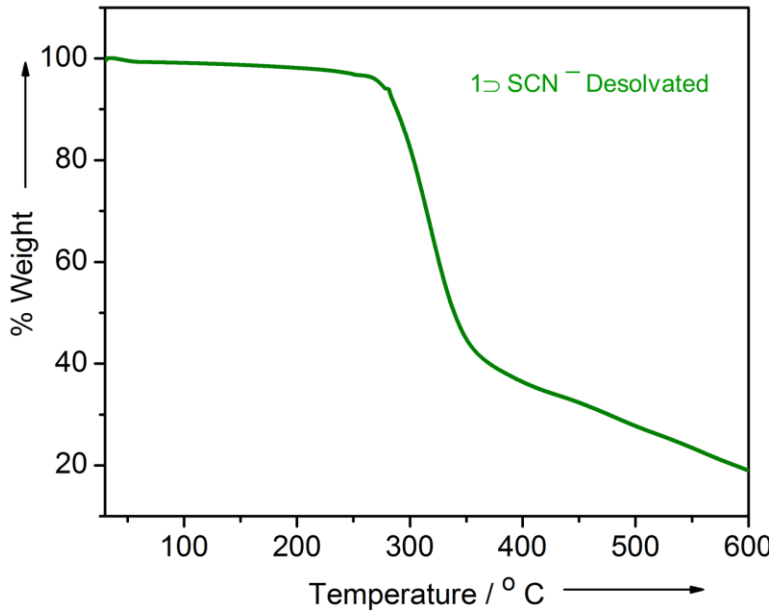

Appendix 3.11: *TGA pattern of the desolvated compound 1⊃SCN¯*

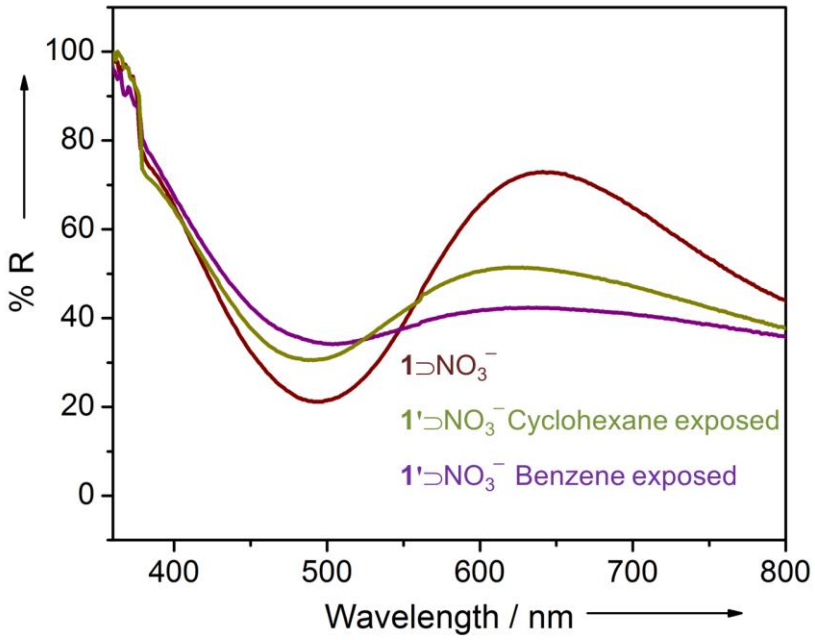

Appendix 3.12*: UV-VIS reflectance spectra benzene and cyclohexane exposed phases of 1′ ⊃NO_3^-.*

Appendix 3.13*: Benzene Cyclohexane separation results of some known porous materials.*

No.	Type of Porous Material	Compound name/ Formula	Uptake amount of Benzene/Cyclohexane (A/ mlg^{-1}, A/ $mmolg^{-1}$, A/ mg g^{-1}, A/ formula unit, wt. %)	Year	Journal name	Reference
1.	Metal-Organic framework (present work*)	$[Cu_2L_4(NO_3)_4]_n$	~2 / ~0.25 molecules per formula unit	2015	Present work	1.
2.	Zeolite membrane	FAU-type	35.89/26.51 molecules/formula unit	2003	*Journal of Membrane Science*	2.
3.	Metal-Organic framework	{[Zn(μ-4-TCNQ-TCNQ)bpy]. 1.5benzene}$_n$	~80mlg^{-1}/~15mlg^{-1}	2007	*J. Am. Chem. Soc.*	3.
4.	Metal-Organic framework	MAF-2	3.0 / 0.1 per formula unit	2008	*J. Am. Chem. Soc.*	4.
5.	Covalent Organic Framework(COF)	PAF-2	138 mg g^{-1} / 7 mg g^{-1}	2009	*Chem. Commun.*	5.
6.	Metal-Organic framework	$[Cu_2I_2$ (BTTP4)$]_n$	20.3 wt %/ >10 wt. %	2010	*Chem. Asian J.*	6.
7.	Metal-Organic framework	CID-23	27 mLg^{-1}/~2mLg^{-1}	2011	*Chem. Eur. J.*	7.
8.	Metal-Organic framework	$[Ni_3(OH)(Ina)_3(BDC)_{1.5}]_n$	22.60 / 1.40 wt%,	2011	*J. Mater. Chem.*	8.
9.	Microporous polyimide networks	MPI-1 MPI-2 MPI-3	119.8/ 50.1 (wt. %) 76.6/ 44.8 (wt. %) 54.9/ 41.5(wt. %)	2013	*Macromolecules*	9.
10.	Metal-Organic framework	$[Zn(BCbpy)(PMA)_{0.5}].7H_2O.DMF$(**1-bpy**) and $[Zn(BCbpe)(PMA)_{0.5}].8H_2O.DMF$ (**2-bpe**)	1.5 /~0.15 molecules per ring unit and 0.6 / 0.13 molecules per ring unit)	2014	*J. Mater. Chem.*	10.

References:

1) Karmakar, A., Desai, A. V., Manna, B., Joarder, B. Ghosh S. K. *Chem. Eur. J*. **2015**, *21*, 7071 – 7076

2) Jeong, B. H., Hasegawa,Y., Sotowa, K.I,. Kusakabe, K., Morooka, S. *J. Mem. Sci*. **2003**, *213*, 115–124.

3) Shimomura, S., Horike,S., Matsuda, R., Kitagawa. S. *J. Am. Chem. Soc*. **2007**, *129*, 1099- 10991.

4) Zhang, J.-P., Chen, X.-M. *J. Am. Chem. Soc*., **2008**, *130*, 6010–6017.

5) Ren, H., Ben, T., Wang, E., Jing, X., Xue, M., Liu, B., Cui, Y., Qiu, S., Zhu, G. *Chem. Commun*. **2010**, *46*, 291–293.

6) Yang, R., Li, L., Xiong, Y., Li, J. R., Zhou, H.C., Su, C. Y., *Chem. Asian J*. **2010**, *5*, 2358–2368.

7) Hijikata, Y., Horike, S., Sugimoto, M., Sato, H., Matsuda, R., Kitagawa, S. *Chem. Eur. J*. **2011**, *17*, 5138 – 5144

8) Liu, G. S., Ma, F., Wei, F., Tang, Q., Yang, Y., Liang, D., Li , S., Chen,Y. *J. Mater. Chem*. **2011**, *21*, 15909.

9) Li, G., Wang, Z. *Macromolecules*. **2013**, *46*, 3058−3066.

10) Ren, C. X., Cai, L.X., Chen, C., Tan, B., Zhang, Y.J., Zhang, J. *J. Mater. Chem. A*, **2014**, *2*, 9015–9019.

Chapter -4

A Post-synthetically Modified MOF for Selective and Sensitive Aqueous Phase Detection of Highly Toxic Cyanide ion

Cover page for Chapter 4

Appendix:

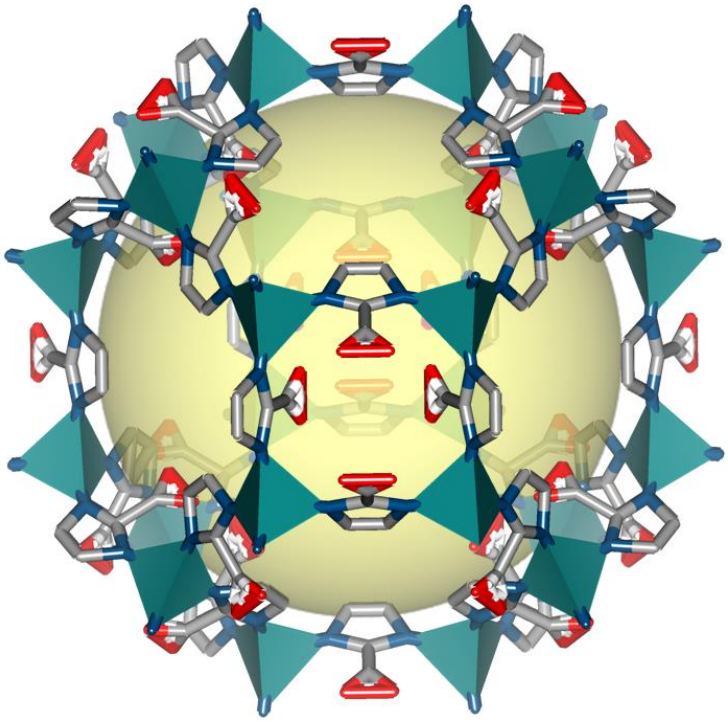

Appendix 4.1*: Cage structure of ZIF-90 showing void space (Yellow ball) in between.*

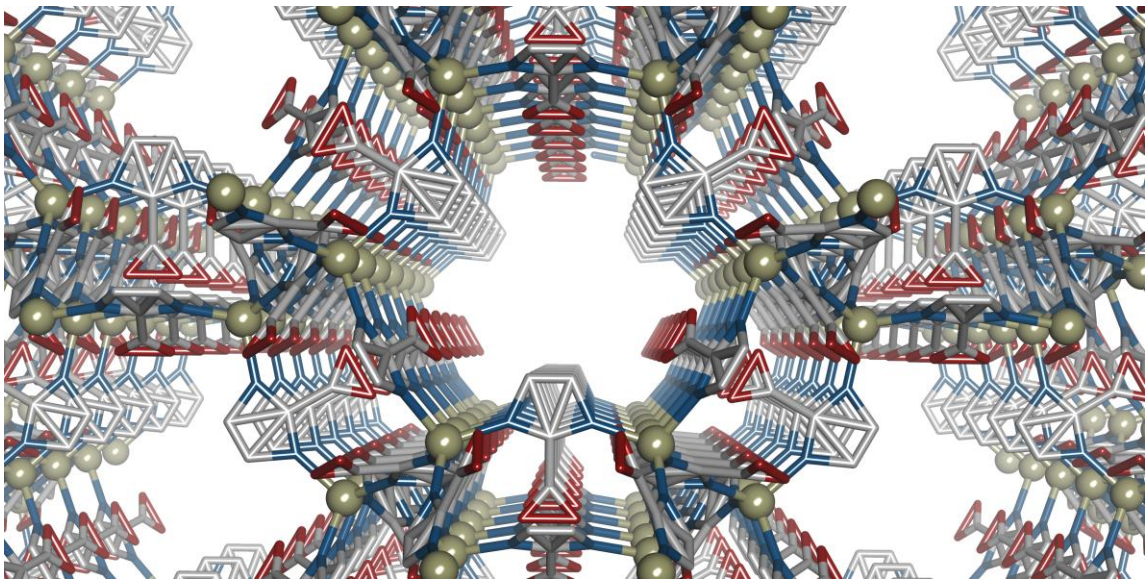

Appendix 4.2*: Perspective view of ZIF-90 showing porous channels.*

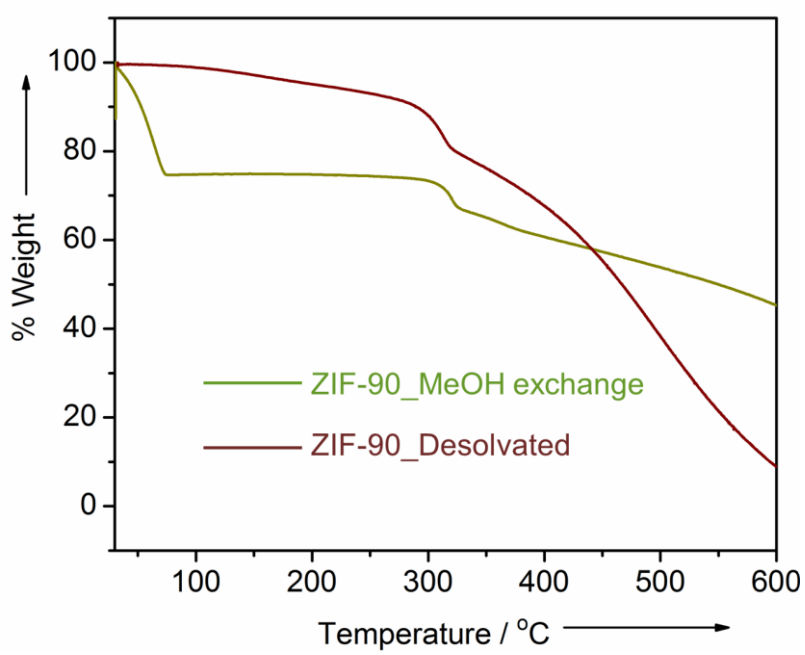

***Appendix 4.3**: TGA curve of ZIF-90; MeOH exchanged (green) and desolvated (wine red).*

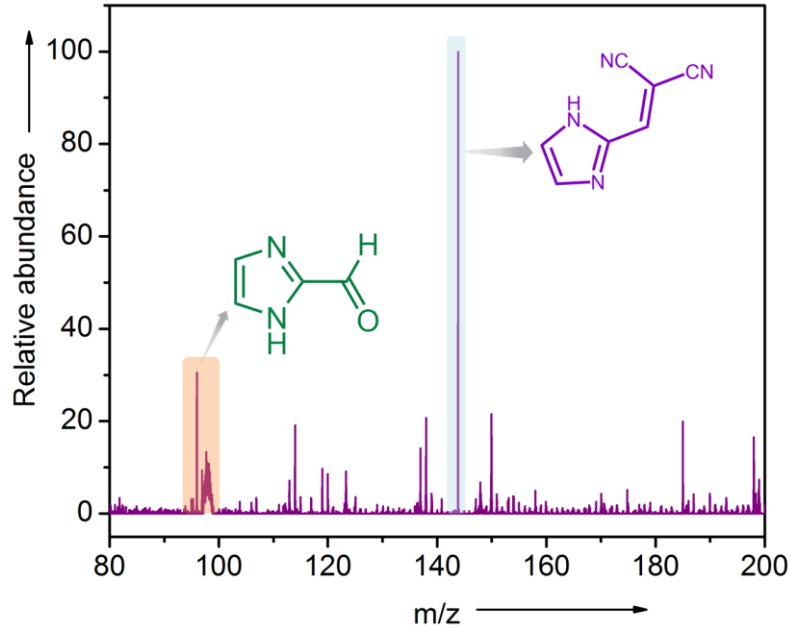

***Appendix 4.4**: Mass spectra of digested M-ZIF-90 in DCl/D_2O showing highlighted bands for the imidazole carboxyaldehyde and the malononitrile functionalized ligand after PSM.*

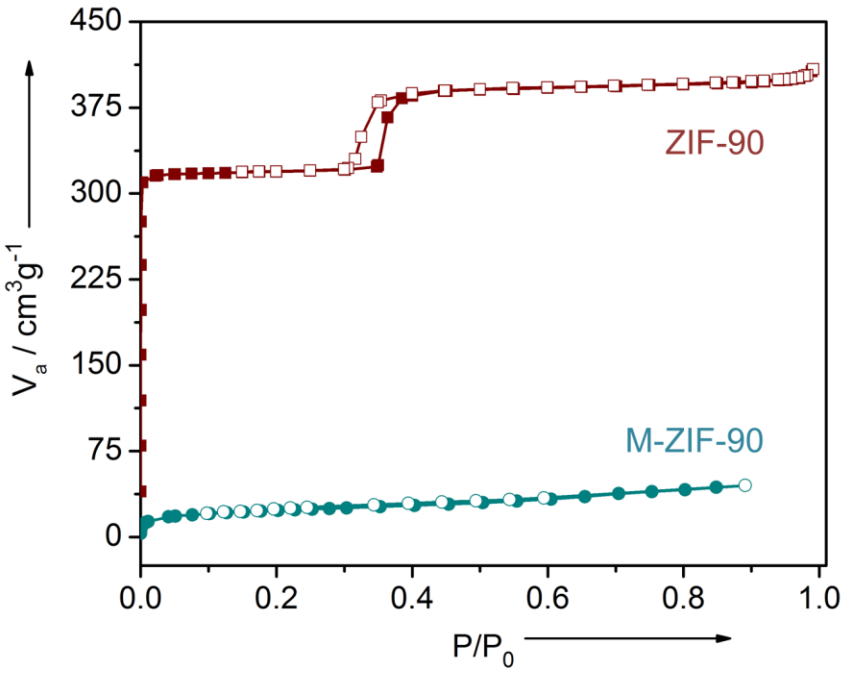

***Appendix 4.5**: N_2 adsorption isotherm of ZIF-90 and M-ZIF-90 at 77K.*

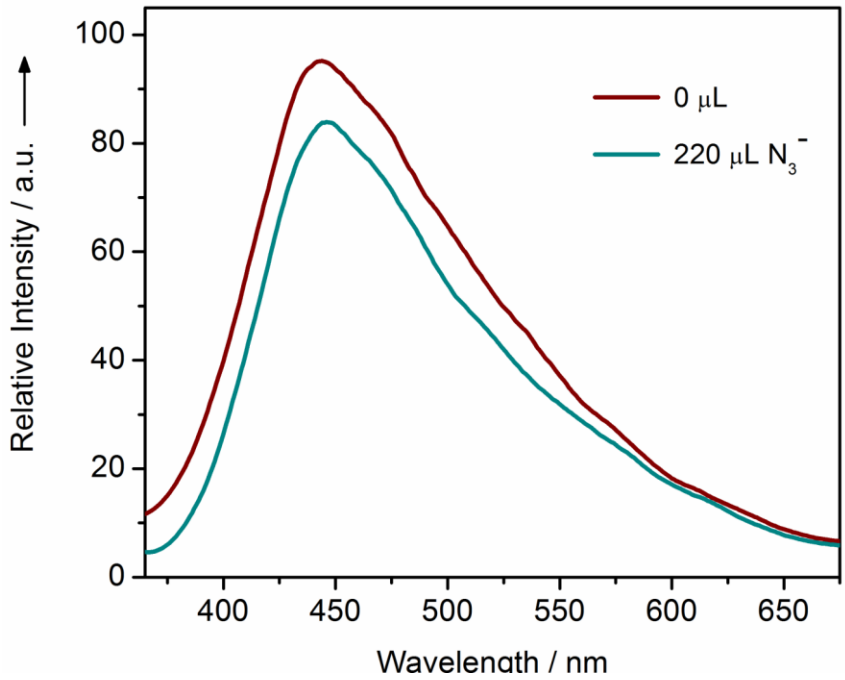

***Appendix 4.6**: Fluorescence changes of upon addition of N_3^- as Sodium salt in (1:1) H_2O/ DMSO to M-ZIF-90.*

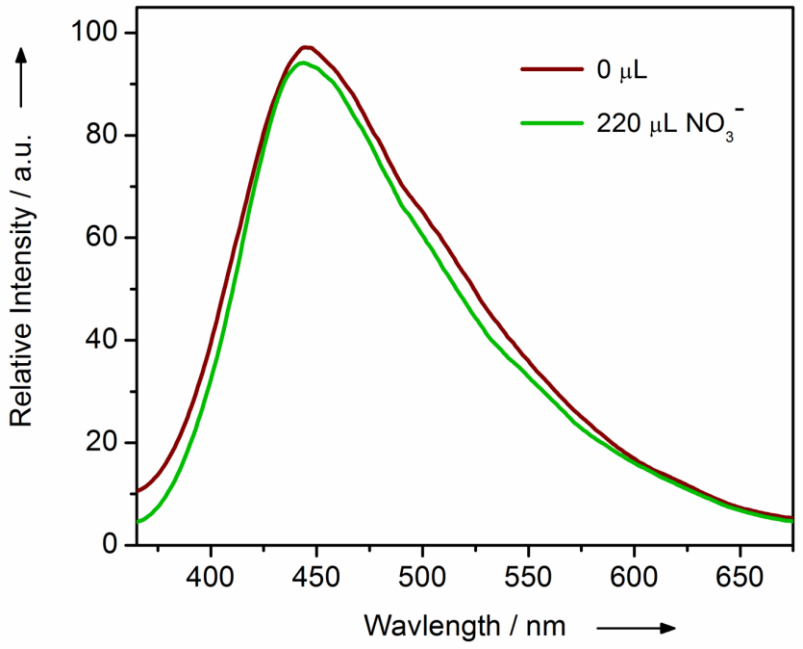

***Appendix 4.7**: Fluorescence changes of upon addition of NO_3^- as tetrabutyl salt in (1:1) H_2O/ DMSO to M-ZIF-90.*

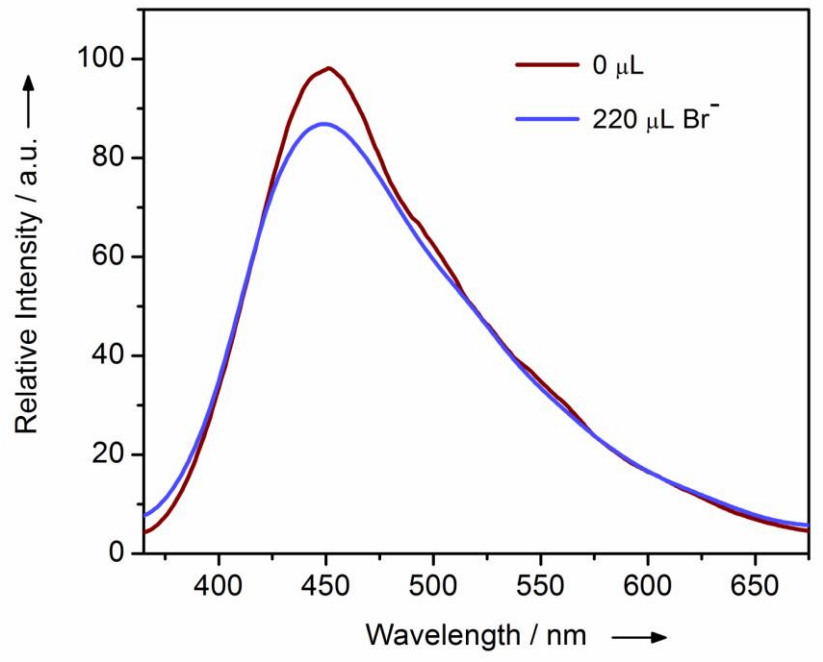

***Appendix 4.8**: Fluorescence changes of upon addition of Br^- as tetrabutyl salt in (1:1) H_2O/ DMSO to M-ZIF-90.*

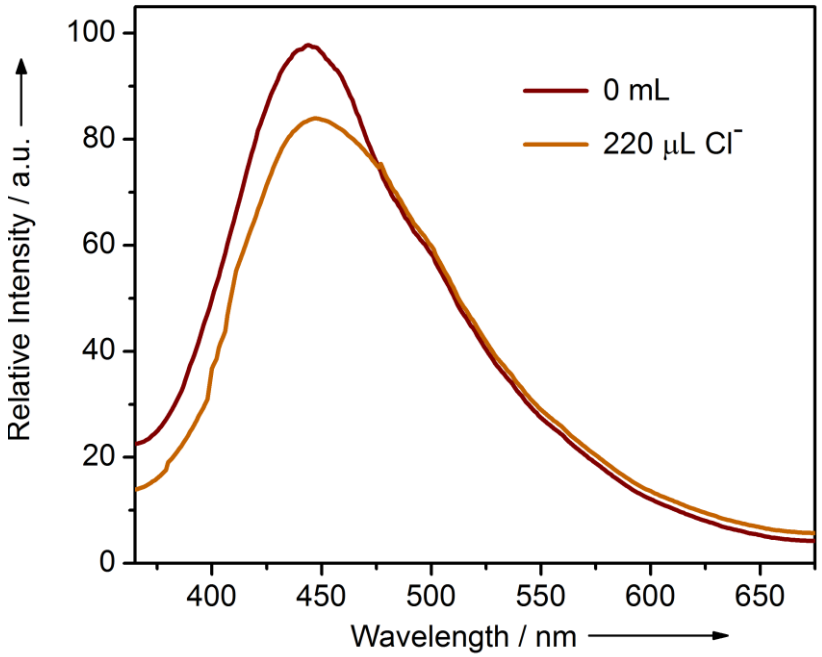

***Appendix 4.9**: Fluorescence changes of upon addition of Cl^- as tetrabutyl salt in (1:1) H_2O/ DMSO to M-ZIF-90.*

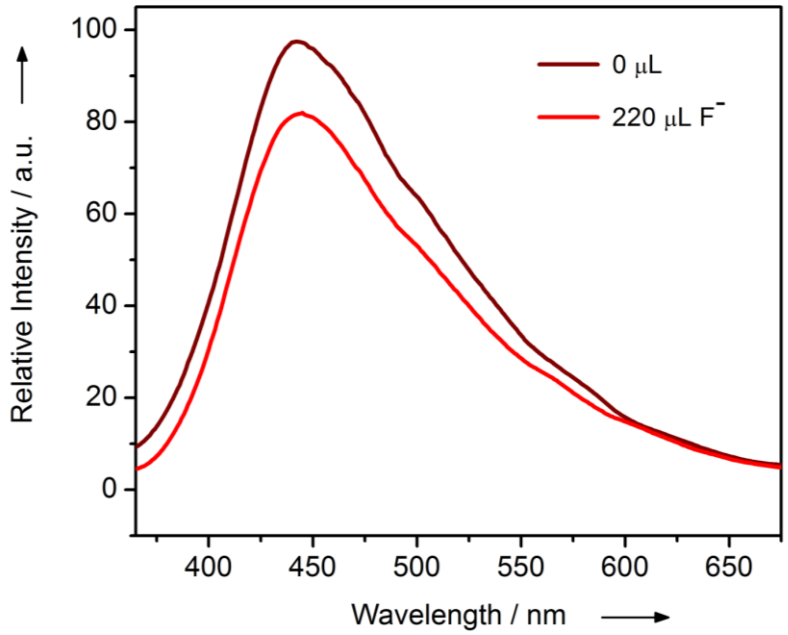

***Appendix 4.10**: Fluorescence changes of upon addition of F^- as tetrabutyl salt in (1:1) H_2O/ DMSO to M-ZIF-90.*

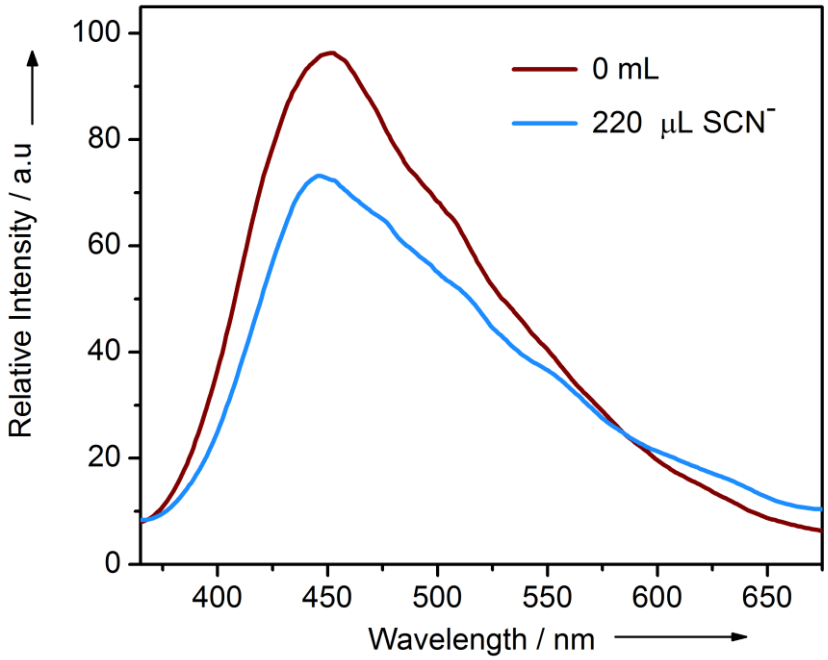

***Appendix 4.11**: Fluorescence changes of upon addition of SCN^- as tetrabutyl salt in (1:1) H_2O/ DMSO to M-ZIF-90.*

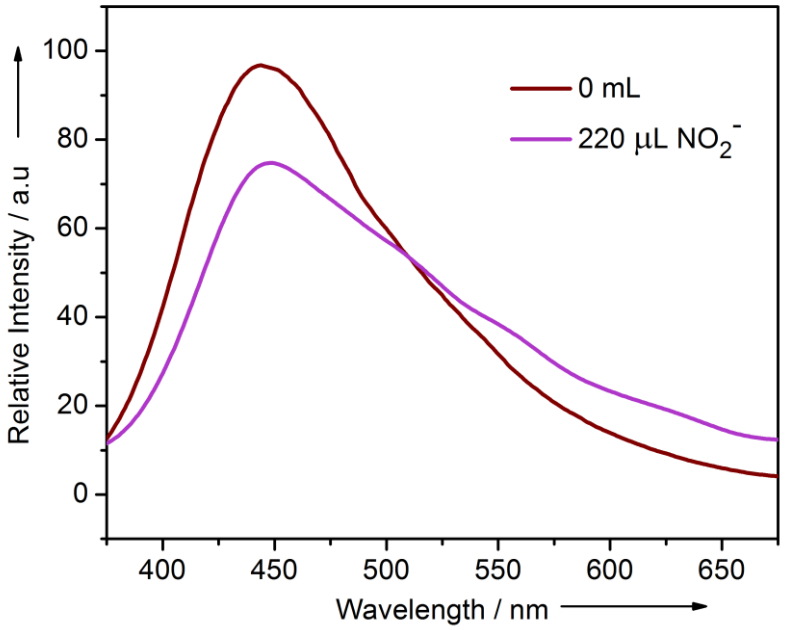

***Appendix 4.12**: Fluorescence changes of upon addition of NO_2^- as tetrabutyl salt in (1:1) H_2O/ DMSO to M-ZIF-90.*

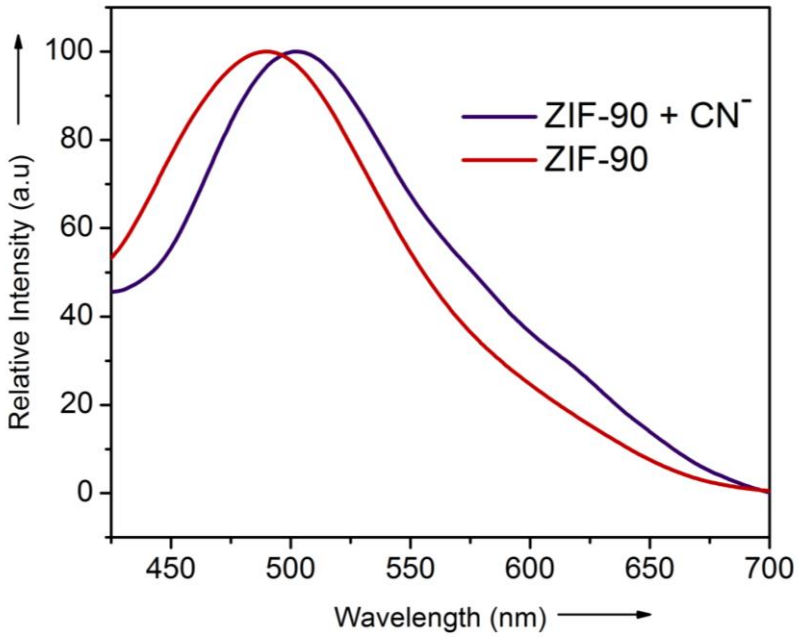

***Appendix 4.13**: Fluorescence response of ZIF-90 upon addition of CN^- as tetrabutyl salt in (1:1) H_2O/ DMSO.*

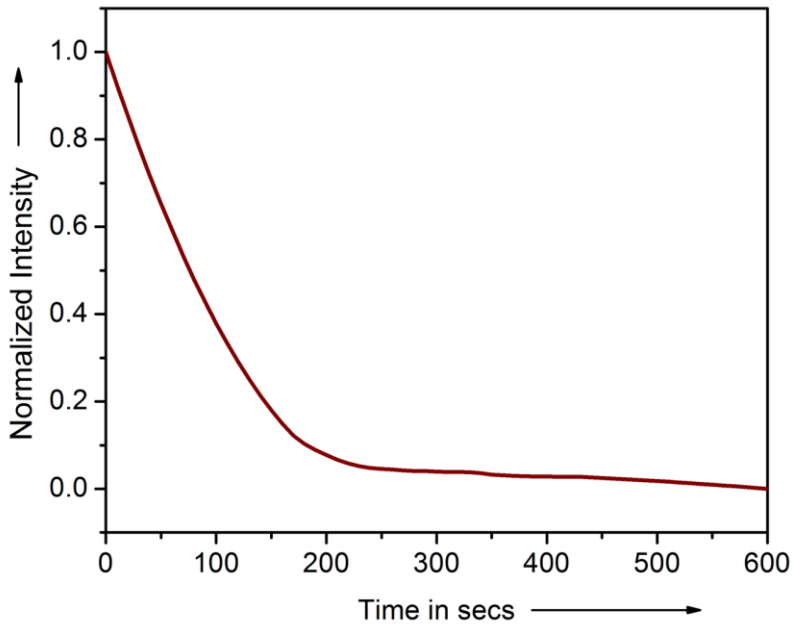

***Appendix 4.14**: Fluorescence decay profile of M-ZIF-90 upon addition of CN^- ions w.r.t. time in seconds.*

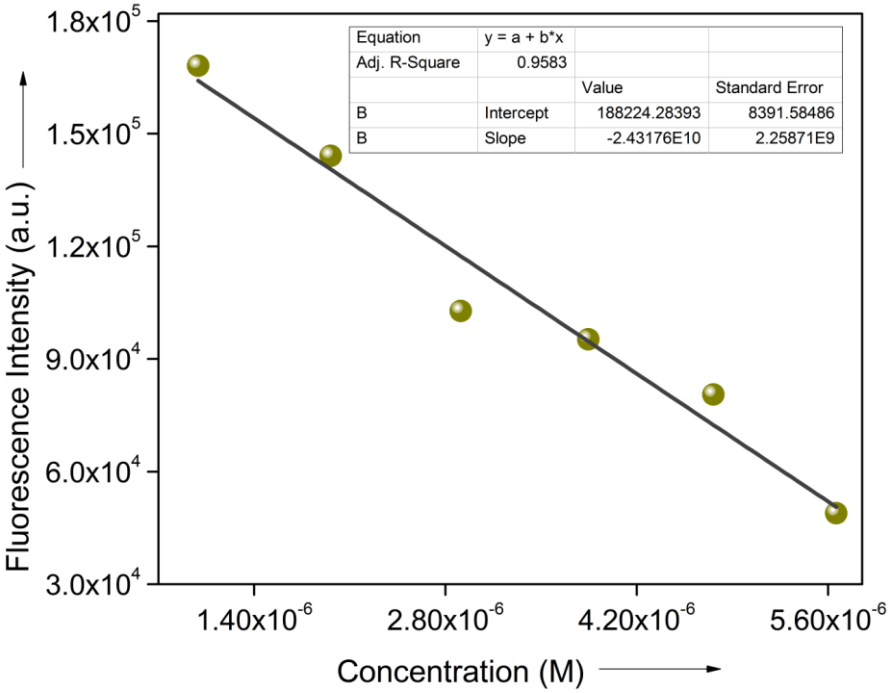

***Appendix 4.15**: Linear region of fluorescence intensity of probe upon addition of CN^-(20 – 200 µL, 0.1 stock solution) at λ_{em} = 450 nm (upon λex = 365 nm) (R^2 = 0.96).*

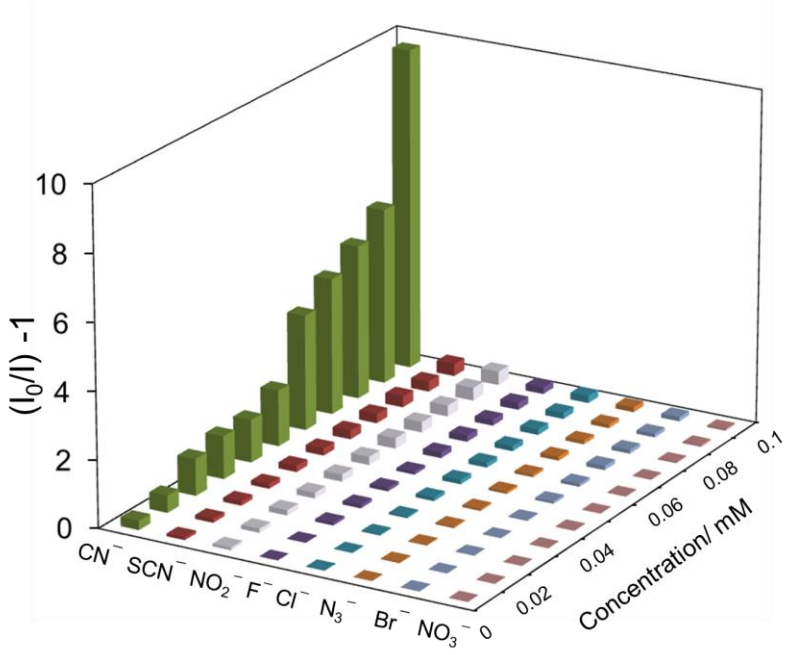

***Appendix 4.16**: Stern-Volmer plot of different anions with concentration.*

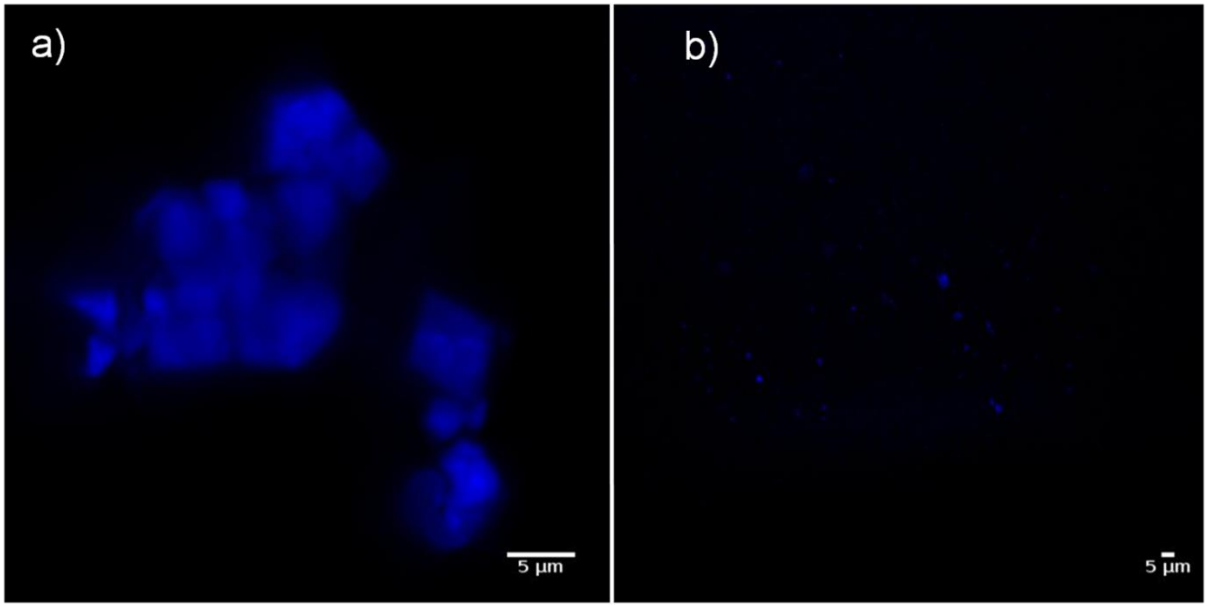

***Appendix 4.17**: Dark field confocal images of a) M-ZIF-90 and b) upon addition of CN^- anions to it showing quenching effect.*

Chapter -5

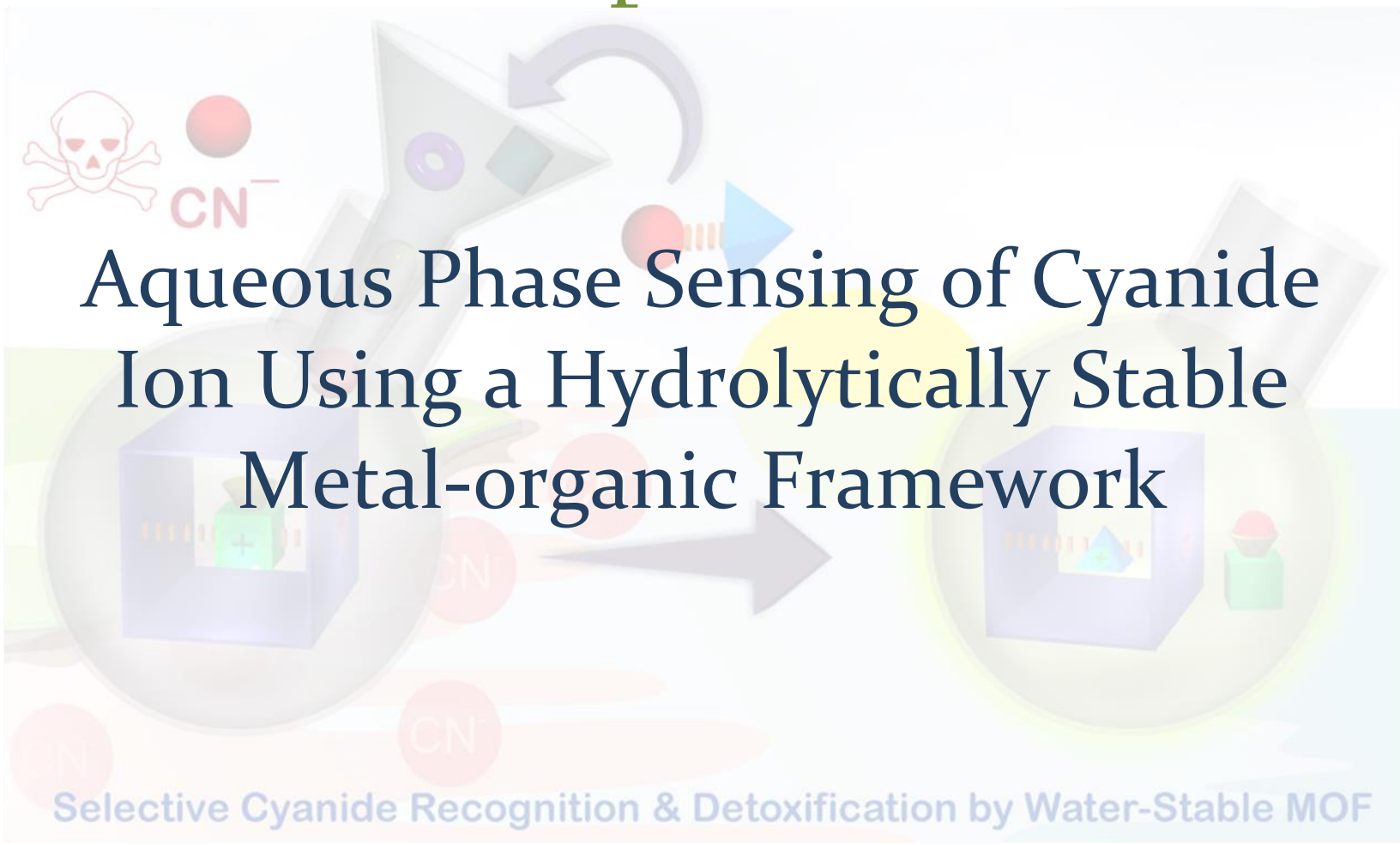

Aqueous Phase Sensing of Cyanide Ion Using a Hydrolytically Stable Metal-organic Framework

Cover page for Chapter 5

5.1 Introduction:

Cyanide ion is one of the most toxic chemical species to living animals as listed by Environment Protection Agency (EPA) and the World health Organization (WHO).[1] The release of cyanide ion in any form can be lethal, as owing to its negative charge it can bind to the Fe^{3+} ion of the cytochrome oxidase and inhibits normal functioning of lungs and brain leading to eventual death. Moreover, since CN^- is a chemical warfare agent (CWA), it is imperative to monitor, control and simultaneous detoxification of cyanide ions.[2] Since the source of cyanide ion is mostly from industrial wastes and even biogenic processes, a significant attention is required for quantification and management of its concentration in drinking water, waste water or any other natural/artificial sources. The currently known methods of removal/detoxification of cyanides involving inorganic nitrites, thiosulfates or organic based aminophenols, glucose etc. have demerits because of their own toxicity issues in few cases and dependence of usage in binary combinations in other cases. Further, detoxifications by standard chemical means (sulphite, hydrogen peroxide or Caro's acid) that have been employed by many industries often involve the formation of toxic cyanogen derivatives.[3]Additionally, the extent of reusability of such materials poses a key challenge to design near perfect tools for cyanide sequestration. Therefore the International Cyanide Management Institute (ICMI) devotes a considerable attention to the detoxification techniques of ionic cyanides by alternative eco-friendly pathways.

Metal-organic Frameworks (MOFs) have emerged as a new class of solid-state crystalline materials where their intrinsic pervious nature allows a wide spectrum of applications.[4] Very recently MOFs have shown promising potential as "crystalline molecular flasks" where solution phase reactions can be mimicked in solid state with greater degree of molecular recognition and reaction sensitivity.[5] MOFs as molecular flasks/reaction vessels have often been employed to achieve important applications such as sensing, catalysis, chiral separation etc.[6] Due to the molecular sieving effect in combination with the confinement effect in MOFs, these materials can act as the prefect host materials for a wide variety of analytes, often rendering toxic/harmful chemicals inactive by subsequent reduction in their chemical reactivity.[6]

In recent times MOFs have proven to be one of the prime candidates for recognition and counter measure of toxic chemical species from the environment. Although chemical adsorption based methods are prevalent in MOFs for capturing of toxic species, capturing of such toxic

species/pollutants and consequent sequestration techniques by MOFs is required for environmental remediation purposes.[7] An irreversible reaction based approach i.e. the chemodosimetric approach for capturing a particular analyte is more reliable as it proves to be a more concrete and efficient way of recognition of a particular species. Also the added advantage of heterogeneous phase reactions allow for the recovery of the MOFs for recyclability purposes. If such a reaction can be monitored by fluorometric methods using MOFs as reaction vessels, then suitable signal transduction can be achieved paving way for segregation of toxic entities.[8] Fluorometric methods of sensing score over the other conventional techniques owing to their ease of handling, high signal output and easy fabrication into devices. Conjointly, a turn-on fluorescence response in aqueous phase is desired because it does not lead to any loss of signal after capturing of the analyte(s).[9]

Ionic MOFs (i-MOFs) are perhaps the best manifestations of MOF based host matrices because the residual charge (positive or negative) can often be exchanged with more suitable cations/anions which may be responsible in imparting a suitable functional behaviour.[10] In this regime, bio-MOF-1 which is a hydrolytic stable and porous anionic MOF, has been the forerunner because the freely lying dimethyl ammonium (DMA) cations can be exchanged resulting in versatile applications in sensing, non-linear optics, catalysis and drug delivery.[11] Strategic incorporation of a cationic dye molecule in such anionic MOF may not only result in tuning the electronic properties of the composite material, but also depending upon the nature of the dye molecule loaded, one can induce specific recognition sites for a particular analyte in the host framework.

Herein in this chapter, I have shown the incorporation of a cationic dye 3, 6-Diaminoacridinium cation (DAAC) inside the porous channels of bio-MOF-1 by the conventional cation exchange process. The dye loaded bio-MOF-1 i.e. bio-MOF-1⊃DAAC serves as a molecular flask for selective reaction with toxic CN^- anion via Michael type addition[12a] at the electrophilic position (C9 position) of the dye molecules confined in the pores. This results in the high signal output via turn on response (Figure 1) and synergistically reducing the toxicity factor of CN^- via formation of a covalent bond with the dye molecules. The cyanide detoxification via fluorescence switch on response has been utilized to check the efficacy of the MOF to monitor the cytoplasmic CN^- concentration in human breast cancer cell lines (MCF-7). In addition, the heterogeneous phase reaction based approach allow for the reusability of the MOF for practical

applications in cyanide detection and detoxification. Notably, this report not only inaugurates the utilization of MOFs as crystalline molecular flask for pure aqueous phase recognition of trace amount toxic molecule such as CN^- ion both in chemical and biological systems (human cells) , but its consequent detoxification in heterogeneous phase has also been achieved.

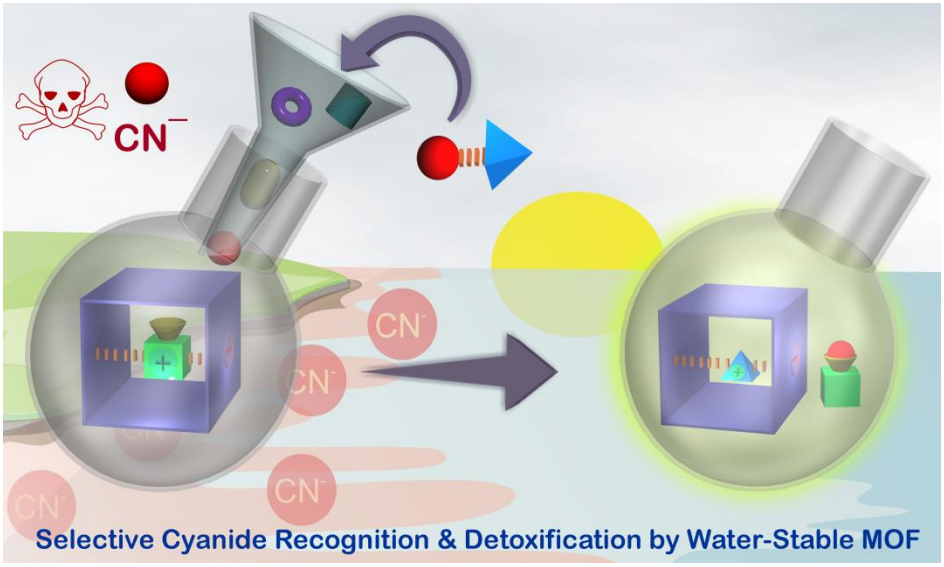

Scheme 5.1:*Schematic overview of selective sensing of CN^- ion by MOF which as a molecular reaction flask.*

5.2 Experimental Section:

5.2.1 General remarks:

5.2.1.1 Materials: All the reagents and solvents were commercially available and used without further purification.

5.2.1.2 Physical measurements: Powder X-ray diffraction (PXRD) patterns were measured on Bruker D8 Advanced X-Ray diffractometer at room temperature using Cu-Kα radiation (λ= 1.5406 Å) with a scan speed of 0.5° min^{-1} and a step size of 0.01° in 2 *theta*. Thermogravimetric analysis was recorded on Perkin-Elmer STA 6000, TGA analyzer under N_2 atmosphere with heating rate of 10° C/min. FT-IR spectra were recorded on NICOLET 6700 FT-IR Spectrophotometer using KBr Pellets. The fluorescence images of cells were taken using Olympus Inverted IX81 equipped with Hamamatsu Orca R2 microscope.

5.2.1.3 Sorption Measurements: Gas sorption measurements were performed using BelSorpmax (Bel Japan). All of the solvents used were of 99.99% purity. The desolvated samples was obtained by heating sample at 120 °C under vacuum for 8h and the dehydration was confirmed by TGA and PXRD. Prior to adsorption measurement the desolvated sample was pre-treated at 100 °C under vacuum for 3h using Bel Prepvac II and purged with N_2 on cooling.

5.2.2 Synthesis:

5.2.2.a Synthesis of bio-MOF-1: The synthesis method of bio-MOF-1 was carried out according to previous literature reports 1. To a solution of adenine (0.25 mmol) and 4,4'-biphenyl dicarboxylic acid (H_2BPDC) (0.39 mmol) in DMF (30 ml), was added dropwise a solution of Zinc acetate dihydrate (0.15 mmol) in water (5 ml). A white precipitate formed was dissolved after the addition of nitric acid (0.3 ml), and the resultant solution was heated at 130˚C for 24 h to afford transparent rod-like crystals. Crystals of regular morphology were collected by filtration, washed with DMF and dried in air. Elemental analysis: $C_{132}H_{158}N_{30}O_{44}Zn_8$ = $Zn_8(Ad)_4(BPDC)_6O\bullet$ $2(NH_2(CH_3)_2)^+$, 8DMF, $11H_2O$ Calcd. C, 46.74; H, 4.70; N, 12.39. Found C, 47.55; H, 4.74; N, 12.4.

5.2.2.b Synthesis of bio-MOF-1⊃DAAC: Crystals of bio-MOF-1 were immersed in a aqueous solution of solution of DAAC.HCl (1mmol) for 7 days to yield bio-MOF-1⊃DAAC MOF/ dye composites. The products were washed thoroughly with MeOH, DMF, H_2O four times each to remove residual DMASMI on the surface of bio-MOF-1 and dried at 100˚C for 4 h. The resulting deep yellow compound was obtained as crystalline powder form. Elemental Analysis: Found C, 52.55; H, 5.34; N, 13.7.

5.2.3. Recyclability Experiment: To check the Recyclability about 30 mg of desolvated bio-MOF-1⊃DAAC in H_2O was taken and 0.75 mmol of tetrabutylammonium cyanide was added and kept for about 10 days. After the completion of the reaction the solid compound was further dipped in aqueous solution of DAAC.HCl (1mmol) for about 7-10 days. Elemental Analysis: Found (for recycled bio-MOF-1⊃DAAC): C, 54.43; H, 4.11; N, 11.7.

5.2.4. Cell viability assay: 5 x 10^3 MCF-7 (human breast cancer) cell lines were seeded per well in 96-well µL plate and incubated at 37°C in a 5% CO_2 incubator overnight for attachment. Cells were then treated with bio-MOF-1⊃DAAC and DACC-CN in different concentrations (0, 3, 6.25, 12.5, 25, 50 µg/ml). After 24 h, 20 µl of MTT reagent (5 mg/ml) was added to each well

and incubated for another 4 h at 37°C. Formazan crystals were then solubilized in 100 µL of the solubilization buffer (10 gm SDS in 0.1 N HCl) and incubated overnight. Absorbance was measured by spectrophotometer at 550 nm. The percent cell viability was calculated considering the untreated cells as 100 percent viability and thus cytotoxicity of the bio-MOF-1⊃DAAC and DACC-CN was determined.

5.2.5. Cellular internalization: 1.5 x 10^4 MCF-7 cells were seeded in a lab tek chamber slide 8 well (per well) and incubated at 37°C in a 5% CO_2 incubator overnight for attachment. Cells were then treated with 20 µl MOF-1⊃DAAC (1 mg/2 ml autoclaved water with constant sonication) for 6 h. Cells were then washed thrice with PBS (pH = 7.4) and treated with CN^- (0.01mmol) and incubated in dark at 37 °C for 30 min. Staining solution was aspirated and cells are washed thrice with PBS. The lab-tek chamber slide 8 wells were subjected to fluorescence imaging using a CLSM (Zeiss LSM 710).

5.3. Result and discussions:

bio-MOF-1 having molecular formula $[Zn_8(ad)_4(BPDC)_6O•2Me_2NH_2]•G$(G=DMF and water) was prepared according to previous literature reports (see the SI). The infinite zinc–adeninate secondary building units (SBUs) are interconnected by BPDC (BPDC=biphenyl dicarboxylic acid) linkers to constitute a 3D porous extended framework (**Figure 5.1 and Appendix 5.1**). The 1D channels along crystallographic *c* axis containing the DMA cations are sufficiently porous to accommodate large cationic dye molecules. Bearing this in mind, the DMA cations were exchanged by DAAC molecules by simple cation exchange process resulting in the formation of bio-MOF-1⊃DAAC. The progress and completion of the cation exchange reaction was monitored by CHNS, UV, Powder X-ray diffraction (PXRD), gas-adsorption, fluorescence results. The PXRD data reveals that the pristine framework of bio-MOF-1 is maintained even after the cation exchange process (**Figure 5.2 a**). The UV absorption data reveals a clear change in the profile with new absorption band between 420-460 nm owing to the incorporated DAAC moieties in the anionic framework (**Figure 5.4 a**). In the emission spectra also I saw that characteristic peak of the bio-MOF-1 at 420 nm (blue region) being gradually quenched with new peak at ~510 nm which corresponds to the green region of the spectrum (**Figure 5.3 and 5.4 b**). This is mainly because of the energy

transfer from the MOF to the encapsulated dye molecules. The ^{1}H-NMR of the digested samples of bio-MOF-1⊃DAAC showed peaks corresponding to the DAAC molecules in the

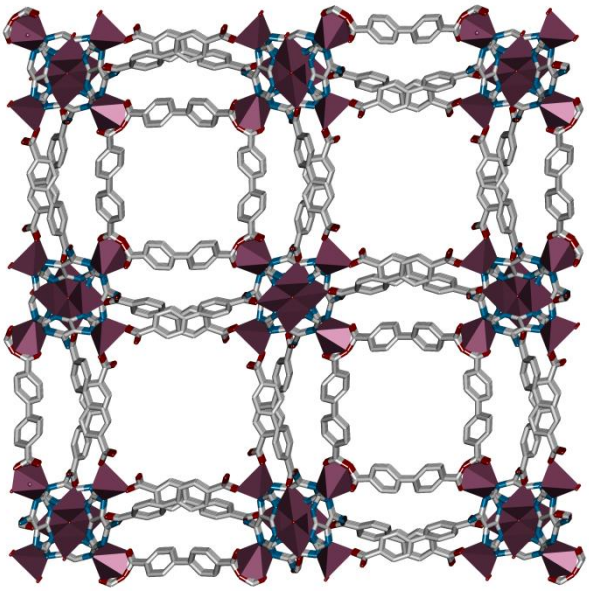

***Figure 5.1**: Porous view of bio-MOF-1 along c axis.*

framework (**Appendix 5.2**). From the CHNS and ^{1}H-NMR data the percentage of dye loaded inside the bio-MOF-1 framework were calculated to be ~70%. From the N_2 gas adsorption

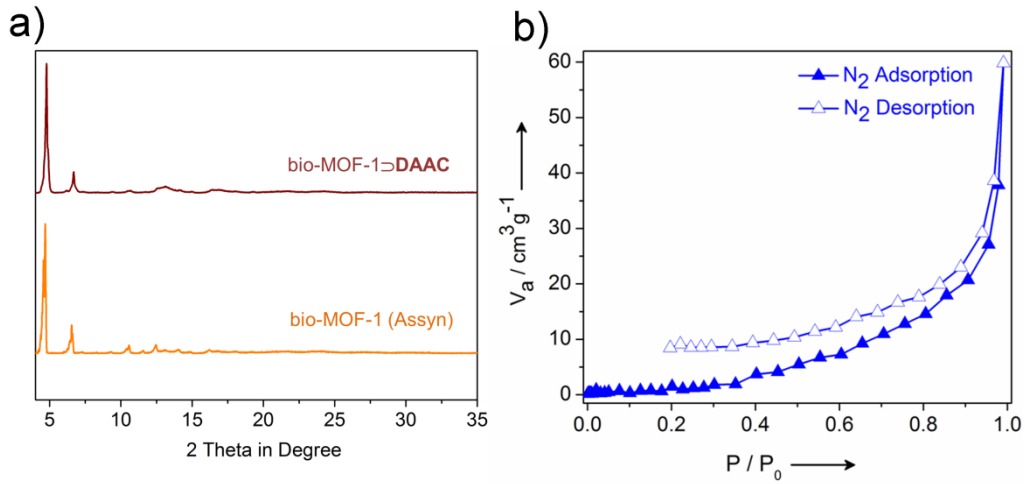

***Figure 5.2**: a) PXRD of bio-MOF-1 (assyn.) and to bio-MOF-1⊃DAAC (assyn.) and b) N_2 adsorption isotherm of bio-MOF-1⊃DAAC at 77K showing considerable decrease in porosity.*

results performed at 77 K, a considerable decrease in porosity (BET surface area 33 m^2g^{-1}) was observed due to blockage of the pores by the bulky DAAC molecules (**Figure 5.2 b**). The DAAC

unit having a positive charge located at the quaternary Nitrogen centre is susceptible to attack at the C9 position by nucleophiles[12b] (**Figure 5.5 a-b**). A conceivable idea such as this, prompted

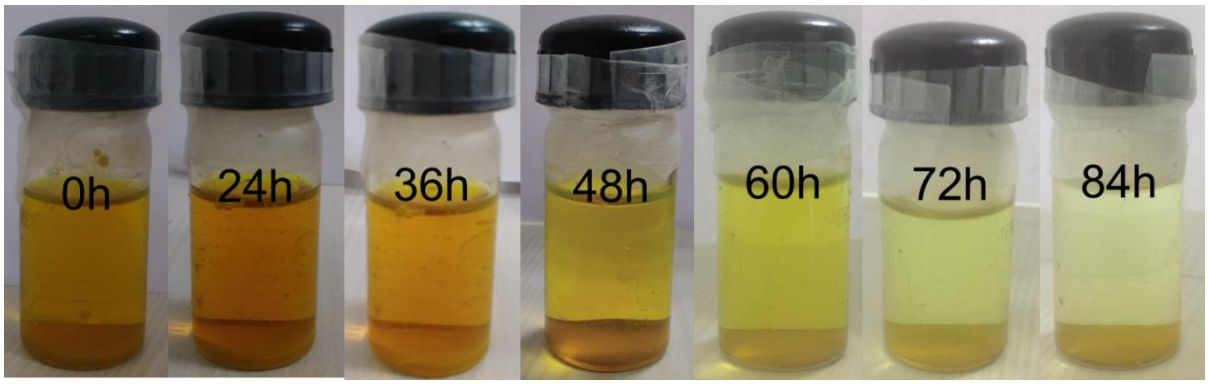

Figure 5.3*: Visual change in the supernatant solution upon exchange of DMA cations with DACC cations in bio-MOF-1.*

me to check the reactivity of different anions assuming that the nucleophile would attack the carbon centre via Michael type addition reaction. To investigate the response of bio-MOF-1⊃DAAC towards different nucleophiles 1 mg of the desolvated MOF compound was dispersed in HEPES buffer solution (10 mM, pH 7.4), and incremental addition of 0.1 mmol of

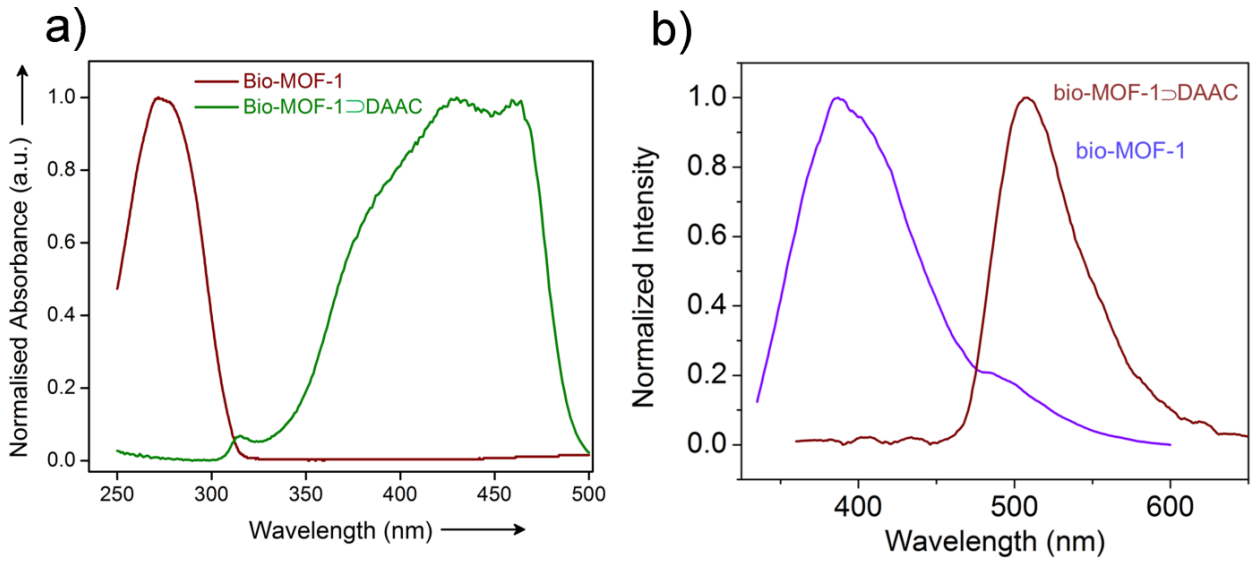

Figure 5.4*: a)UV absorption spectra of bio-MOF-1 and bio-MOF-1⊃DAAC b) Emission profile of bio-MOF-1 and bio-MOF-1⊃DAAC (after 7 days of exchange).*

Tetrabutylammonium (TBA) salts of F^-, Cl^-, Br^-, I^-, SCN^-, NO_3^-, NO_2^-, HCO_3^-, OAc^- and CN^- in 1 ml H_2O was carried out. While in other cases I observed negligible fluorescence response (**Appendix 5.3-5.11**), CN^- gave a very strong fluorescence turn on response (~17 fold) upon addition of 246 µL addition of its solution (**Figure 5.5 f**). The CN^- ions after attacking the C9

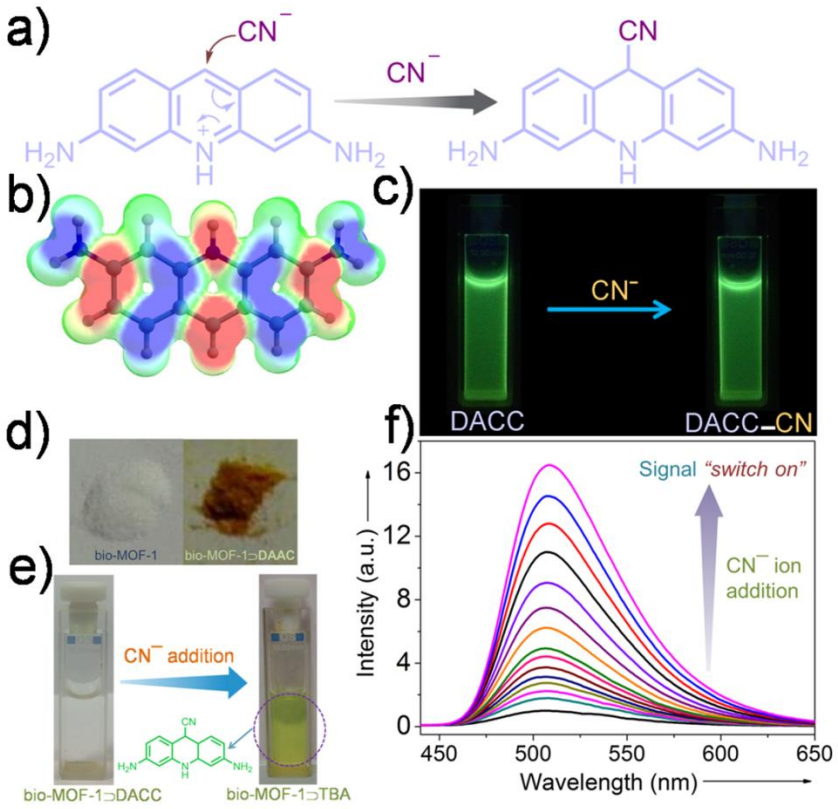

Figure 5.5*:Representation of the reaction of DAAC cation with CN^-, b)electronic potential map of the LUMO energy state of the DACC molecule, c) no change observed upon addition of cyanide ion to DACC molecules only d) colour change observed after incorporation of DAAC in bio-MOF-1 by cation exchange, e) visual change in the supernatant solution upon addition of cyanide ions to bio-MOF-1⊃DAAC and f) changes in fluorescence intensity via turn-on response upon addition of CN^- ions to bio-MOF-1⊃DAAC.*

carbon of the DAAC molecules form a covalent bond with it rendering the cationic dye, neutral. The neutral dye which is also highly fluorescent in aqueous phase (**Figures 5.5 c Appendix 5.12**) then escapes the reaction vessel (MOF) to the solution, which results in "switch on" signal (**Figures 5.7 a-c, Appendix 5.13**). The counter cation i.e. TBA replaces the cationic dye in the

bio-MOF-1⊃DAAC resulting in the formation of bio-MOF-1⊃TBA (**Figure 5.6**), thus maintaining the charge neutrality. This was further supported as the supernatant solution after addition of the CN^- ions shows a distinct visual color change (**Figure 5.5 e**). A peak in the UV absorption profile corresponding to the DAAC molecules arise when CN^- solution was added to bio-MOF-1⊃DAAC at different time intervals (**Figure 5.7 g**).

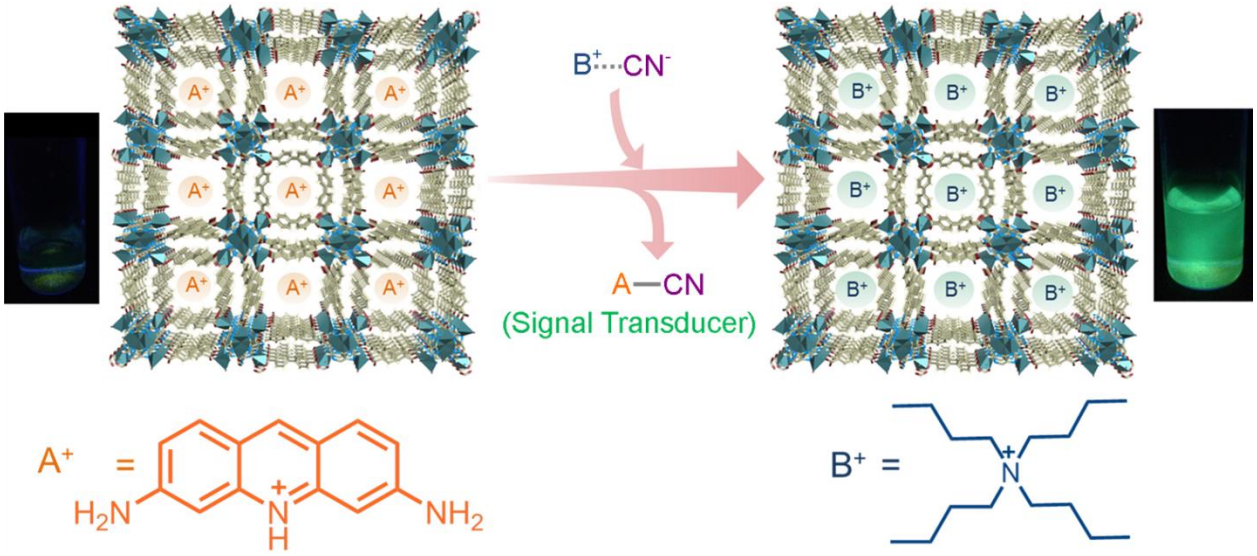

***Figure 5.6**:Figure showing the reaction based (chemodosimetric) approach in bio-MOF-1⊃DAAC prompted by CN^- inspiring in a turn-on fluorescence response.*

The aggregation-caused quenching (ACQ) prevail in both the DACC moiety and bio-MOF-1⊃DAAC and therefore exhibit a weak fluorescence in solid state. However once the neutral dye is released in the solution upon the addition of cyanide, there is a release in stress from both the π-π interactions of the dye with the framework and the aggregation as otherwise observed in the solid state. Thus an increase in fluorescence intensity is observed. The mass spectroscopic analysis of the supernatant solution shows peaks for the neutral dye molecule (**Appendix 5.19**) in which the cyanide is covalently linked to it. Such a concerted reaction in the molecular reaction vessel does not lead to any changes in the overall framework which is evident from the PXRD pattern and SEM images even after dipping bio-MOF-1⊃DAAC in aqueous CN^- solution for a period of 1 month (**Figures 5.7 d, Appendix 5.17**). The linear fit of the kinetics gave a linear progression of intensity with time and concentration which prove the fact that the receptor (DAAC) has a strong affinity for CN^-, which is the strongest nucleophile as compared to the

other anions (**Figures 5.7 e, Appendix 5.14-5.15**). In an effort to check the efficiency of the MOF to detect CN^- in presence of other anions equimolar concentration of other intrusive anions were added after which CN^- ions were added to the same solutions systematically. No spectral was observed in the case of other anions,whereas CN^-ions incurred almost the same increase in fluorescence intensity as previously observed insingle component analysis (**Figure 5.7 f**). Thus

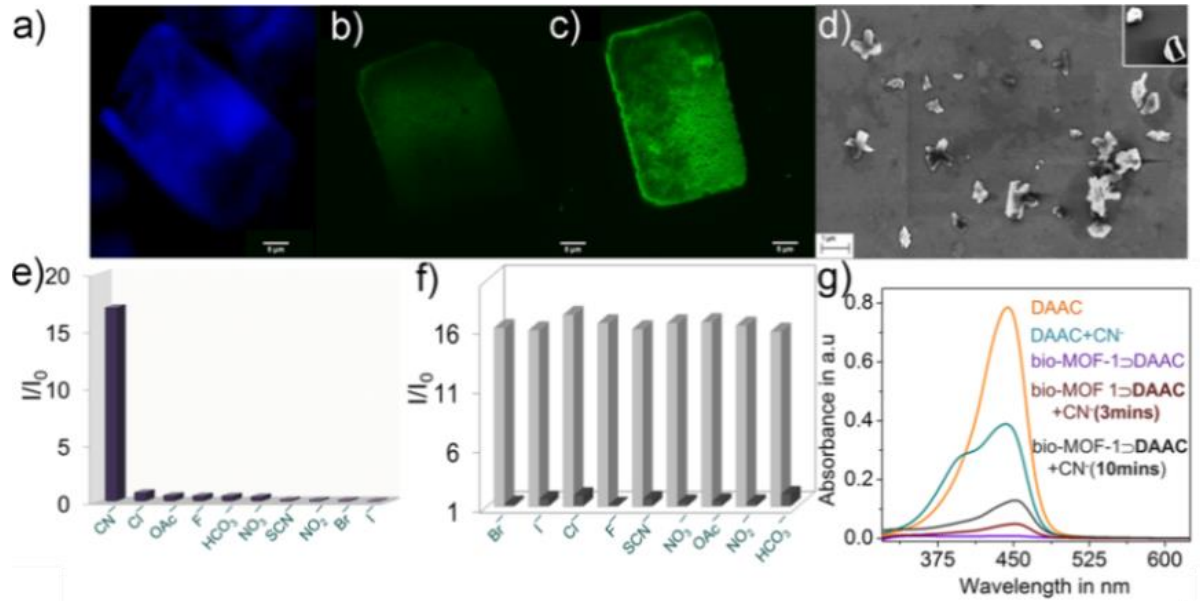

Figure 5.7*:a) Confocal images of (a) bio-MOF-1, (b) bio-MOF-1⊃DAAC and (c) bio-MOF-1⊃DAAC +CN^- in dispersed phase (d) SEM images of bio-MOF-1⊃DAAC and bio-MOF-1⊃DAAC +CN^- (inset) showing crystalline morphology in both the cases (e) response in fluorescence of other anions as compared to CN^- ions (f) fluorescence change of bio-MOF-1⊃DAAC upon addition of other anions (black) followed by the addition of cyanide ion (gray) and g) change in the absorption spectra bio-MOF-1⊃DAAC upon addition of CN^- ions to it.*

the MOF could be used in practical purposes for detecting cyanide even in presence of other interfering anions. Also, when bio-MOF-1⊃TBA was further exchanged with DACC to form bio-MOF-1⊃DAAC to check the reversibility of such a cation exchange process, an almost similar response was observed when $CN^-$was added to it (**Figures 5.8 a and Appendix 5.17**). This was testimonial of the fact that that the MOF could be recycled even after the reaction inside its nano-porous channels and thereafter regenerated for further usage via simple and rapid cation exchange process. The limit of detection (LOD) was calculated to be 5.2 ppb (**table 5.1**

and 5.2) which is well within the permissible limit of cyanide concentration in drinking water as set by WHO/EPA.

Table 5.1*: Standard deviation for probe.*

Blank Readings (only probe)	FL Intensity
Reading 1	50430
Reading 2	58595
Reading 3	64514
Reading 4	74235
Standard Deviation (σ)	10024

Moreover it is a well-known fact that ionic cyanides are much more toxic to living cells than covalently linked cyanides mainly due their superior reactivity. In order to check the cytotoxicity of bio-MOF-1⊃DAAC for sensing and detoxification of CN^- ions in living cells, I carried out MTT [3-(4,5-Dimethylthiazol-2-yl)-2,5-DiphenyltetrazoliumBromide] assay in human breast cancer cell lines (MCF7). After about incubation of the cells with bio-MOF-1⊃DAAC for 24 h, the cells were found to ~75% viable at higher concentration of the MOF (50 μg/mL) which was then used for live cell imaging (**Figure 5.8 b**). For in vitro live cell imaging, we incubated bio-MOF-1⊃DAAC for 6 h at 37˚C and thereafter washed three times with PBS buffer and performed confocal laser scanning microscopy (CLSM). A weak fluorescence was observed for

the bio-MOF-1⊃DAAC incubated cells (**Figure 5.8 c**). However, when the same experiment was repeated with the addition of the CN^- for about 30 minutes, a strong fluorescence turn on signal

***Table 5.2**: Calculattion of limit of detection (LOD).*

Slope from Graph (m)	1.48×10^{8}	mM^{-1}
Detection limit ($3\sigma/m$)	2.01×10^{-4}	mM

was observed (~16 folds) which was in accordance to the response observed in fluorescence microscopy (**Figure 5.8 d**). The morphology of the MCF-7 cells was intact during the course of

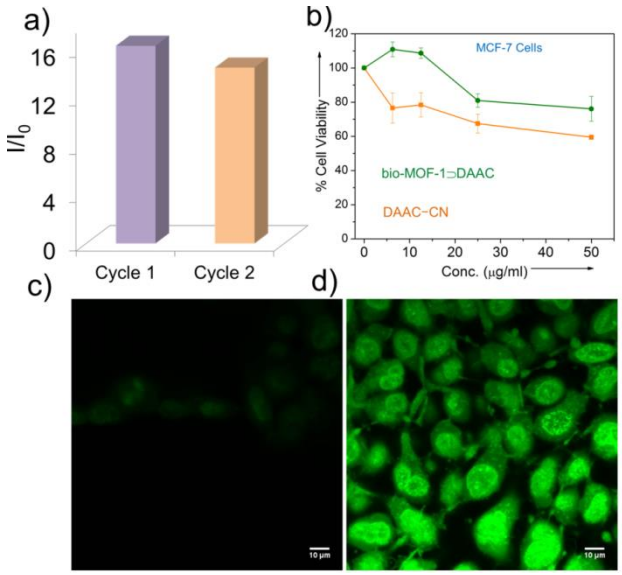

***Figure 5.8**:Fluorescence response of the MOF compound after recyclability test b) MTT assay of bio-MOF-1⊃DAAC and the neutral dye compound formed after addition of cyanide ions ,CLSM images of bio-MOF-1⊃DAAC before c) and d) after the addition of cyanide showing drastic change in fluorescence.*

the imaging experiment (Figure S33). This result corroborated to the fact that the MOF could be used to detect even trace amount CN^- ions in living cells and thus could beefficiently used for monitoring its concentration. In order to check the cytotoxicity of the neutral dye, we incubated the cells again with the supernatant solution of the bio-MOF-1ↃDAAC after addition of the CN^- ions and checked its cytotoxicity. Interestingly, we observed a high viability of cells (62%) after the cells were incubated with the DACC molecules treated with CN^- ions (**Figure 5.8 b**). Thus the highly reactive nature of the ionic cyanides was rendered ineffective by a reaction based approach in heterogeneous medium inside the MOF.

In conclusion a bio-compatible anionic MOF has been utilized as a crystalline reaction flask to recognize a highly toxic chemical species i.e. CN^- ions. The heterogeneous phase reaction inside the MOF results in a signal turn on response in presence of CN^- ions thus proving as an efficient sensor of such a chemically reactive pollutant. The pure aqueous phase recognition and very low detection limit are in well accordance to the standard set by WHO/EPA for monitoring CN^- ion concentration in natural and artificial sources. In vitro studies have been carried out to monitor the efficacy of the MOF to detect trace amount of CN^- in the cytoplasm. This work paves way to a new approach for bio-sensing and presents a new platform for development of antidotes for the highly toxic CN^- ions.

5.4. References:

1. a) Guidelines for Drinking-Water Quality, World Health Organization, Geneva (Switzerland). **1996.**
2. a) Argoti,D; Liang, L.;Conteh,A.; Chen,L.; Bershas,D.; Yu,C. P.;Vouros, P.; Yang,E.*Toxicology*, **2005**, *214*, 167; b) Kuhn, R. G. United States Patent **1971**, (US3586623 A).
3. a) Borbely, G.J.; Devuyst, E.A.; Ettel, V.A.; Mosoiu, M.A; Schitka, K.J. Cyanide removal from aqueous streams. *US Patent*, *4*, 537,686 (INCO Limited), **1985**.
4. a) Banerjee, D.; Kim, D.; Schweiger, M. J.; Kruger, A. A.; Thallapally, P. K. *Chem. Soc. Rev*., **2016**, *45*, 2724; b) Meek, S. T.; Greathouse, J. A.; Allendorf, M. D. *Adv. Mater*., **2011**, *23*, 249; c) Stock, N.; Biswas, S. *Chem. Rev*., **2012**, *112*, 933; d) Aguilera-Sigalat,J.; Bradshaw, D. *Coord. Chem. Rev*., **2016**, *307*, 267.
5. a) Ikemoto, K.; Inokuma, Y.; Fujita, M. *J. Am. Chem. Soc*., **2011**, *133*,16806; b) Hu, Z.; Deibert, B. J.; Li, J. *Chem. Soc. Rev*., **2014**, *43*, 5815; c) Kreno, L. E.; Leong, K.; Farha, O. K.; Allendorf, M.; van Duyne, R. P.; Hupp, J. T.*Chem. Rev*., **2012**, *112*, 1105; dLi, B.; Wen, H. –M.; Cui, Y.; Zhou, W.; Qian, G.; Chen, B. *Adv. Mater*., **2016**, DOI: 10.1002/adma.201601133.
6. a) Mondloch, J. E.; Katz, M. J.;Isley,W. C.; Ghosh, P.; Liao,P.; Bury, W.; Wagner, G. W.; Hall, M. G.; DeCoste, J. B.; Peterson, G. W.; Snurr, R. Q.; Cramer,C. J.;Hupp, J. T.;Farha,O. K. *Nat. Mater*., **2015**, *14*, 512; b) Moon, S.Y.; Liu, Y.; Hupp, J. T.; Farha, O. K.*Angew. Chem. Int. Ed*., **2015**, 54, 6795; c) Rudd, N. D.; Wang, H.; Fuentes-Fernandez, E. M. A.; Teat, S. J.; Chen, F.; Hall, G.; Chabal, Y. J.; Li,J. *ACS Appl. Mater. Interfaces*, **2016**, *8*, 30294.
7. a) López-Maya, E.; Montoro, C.; Rodríguez-Albelo, L. M.; Cervantes, S. D. A.; Lozano-Pérez, A. A.; Cenís, J. L.; Barea, E.; Navarro, J. A. R. *Angew. Chem. Int. Ed*., **2015**, *54*, 6790; b) Desai, A. V.; Manna, B.; Karmakar, A.; Sahu, A.; Ghosh, S. K.*Angew. Chem. Int. Ed*., **2016**, *55*, 7811.
8. a) Barea, E.; Montoro, C.; Navarro,J. A. R. *Chem. Soc. Rev*., 2014, *43*, 5419; b) Cui, J.; Wong, Y.-L.; Zeller, M.; Hunter, A. D.; Xu, Z. *Angew. Chem. Int. Ed*., **2014**, *53*, 14438.

9. a) . Du, J.; Hu, M.; Fan. J.; Peng, X.*Chem. Soc. Rev*., **2012**, *41*, 4511; b) D.G. Cho and J. L. Sessler, *Chem. Soc. Rev*., **2009**, *38*, 1647.

10. a) Karmakar, A.; Desai, A. V.; Ghosh, S. K.Coord. Chem. Rev., 2016, *307*, 313; b) Maji, T. K.; Matsuda, R.; Kitagawa, S. *Nat. Mater*., **2007**, *6*, 142.

11. a) An, J.; Geib, S.J.; Rosi, N.L. J. Am. Chem. Soc., **2009**, *131*, 8376; b) Yu, J.; Cui, Y.; Xu, H.; Yang, Y.; Wang, Z.; Chen, B.; Qian, G.*Nat. Commun*., 2013, 4, 2719; c) An, J.; Rosi, N. L.*J. Am. Chem. Soc*., **2010**, *132*, 5578.

12. a) Happ, J. W.; Janzen, E. G.; Rudy, B. C.*J. Org. Chem*. 1970, *35*, 3382; b) Yang, Y.K.; Tae. J.*Org. Lett*., **2006**, *8*, 5721.

Appendix

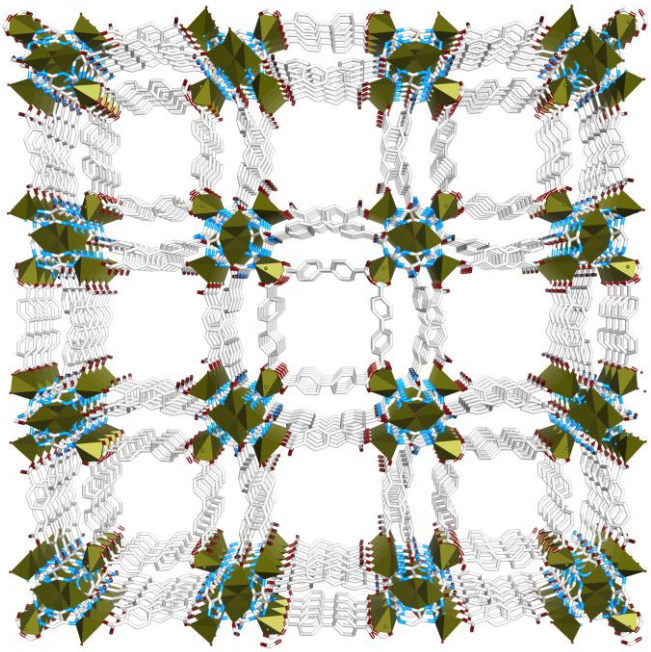

***Appendix 5.1**: Perspective view of bio-MOF-1 along c axis.*

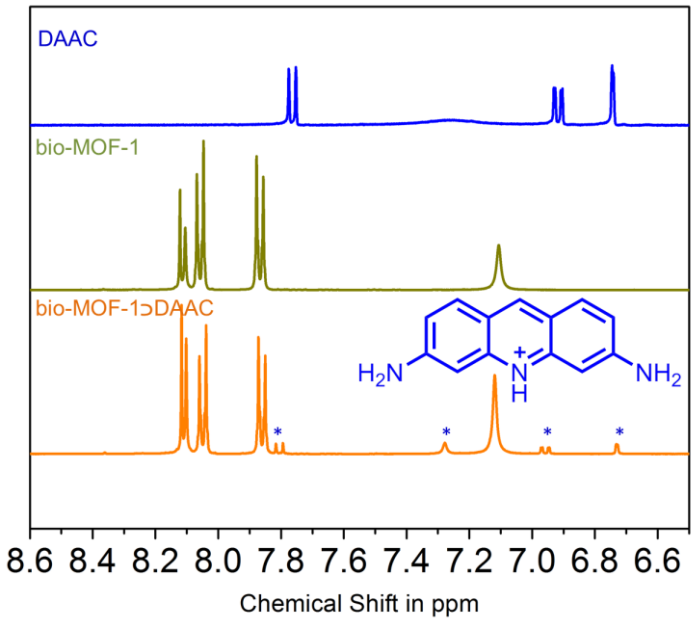

***Appendix 5.2**: ^{1}H-NMR spectra of DAAC, bio-MOF-1 and bio-MOF-1⊃DAAC digested in HF and dmso-d^{6} showing peaks for DAAC molecules (shown with blue asterisk).*

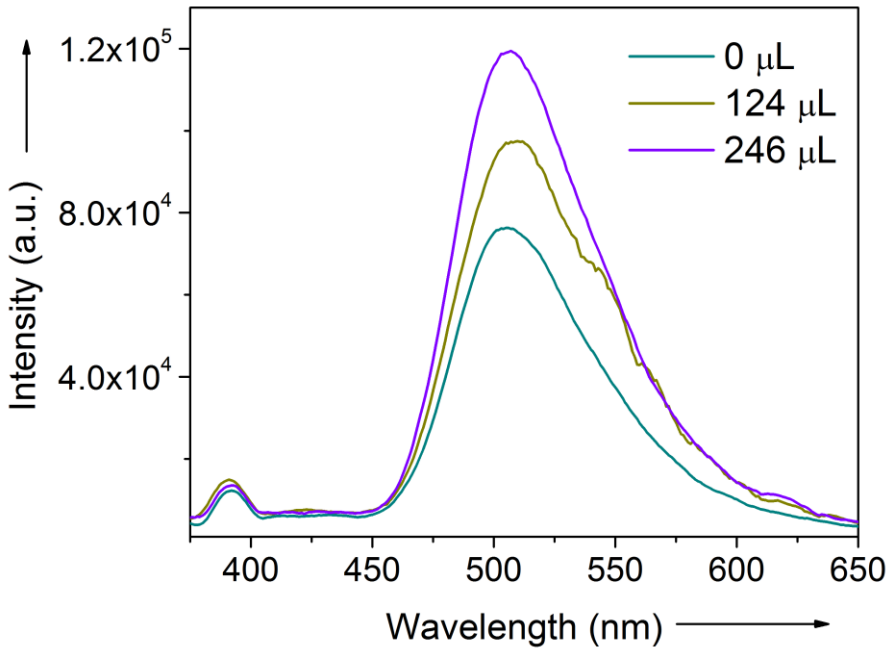

***Appendix 5.3**: Fluorescence changes of upon addition of F^- as Tetrabutylammonium salt in aqueous phase to bio-MOF-1⊃DAAC.*

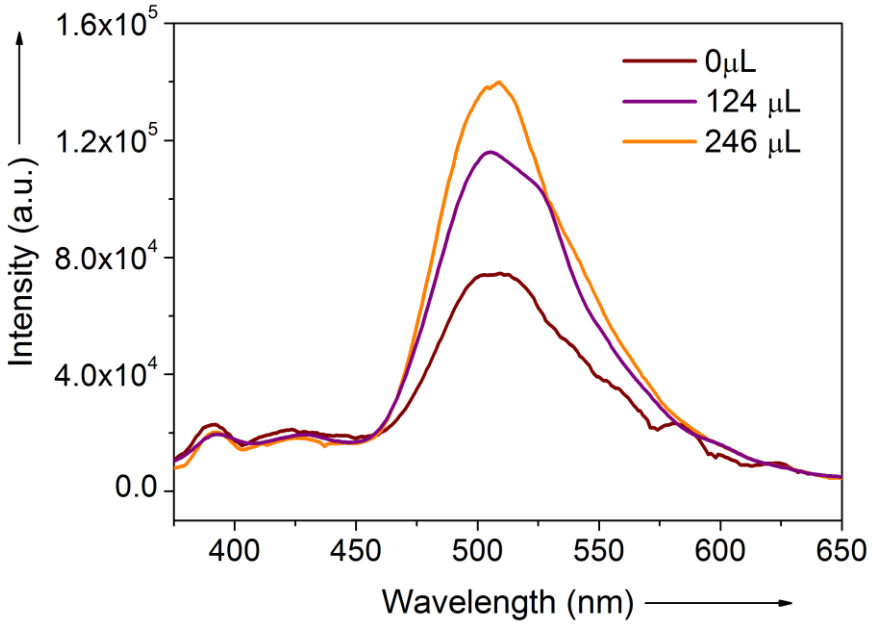

***Appendix 5.4**: Fluorescence changes of upon addition of Cl^- as Tetrabutylammonium salt in aqueous phase to bio-MOF-1⊃DAAC.*

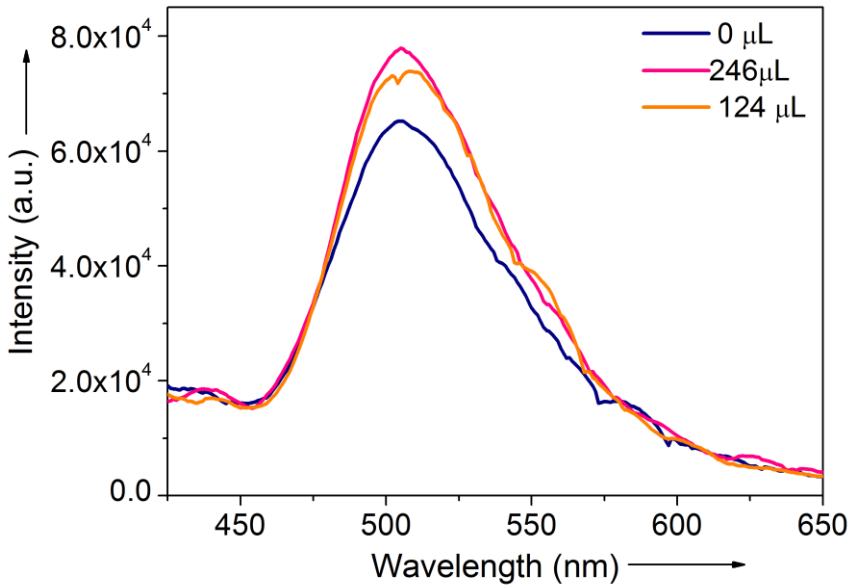

***Appendix 5.5**: Fluorescence changes of upon addition of Br^- as Tetrabutylammonium salt in aqueous phase to bio-MOF-1⊃DAAC.*

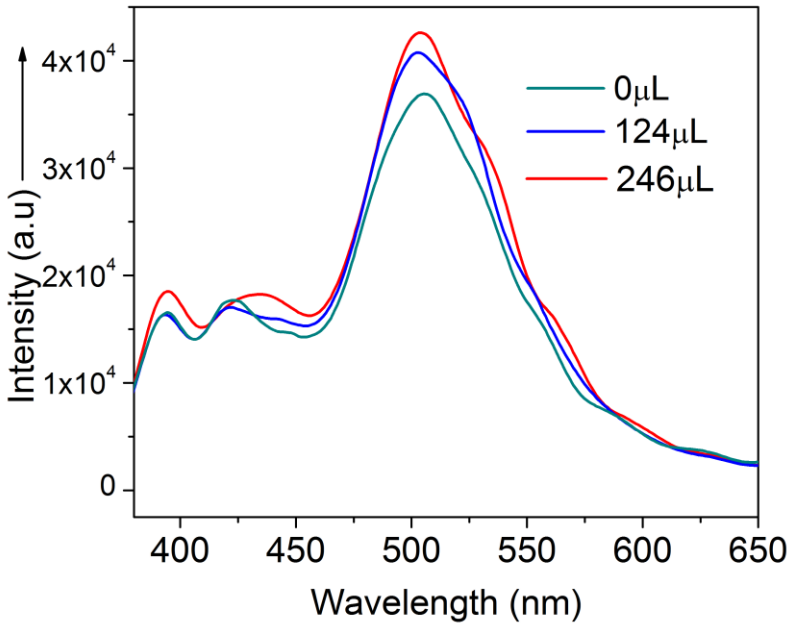

***Appendix 5.6**: Fluorescence changes of upon addition of I^- as Tetrabutylammonium salt in aqueous phase to bio-MOF-1⊃DAAC.*

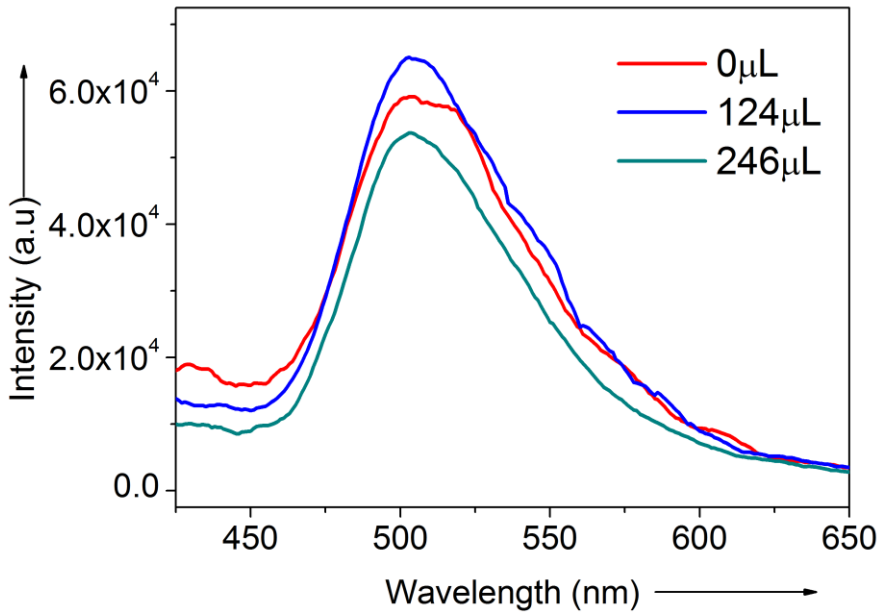

***Appendix 5.7**: Fluorescence changes of upon addition of NO_2^- as Tetrabutylammonium salt in aqueous phase to bio-MOF-1⊃DAAC.*

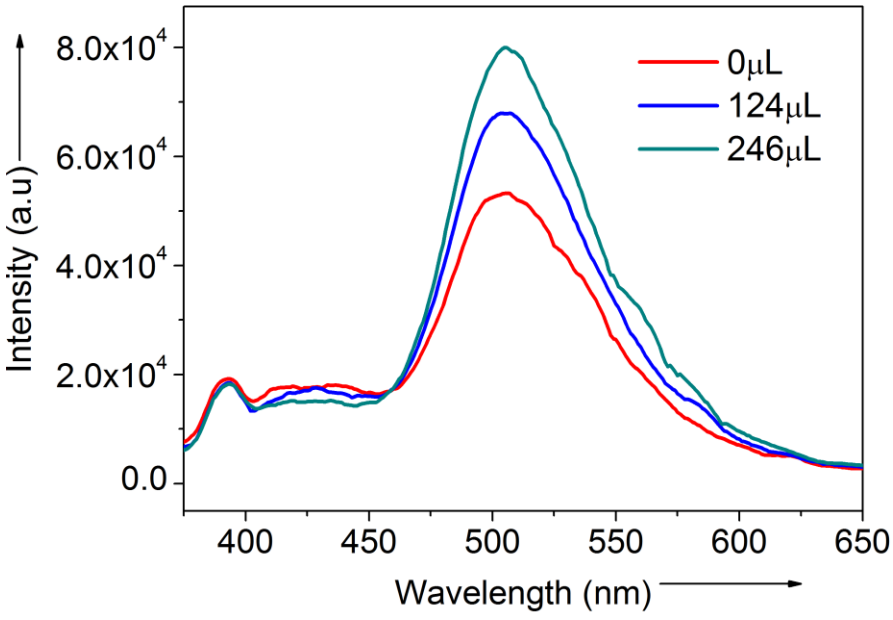

***Appendix 5.8**: Fluorescence changes of upon addition of NO_3^- as Tetrabutylammonium salt in aqueous phase to bio-MOF-1⊃DAAC.*

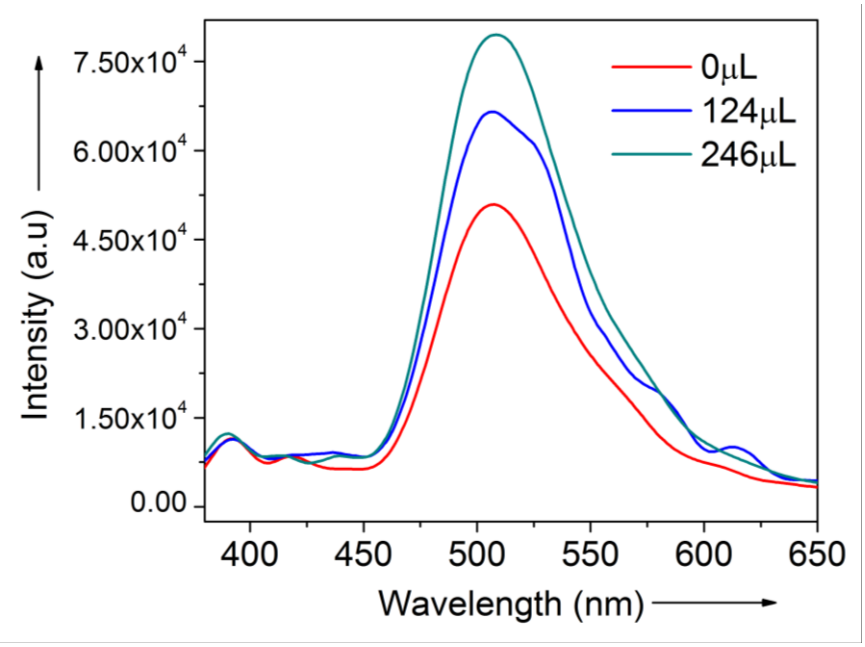

***Appendix 5.9**: Fluorescence changes of upon addition of HCO_3^- as Tetrabutylammonium salt in aqueous phase to bio-MOF-1⊃DAAC.*

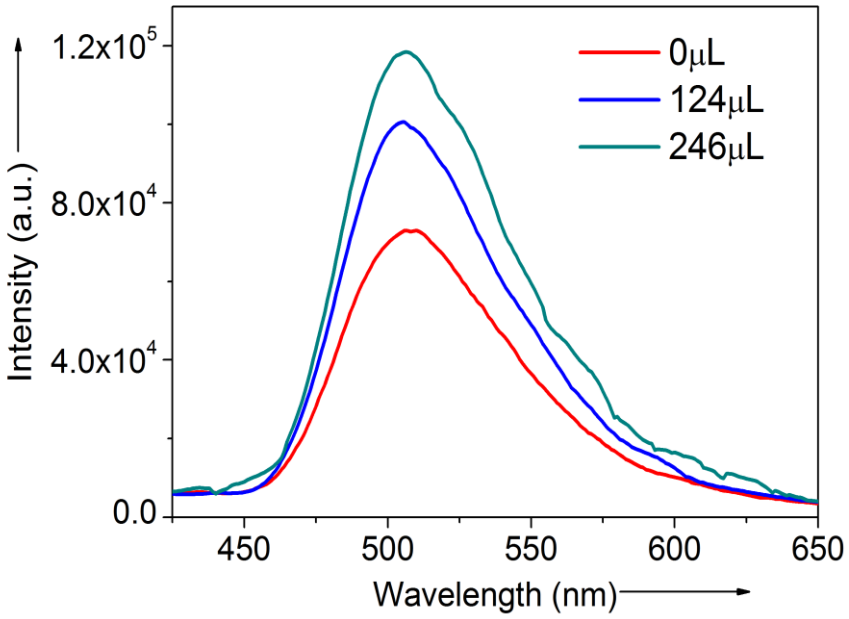

***Appendix 5.10**: Fluorescence changes of upon addition of OAc^- as Tetrabutylammonium salt in aqueous phase to bio-MOF-1⊃DAAC.*

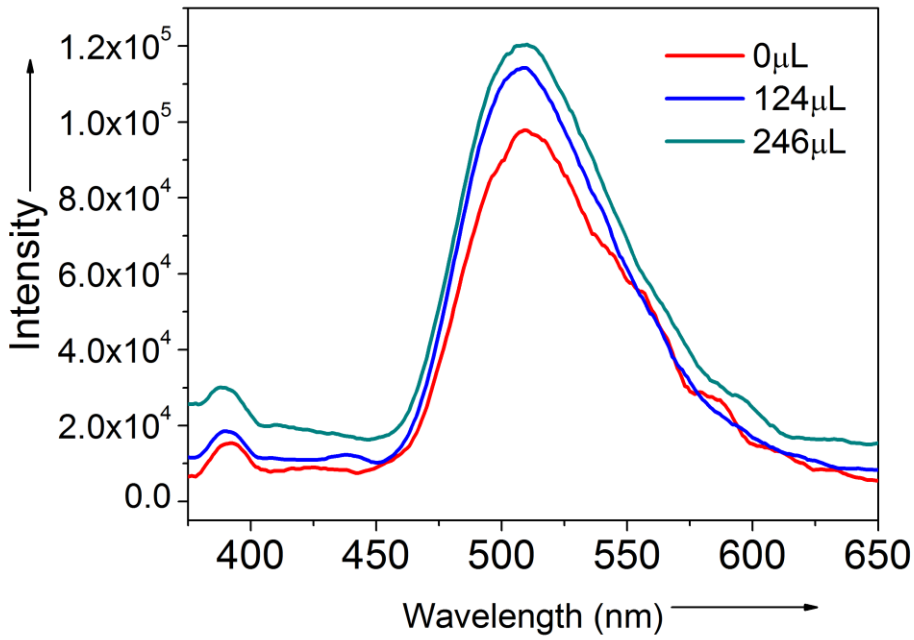

Appendix 5.11*: Fluorescence changes of upon addition of SCN^- as Tetrabutylammonium salt in aqueous phase to bio-MOF-1⊃DAAC*

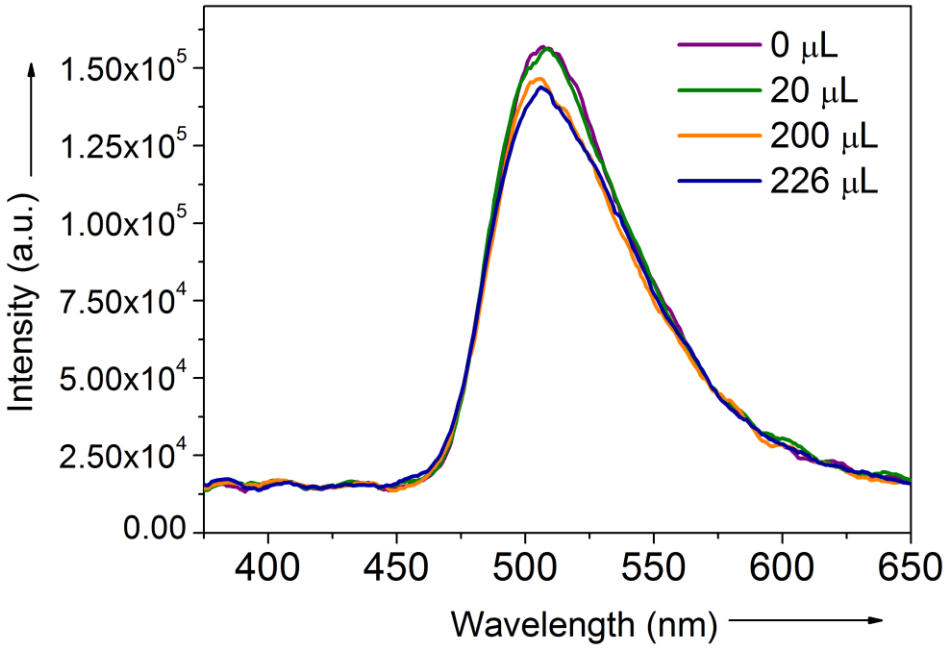

Appendix 5.12: *Fluorescence response upon addition of CN^- ions to 3,6-Diaminoacridine hydrochloride.*

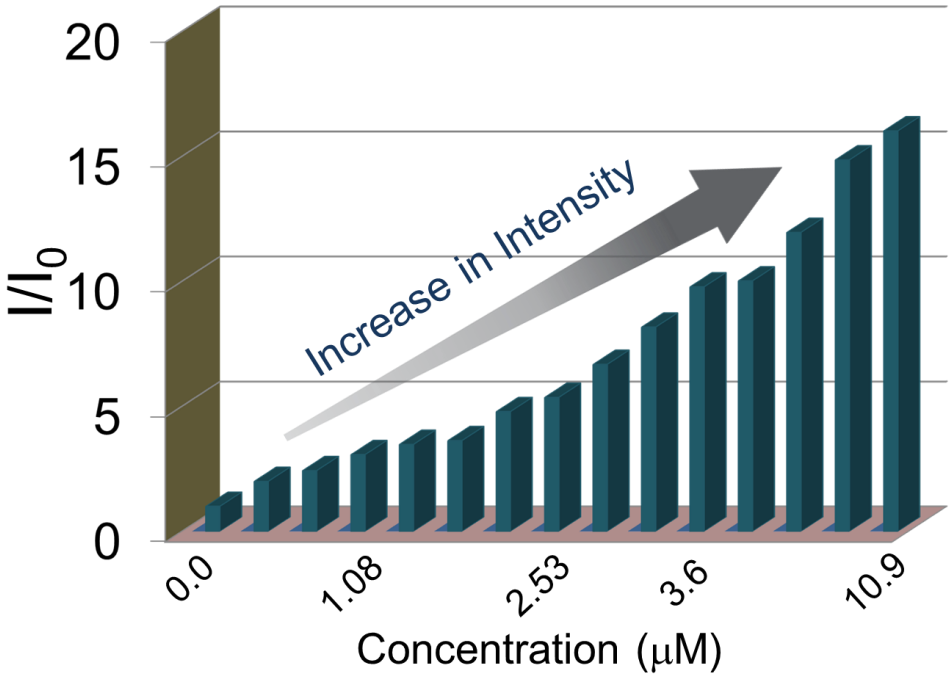

***Appendix 5.13**: Turn on response upon gradual addition of CN^- as Tetrabutylammonium salt in aqueous phase to bio-MOF-1⊃DAAC.*

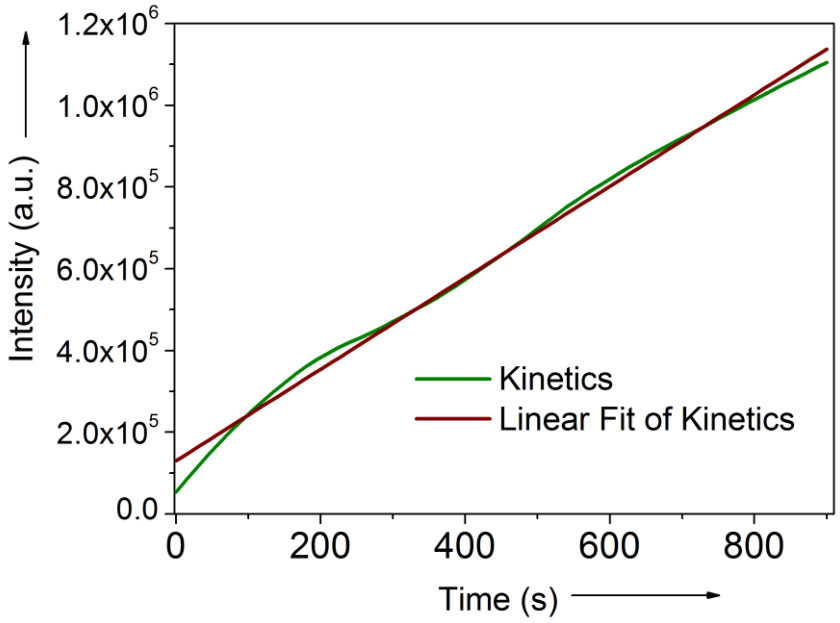

***Appendix 5.14**: Fluorescence response upon addition of CN^- ions to bio-MOF-1⊃DAAC w.r.t. time in seconds*

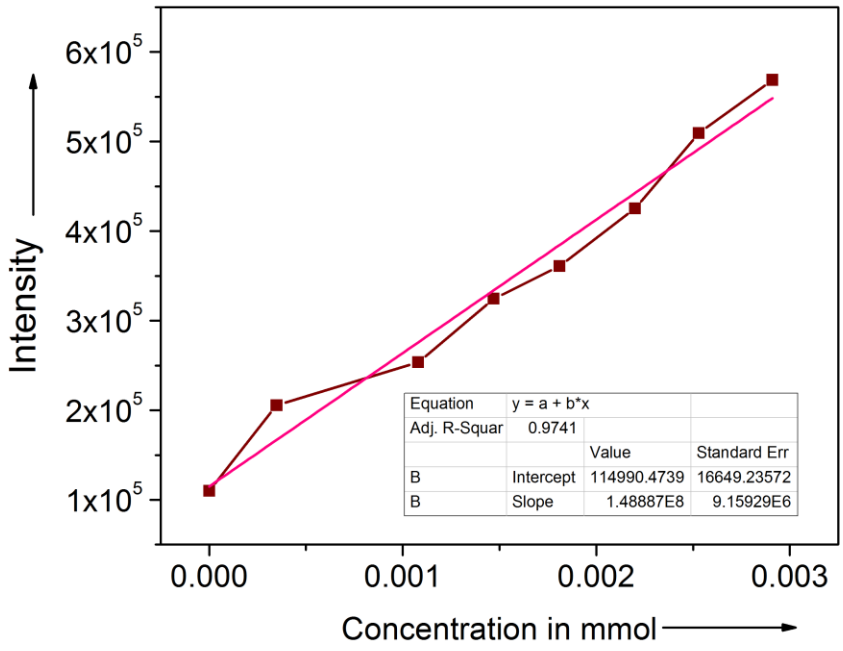

***Appendix 5.15**: Linear fit of Fluorescence change vs. conc. upon addition of CN^- ions.*

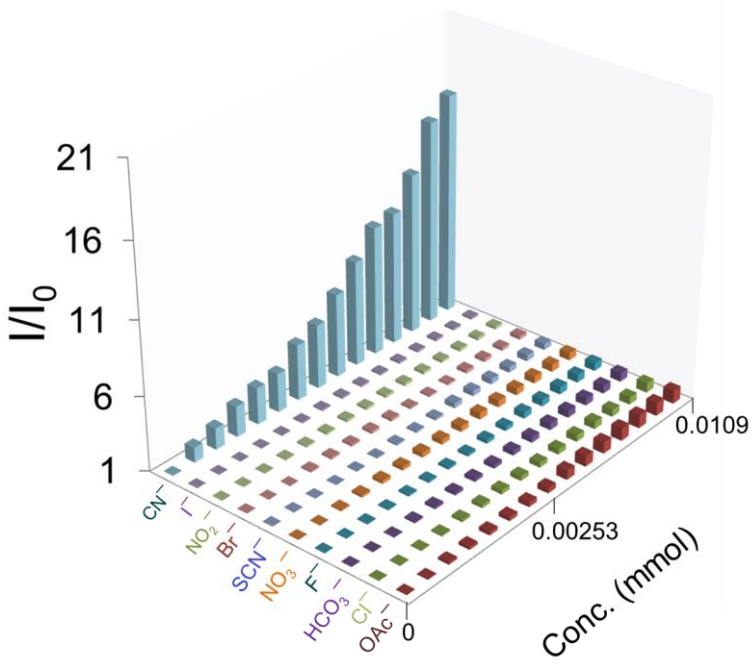

***Appendix 5.16**: Fluorescence response of CN^- ions compared to other anions when the anions w.r.t to different concentration of anions.*

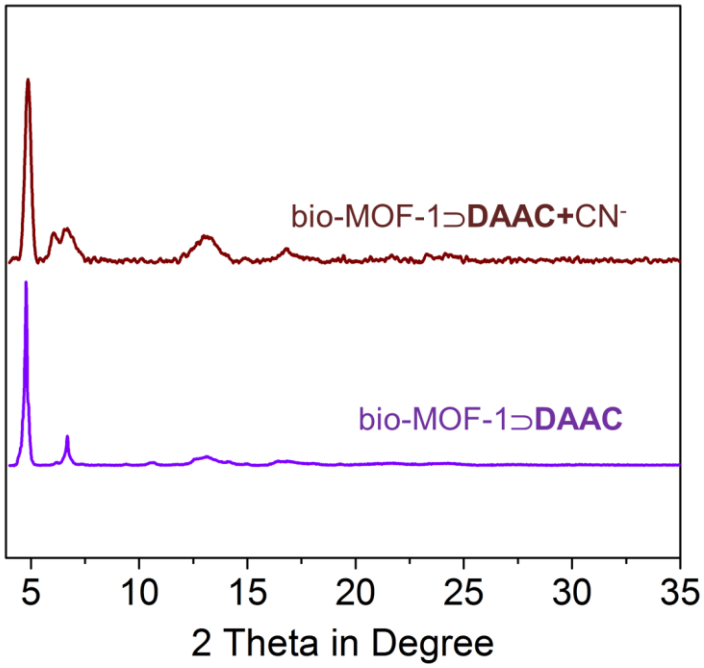

***Appendix 5.17**: PXRD pattern of bio-MOF-1⊃DAAC and bio-MOF-1⊃DAAC dipped in CN^- for about 1 month showing bulk crystallinity and structure retainment.*

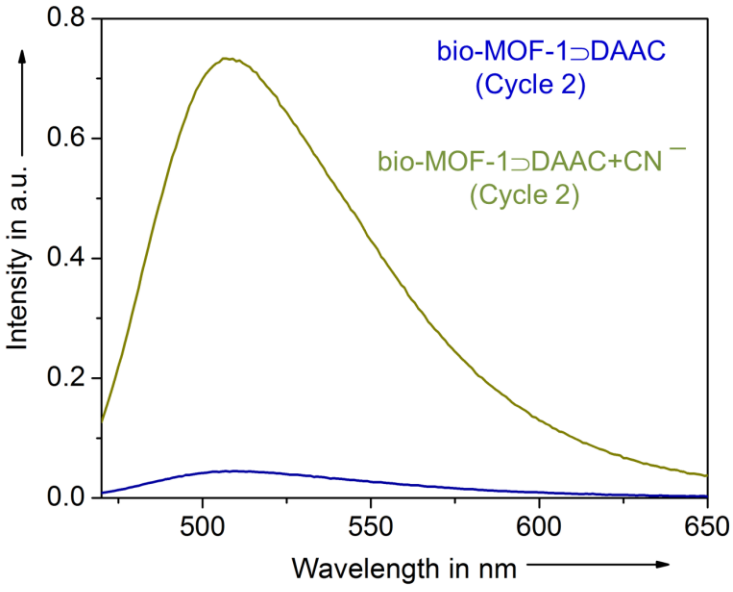

***Appendix 5.18**: Fluorescence response in presence of cyanide ions after recyclability experiments.*

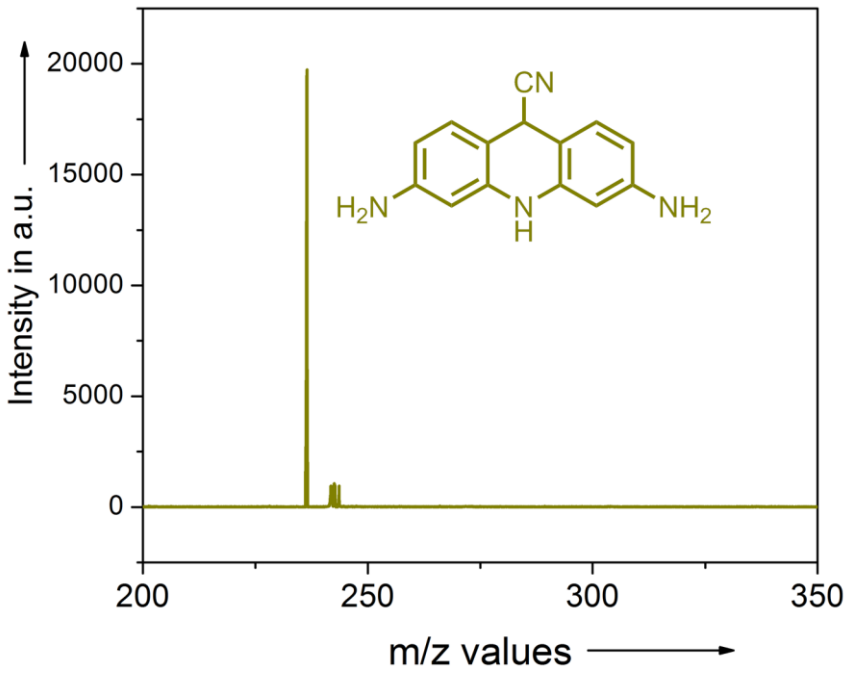

***Appendix 5.19**: MALDI-TOF spectra of the supernatant solution of spectra of bio-MOF-1⊃DAAC treated with CN^-.*

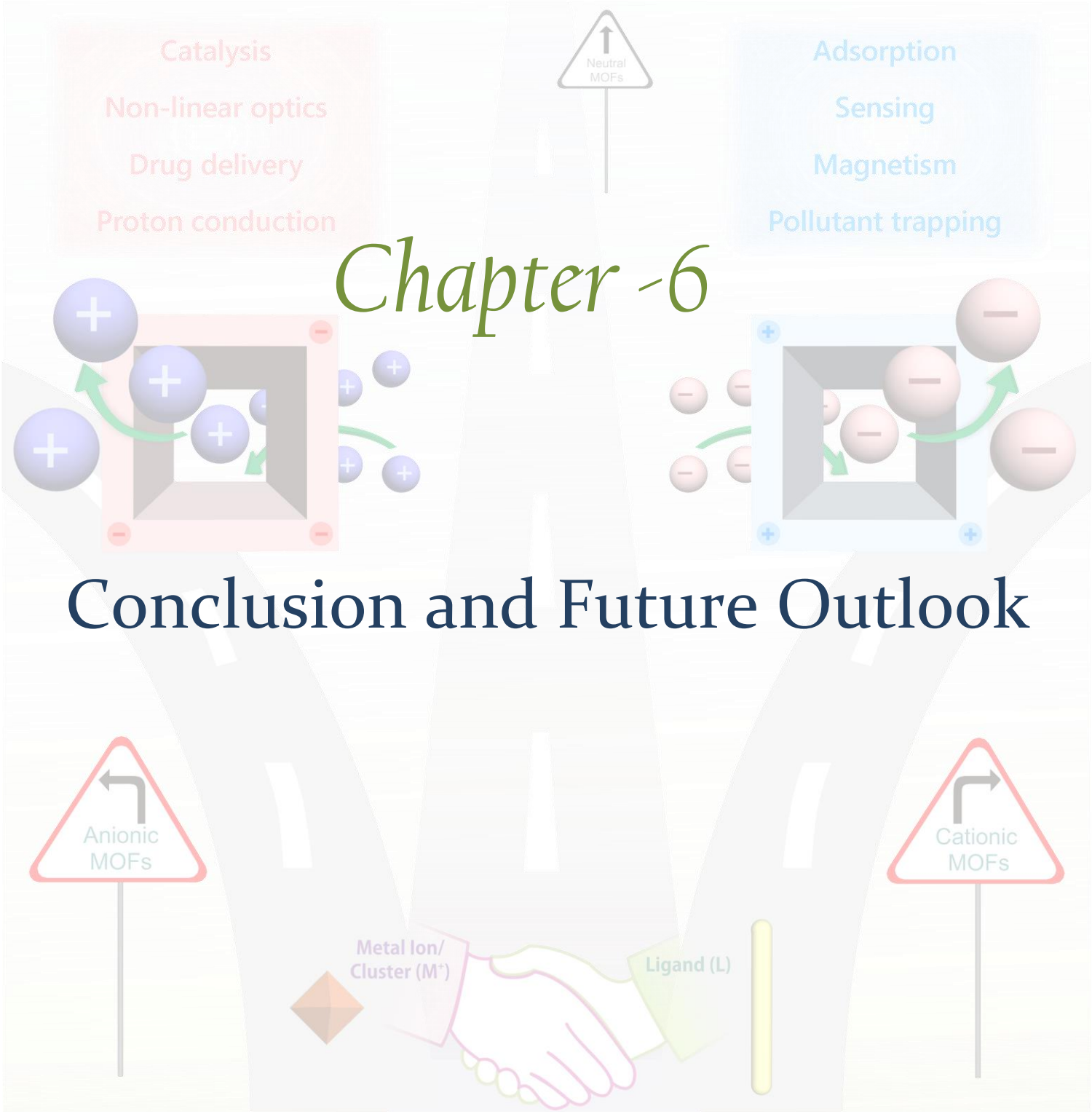

Chapter -6

Conclusion and Future Outlook

Cover page for Chapter 6

6.1. Conclusion and Future Outlook

In view of the tremendous amount of research devoted to the sensing and recognition of anions which play a crucial role in biological and chemical processes, the present thesis can add a new dimension towards escalating research on this aspect of supramolecular chemistry. Anions recognition are mostly realized by changes in optical and visual changes upon interaction/binding to the host receptor. MOFs, due to their tunable opto-electronic properties can be an efficient sensory probes for anions which has been demonstrated by following various approaches in this thesis. While the conventional anion exchange process has been illustrated in exploring the tunable luminescence and colorimetric changes w.r.t. different anions, other important strategy that can be employed in recognition of a particular anion is the post-synthetic modification, which imparts specific recognition sites in the framework. Also the inherent iconicity of the MOFs, which can be obtained by judicious choice of metal or ligands can offer that extra liberty of changes in luminescence modulation which can be tuned for selective recognition of even toxic anionic species.

Halogen-bonding-based anion receptors and utility of anion receptors in organo catalysis are some of the fields that has seen tremendous growth in the last few years. Since halogen bonding receptors are operative even in polar solvents, they are more competent than even the conventional hydrogen bonding that has been extensively studies for anion binding and recognition over the years. Since MOFs have proven to be one of the efficient class of materials for sensing applications due to their structural tailor ability, good physio-chemical stability and possibility of fabrication into smart devices, they hold great promise for the future for real time applications based on anion sensing.

Rights and Permission

Chapter 1:

Reprinted (adapted) with permission from *Coord. Chem. Rev*. **2016**, *307*, 313-341. Copyright 2016: Elsevier

Chapter 2:

Reprinted (adapted) with permission from *Inorg. Chem*. **2014**, *53*, 12225-12227 Copyright 2015 American Chemical Society.

Chapter 3:

Reprinted (adapted) with permission from *Chem. Eur. J*. **2015**, *21*, 7071-7076 Copyright 2015: John Wiley and Sons.

Chapter 4:

Reprinted (adapted) with permission from *Chem. Eur. J.* **2016**, *22*, 864-868. Copyright 2016: John Wiley and Sons.

Chapter 5:

Reprinted (adapted) with permission from *Chem. Commun.* **2017**, *DOI: 10.1039/C6CC08557A*. Copyright 2017: Royal Society of Chemistry

Coordination Chemistry Reviews 307 (2016) 313–341

Contents lists available at ScienceDirect

Coordination Chemistry Reviews

journal homepage: www.elsevier.com/locate/ccr

Review

Ionic metal-organic frameworks (iMOFs): Design principles and applications

Avishek Karmakar, Aamod V. Desai, Sujit K. Ghosh*

Dept. of Chemistry, Indian Institute of Science Education and Research (IISER), Pashan, Pune, Maharashtra 411008, India

Contents

Abbreviations: MOF, metal-organic framework; PCP, porous coordination polymer; CP, coordination polymer; 3D, 3 dimensional; DMF, dimethylformamide; DEF, diethylformamide; BDC, benzene-1,4-dicarboxylic acid; BTC, 1,3,5-benzenetricarboxylate; DMA, dimethyl ammonium system; SBU, secondary building unit; ZMOF, zeolite-like metal-organic frameworks; BPTC, biphenyltetracarboxylic acid; TMA, tetramethylammonium cation; TEA, tetraethylammonium cation; TBA, tetrabutylammonium cation; TCPT, 2,4,6-tris-(4-carboxyphenoxy)-1,3,5 triazine; Q_{st}, isosteric heat of adsorption; CCS, carbon capture and sequestration; H_2ppz^{2+}, piperazinium cation; DMNB, 2,3-dimethyl-2,3-dinitrobutane; Bpp, 1,3-bis(4-pyridyl)propane; Btapa, 1,3,5-benzene tricarboxylic acid tris[N-(4-pyridyl)amide]; EDTPN, ethylenediaminetetrapropionitrile; Mtpm, mtpm=tetrakis(m-pyridyloxy methylene)methane; tatrz, 1-(9-(1H-1,2,4-triazol-1-yl)anthracen-10-yl)-1H-1,2,4-triazole; dpzm, di-2-pyrazinylmethane; bpe, 1,2-bis(4-pyridyl)ethane; bipy, 4-4′-bipyridine; POM, polyoxometalates; RH, relative humidity; DFT, density functional theory; RTMPyP, 5,10,15,20-tetrakis(1-methyl-4 pyridinio)porphyrin; COD, 1,5-cyclooctadiene; Bpy, 4-4′-bipyridine; Dppe, 1,2-bis(diphenylphosphino)ethane; NLO, non-linear optics; SHG, second harmonic generation; DPASM, 4-(4-(diphenylamino)styryl)-1-methylpyridinium; DPASB, 1-butyl-4-(4-(diphenylamino)styryl)pyridinium; DPASN, 4-(4-(diphenylamino)styryl)-1-nonylpyridinium; DPASD, 4-(4-(diphenylamino)styryl)-1-dodecylpyridinium; PBS, phosphate-buffered saline; TNP, 2,4,6-trinitrophenol; TNT, 2,4,6-trinitrotoluene; DMNB, 2,3-dimethyl-2,3-dinitrobutane; 2,6-DNT, 2,4-dinitrotoluene; 2,4-DNT, 2,4-dinitrotoluene; NM, nitromethane; p-XBP4, N,N′-p-phenylenedimethylenebis(pyridin-4-one); LDH, layered double hydroxides; EDS, 1,2-ethanedisulfonate; Btr, 4,4′-bis(1,2,4-triazole); CD, cicular dichroism; MTT, 3-(4,5-dimethylthiazol-2-yl)-2,5-diphenyltetrazolium bromide; Imid, 3-bis(4-carboxy-2,6-dimethylphenyl)-1*H*-imidazolium; NHC, N-heterocycliccarbenes; NOTT, University of Nottingham; PC, proton conduction; OG, orange gelb.

* Corresponding author. Tel.: +91 20 25908076.
E-mail address: sghosh@iiserpune.ac.in (S.K. Ghosh).

http://dx.doi.org/10.1016/j.ccr.2015.08.007

Inorganic Chemistry

Communication

pubs.acs.org/IC

Dynamic Metal–Organic Framework with Anion-Triggered Luminescence Modulation Behavior

Avishek Karmakar, Biplab Manna, Aamod V. Desai, Biplab Joarder, and Sujit K. Ghosh*

Department of Chemistry, Indian Institute of Science Education and Research, Dr. Homi Bhabha Road, Pashan, Pune 411021, India

Supporting Information

ABSTRACT: A three-dimensional cationic framework based on a flexible neutral nitrogen-donor ligand was synthesized and undergoes guest-driven structural dynamics in a reversible way. Size-selective anion-exchange and tunable luminescent behavior of the framework has been explored.

Porous coordination polymers or metal–organic frameworks (MOFs) with tunable properties have emerged as an exciting class of multifunctional materials because of their applications over a wide range.[1] In particular, "soft porous frameworks" have attracted much attention in recent years because of their highly ordered network along with structural flexibility.[2] They score over the conventional rigid porous frameworks in a way that they respond to a specific guest molecule and change their microcavities into those that match the shape and affinity of the incoming guest molecule. These materials undergo solid-state structural transformation when a guest molecule comes in or goes out of the framework. Such guest-responsive tailorable behavior along with enzyme-like specificity makes it a stimulus-responsive smart host material, thereby triggering a manifold increase in the host–guest interactions.[2,3] Combinations of a neutral flexible ligand and metal ions generally give rise to cationic frameworks.[4] These frameworks usually harbor solvents as guests in their porous cavities. Upon drying, these loosely trapped guests escape, thus leading to structural transformations.[5] These guest-driven structural transformations often find a way to build up a dynamic framework.[4b] In addition, these cationic MOFs have extra counteranions to neutralize the overall charge of the framework, which usually weakly coordinates to the metal ions or sometimes remains free in the framework lattice.[6] The incorporation of a d^{10} metal ion in complexation with a nitrogen-donor ligand at room temperature often provides luminescent cationic frameworks.[7] Variation of the counteranions in a luminescent cationic framework by other foreign anions of different size, shape, and geometry may often regulate the framework functionalities.[8] Especially, the anion-switchable fluorescence of a luminescent cationic framework has been one of the most investigated topics in this regard because it finds very useful application such as chemical sensors and anion receptors, paving the way for a concoction of new materials.[4b,7,9] In spite of a lot of reports on dynamic frameworks, anion/guest-switchable fluorescence tuning of a MOF mixed with its inherent framework flexibility is not so common.[10,4b]

Herein, we present a three-dimensional (3D) cationic luminescent framework built from a newly designed nitrogen-donor ligand [(*E*)-*N*′-[1-(pyridin-4-yl)ethyidene]hydrazine carbohydrazide; Scheme S1 in the Supporting Information (SI)] with a flexible skeleton (Figure S1a in the SI) with multiple coordinating sites in combination with zinc(II). The framework shows guest-driven structural dynamics in a reversible way. The air-dried phase of the compound exhibits size-dependent anion-exchange behavior, and this is well demonstrated by single crystal-to-single crystal (SCSC) structural transformation experiments along with other spectroscopic techniques. The cationic framework shows interesting anion-responsive tunable luminescent behavior (Scheme 1).

Scheme 1. Schematic Representation of a Guest- and Anion-Responsive Dynamic Framework

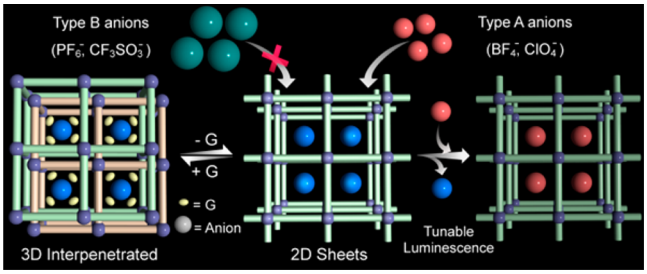

The combination of L (Scheme S1 in the SI) with zinc(II) in a solvent system of methanol/dichloromethane/chlorobenzene at room temperature yielded transparent block-shaped crystals of the compound $[\{Zn(L)_2\}(NO_3)_2{\cdot}xG]_n$ (**1**′⊃NO_3^-; G is a disordered guest molecule). Single-crystal X-ray diffraction (SC-XRD) analysis of **1**′⊃NO_3^- showed that it crystallized in a monoclinic system with space group *C*2/*c*. The asymmetric unit contains two ligands, one zinc(II) ion and two noncoordinated nitrate (NO_3^-) anions. Each zinc(II) ion displays distorted octahedral geometry with a N_4O_2 donor set from four ligands (Figure S1b in the SI). Two ligands bind in a bidentate fashion through amine nitrogen and carbonyl oxygen, and the other two connect the same zinc(II) node via pyridyl nitrogen, thus extending into a 3D structure, as shown in Figures S2 and S3 in the SI. 2-fold interpenetration creates large one-dimensional tubelike channels along the *b* axis, in which disordered solvent molecules and nitrate anions are located.

Received: June 20, 2014
Published: November 18, 2014

ChemPubSoc Europe

DOI: 10.1002/chem.201406233

CHEMISTRY A European Journal Communication

Metal–Organic Frameworks

An Amide-Functionalized Dynamic Metal–Organic Framework Exhibiting Visual Colorimetric Anion Exchange and Selective Uptake of Benzene over Cyclohexane

Avishek Karmakar, Aamod V. Desai, Biplab Manna, Biplab Joarder, and Sujit K. Ghosh*[a]

Abstract: A novel porous metal–organic framework (MOF) architecture is formed by a neutral amide-functionalized ligand and copper(II). Upon desolvation, this compound undergoes a dynamic structural transformation from a one-dimensional (1D) porous phase to a two-dimensional (2D) non-porous phase that shows selective uptake of benzene over cyclohexane. The as-synthesized compound also acts as a visual colorimetric anion sensor for thiocyanate.

Metal–organic frameworks (MOFs) are an important class of materials that have shown astounding applications in conventional proof-of-concept usage in separation, storage of gases, sensing, catalysis, ion-exchange, and fuel cells.[1] The serviceability of such ordered crystalline networks often depends on the incorporation of various functionalities within it, and development of such MOFs that can truly act as a multifunctional material[2] is the demand of the current state of art. In this regard, dynamic/flexible MOFs in which the structures and properties can be tuned in response to an external stimulus are of significant interest.[3] Their structural dynamism can indeed be the key principle for the concoction of diversified functionalities within the MOFs.

The major challenges in chemical industries are development of materials which can address the issues concerning separation and environmental pollution.[4] The conventional separation techniques which can effectively separate two small molecules are often expensive and require processes that are highly energy-demanding.[5] Cyclohexane, which is generally produced by the hydrogenation of benzene in industry, has unreacted benzene in the mixture, and separation of these two components is of considerable significance. In particular, because of the similarity in the boiling points (benzene, 80.1 °C and cyclohexane, 80.7 °C) and comparable Lennard–Jones collision diameters of these two components, conventional techniques often face a serious impediment in such separation procedures.[6] The current methods of separation of these two species involve the removal of residues from the distillate and are often gruesome. MOFs, owing their designable architecture and structural dynamism, score over the other conventional materials in this aspect, because by the virtue of their sieving effect,[7] they can selectively act as an efficient adsorbent for a particular adsorbate over others, such as benzene over cyclohexane, or even among other hydrocarbon congeners.[8] Also, one of the intriguing features of MOFs is the wide variety of organic ligands available for the construction allows syntheses of tailor-made materials for specific interactions with the incoming guest molecules. For instance, an amide-functionalized MOF can form favorable hydrogen-bonding interactions or sometimes because of the inherent basicity of the amide group[2d] can even interact differentially with the C–H protons of benzene and cyclohexane. An amide integrated framework can also discriminate between polar gas molecules such as CO_2 and other nonpolar gases owing to strong dipole–quadrupole interactions with CO_2 and can be an important candidate for carbon dioxide storage and separation.[9,2d]In addition to this, sensing and separation of small anions by cationic/neutral MOFs is one of the important area in the realm of the field of MOFs.[10] Most of the anion exchange/sensing properties of MOFs reported so far are either dependent on fluorescence-based methods of detection or by other spectroscopic techniques. Development of anion receptors that can sense anions by visual chroma are of great current interest as the anion recognition can consequently be realized by the naked eye.[11] Copper(II)-based MOFs are one of the well-known systems for such colorimetric anion sensors.[12] They are known to exhibit Jahn–Teller distortions in which the axial bonds which are usually coordinated by anions are significantly weakened. Anion exchange reactions at these axial sites in such MOFs may often result in visual color change and are getting immense importance in the field of sensors and actuators.[13] Integration of such multiple functionalities such as CO_2 separation/storage, separation of commercially important cyclic C_6 hydrocarbon congeners, and anion sensing by MOFs are rare, and development of such MOFs in a targeted fashion are of considerable importance.

In our endeavor to incorporate multifarious functionality in a MOF, we have synthesized a novel coordination polymer with molecular formula $[\{CuL_2(NO_3)_2\}\cdot o\text{-xylene}\cdot DMF]_n$ ($\mathbf{1}\supset NO_3^-$) by solvothermal reaction of $Cu(NO_3)_2\cdot 6H_2O$ and a newly de-

[a] A. Karmakar, A. V. Desai, B. Manna, B. Joarder, Dr. S. K. Ghosh
Department of Chemistry
Indian Institute of Science Education and Research (IISER) Pune
Dr. Homi Bhabha Road, Pashan, Pune-411008 (India)
Fax: (+91) 2025908186
E-mail: sghosh@iiserpune.ac.in
Homepage: http://www.iiserpune.ac.in/~sghosh/

Supporting information for this article is available on the WWW under http://dx.doi.org/10.1002/chem.201406233.

ChemPubSoc Europe

DOI: 10.1002/chem.201503323

CHEMISTRY
A European Journal
Communication

Sensors

A Post-Synthetically Modified MOF for Selective and Sensitive Aqueous-Phase Detection of Highly Toxic Cyanide Ions

Avishek Karmakar, Naveen Kumar, Partha Samanta, Aamod V. Desai, and Sujit K. Ghosh*[a]

Abstract: Selective and sensitive detection of toxic cyanide (CN^-) by a post-synthetically altered metal–organic framework (MOF) has been achieved. A post-synthetic modification was employed in the MOF to incorporate the specific recognition site with the CN^- ion over all other anions, such as Cl^-, Br^-, and SCN^-. The aqueous-phase sensing and very low detection limit, the essential prerequisites for an effective sensory material, have been fulfilled by the MOF. Moreover, the present detection level meets the standard set by the World Health Organization (WHO) for the permissible limit of cyanide concentration in drinking water. The utilization of MOF-based materials as the fluorometric probes for selective and sensitive detection of CN^- ions has not been explored till now.

Cyanide is considered to be one of the most toxic and lethal pollutants presently occurring in nature. It is known to be a noxious environmental contaminant causing serious health hazards, the production of which is mostly from anthropogenic sources as well as from naturally occurring biogenic processes in various plants.[1] The effect of cyanide in physiological systems in humans and other animals is mostly inhibition of respiration in the mitochondrial respiratory chain, because it binds to cytochrome c and inhibits its normal functions.[2] Various methods, such as mass spectrometry,[3] Raman spectrometry,[4] cyclic voltametry,[5] chromatographic techniques,[6] and electrochemical methods,[7] have been developed to date for the detection of cyanide ions. However, fluorescence-based detection techniques are more effective than the other techniques, because of their simplicity in the handling procedures, prompt response, and their ability to detect any trace amount of analytes with greater accuracy.[8] Although various organic-[9] and inorganic-based[10] chemosensors and chemodosimeters have been utilized to date to sense cyanide ions, the quest for a new class of materials, which could provide a platform for the aqueous-phase detection of toxic anions at very low concentrations, is of major interest at the present time.

Metal–organic frameworks (MOFs) represent examples of metal ions/clusters along with organic struts, which combine together through self-assembly resulting in various architectures.[11] Though the applications of MOFs[12] in fields like gas storage, separation, and heterogeneous catalysis have been comprehensively exploited by researchers, the use of MOFs as sensors is gathering immense importance among material chemists.[13] The pre-designing ability and tunable properties of MOFs sets them apart from other known organic/inorganic chemosensors.[14] Taking advantage of the confinement effect in MOFs, one can also trigger manifold increase in the host–guest interaction, thereby facilitating suitable signal transduction in response to a particular analyte.[15] The intrinsic hydrolytically stable nature in some MOFs could also render an added advantage for the aqueous-phase sensing, which is of great current interest. Moreover, by chemically modifying the organic substituents of the MOF by a post-synthetic modification[16] (PSM), an appropriate functionality can be incorporated within the MOF, which can act as a receptor or recognition site for a particular target/analyte molecule (Scheme 1). Herein, we report for the first time the selective and sensitive aqueous-phase detection of cyanide ions by a MOF-based system. The MOF used in the present study has been chemically modified to graft a specific recognition site for the cyanide ion that exhibits fluorescence modulation behavior with high chemoselectivity to detect the cyanide at very low concentrations.

Zeolitic imidazolate frameworks[17] (ZIFs) are an important subclass of MOFs that have long been known for their chemical and thermal stability. Since the discovery of this subfamily of MOFs, several derivatives of ZIFs have been established and

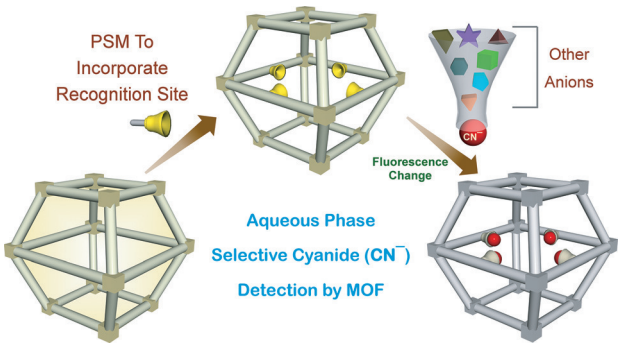

Scheme 1. Schematic overview of the post-synthetic modification in MOF leading to selective sensing of cyanide ion.

[a] *A. Karmakar, N. Kumar, P. Samanta, A. V. Desai, Dr. S. K. Ghosh*
Department of Chemistry
Indian Institute of Science Education and Research (IISER) Pune
Dr. Homi Bhabha Road, Pashan, Pune-411008 (India)
Fax: (+91) 2025908186
Home page:
E-mail: sghosh@iiserpune.ac.in
Homepage: http://www.iiserpune.ac.in/~sghosh/

Supporting information for this article is available on the WWW under http://dx.doi.org/10.1002/chem.201503323.

ChemComm

COMMUNICATION

View Article Online
View Journal

Aqueous phase sensing of cyanide ions using a hydrolytically stable metal–organic framework†

Avishek Karmakar,‡ Biplab Joarder,‡ Abhik Mallick, Partha Samanta, Aamod V. Desai, Sudipta Basu and Sujit K. Ghosh*

Cite this: DOI: 10.1039/c6cc08557a

Received 24th October 2016,
Accepted 22nd December 2016

DOI: 10.1039/c6cc08557a

www.rsc.org/chemcomm

A pure aqueous phase recognition and corresponding detoxification of highly toxic cyanide ions has been achieved by a fluorescent metal–organic framework (MOF). The cyanide detoxification has been shown to be effective even in *in vitro* studies and the MOF could be recycled to show the same efficiency of detoxification.

The cyanide ion is one of the most toxic chemical species to living animals as listed by the Environment Protection Agency (EPA) and the World Health Organization (WHO).[1] The release of a cyanide ion in any form can be lethal, as owing to its negative charge it can bind to the Fe^{3+} ion of the cytochrome oxidase and inhibit the normal functioning of the lungs and brain, leading to eventual death. Moreover, since CN^- is a chemical warfare agent (CWA), it is imperative to monitor, control and simultaneously detoxify cyanide ions.[2] Since the source of cyanide ions is mostly industrial wastes and even biogenic processes, significant attention is required for quantification and management of their concentration in drinking water, waste water or any other natural/artificial sources. The currently known methods of removal/detoxification of cyanides involving inorganic nitrites, thiosulfates or organic based aminophenols, glucose, *etc.*, have demerits because of their own toxicity issues in few cases and dependence of usage in binary combinations in other cases. Further, detoxification by standard chemical means (sulphite, hydrogen peroxide or Caro's acid) that have been employed by many industries often involves the formation of toxic cyanogen derivatives.[3] Additionally, the extent of reusability of such materials poses a key challenge to designing near perfect tools for cyanide sequestration. Therefore, the International Cyanide Management Institute (ICMI) devotes considerable attention to the detoxification techniques of ionic cyanides by alternative eco-friendly pathways.

Department of Chemistry, Indian Institute of Science Education and Research, Dr Homi Bhabha Road, Pashan, Pune 411008, India.
E-mail: sghosh@iiserpune.ac.in; Fax: +91 20 2590 8186; Tel: +91 20 2590 8076

† Electronic supplementary information (ESI) available: Detailed syntheses and characterization, TGA data, absorption and fluorescence results, LOD calculation, SEM images and additional information. See DOI: 10.1039/c6cc08557a

‡ A. K. and B. J. contributed equally.

Metal–organic frameworks (MOFs) have emerged as a new class of solid-state crystalline materials where their intrinsic pervious nature allows a wide spectrum of applications.[4] Very recently, MOFs have shown promising potential as "crystalline molecular flasks" where solution phase reactions can be mimicked in the solid state with a greater degree of molecular recognition and reaction sensitivity.[5] MOFs as molecular flasks/reaction vessels have often been employed in achieving important applications such as sensing, catalysis, chiral separation, *etc.*[6] Due to the molecular sieving effect in combination with the confinement effect in MOFs, these materials can act as perfect host materials for a wide variety of analytes, often rendering toxic/harmful chemicals inactive by subsequent reduction in their chemical reactivity.[6]

In recent times, MOFs have proven to be one of the prime candidates for recognition and as countermeasure of toxic chemical species from the environment. Although chemical adsorption based methods are prevalent in MOFs for capturing toxic species, capture of such toxic species/pollutants and consequent sequestration techniques by MOFs are required for environmental remediation purposes.[7] An irreversible reaction based approach, *i.e.* the chemodosimetric approach for capturing a analyte, is more reliable as it proves to be a more concrete and efficient way of recognition of a particular species. Also the added advantage of heterogeneous phase reactions allows for the recovery of the MOFs for recyclability purposes. If such a reaction can be monitored by fluorometric methods using MOFs as reaction vessels, then suitable signal transduction can be achieved, paving the way for segregation of toxic entities.[8] Fluorometric methods of sensing score over the other conventional techniques owing to their ease of handling, high signal output and easy fabrication into devices. Conjointly, a turn-on fluorescence response in the aqueous phase is desired because it does not lead to any loss of signal after capturing of the analyte(s).[9]

Ionic MOFs (i-MOFs) are perhaps the best manifestations of MOF based host matrices because the residual charge (positive or negative) can often be exchanged with more suitable cations/anions which may be responsible for imparting a suitable